"AUREL VLAICU" UNIVERSITY OF ARAD
FACULTY OF FOOD ENGINEERING, TOURISM AND ENVIRONMENTAL PROTECTION
CHEMICAL AND TECHNOLOGICAL RESEARCH CENTER

Scientific and Technical Bulletin

Series CHEMISTRY, FOOD SCIENCE & ENGINEERING

CHARACTERIZATION BY FTIR-ATR SPECTROSCOPY OF PM10 AND PM2.5 ATMOSPHERIC PARTICLES IN ARAD (ROMANIA) IN NORMAL PERIODS AND IN EPISODES OF SAHARAN DUST

Andreea-Corina MARCU, Andreea Ioana LUPITU, Cristian MOISĂ, Dorina Rodica CHAMBRE

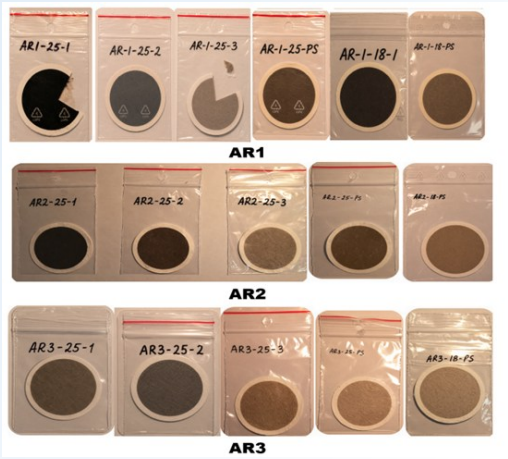

Figure A. Filter sample images

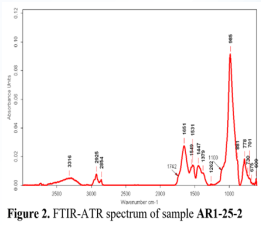

Figure 2. FTIR-ATR spectrum of sample **AR1-25-2**

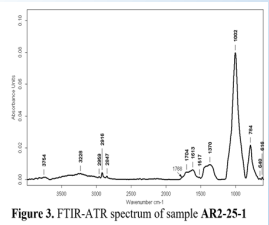

Figure 3. FTIR-ATR spectrum of sample **AR2-25-1**

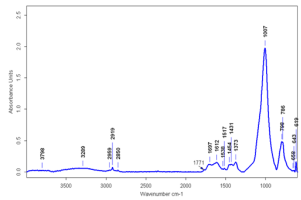

Figure 4. FTIR-ATR spectrum of the **AR3-25-2 sample**

Figure B. FTIR-ATR spectrum of the AR-25-2 sample

Year XXIII, Vol. 22, 2025

https://www.uav.ro/jour/index.php/stb-cfse/index

“AUREL VLAICU” UNIVERSITY OF ARAD

FACULTY OF FOOD ENGINEERING, TOURISM AND ENVIRONMENTAL PROTECTION

CHEMICAL AND TECHNOLOGICAL RESEARCH CENTER

Scientific and Technical Bulletin

Series CHEMISTRY, FOOD SCIENCE & ENGINEERING

Year XXIII, Vol. 22, 2025

ISSN 1582-1021

e-ISSN 2668-4764

EDITURA UNIVERSITĂȚII
AUREL VLAICU
A R A D

EDITURA UNIVERSITĂȚII
AUREL VLAICU
A R A D

CONTENTS

ADDRESS
Faculty of Food Engineering, Tourism and Environmental Protection,
„Aurel Vlaicu" University of Arad, Elena Dragoi St., Nr. 2, L31, Arad, Romania
Phone: 0040257369091; *E-mail:* dana.copolovici@uav.ro
Scientific and Technical Bulletin, Series: Chemistry, Food Science and Engineering is covered/indexed/abstracted in:

Directory of Research Journals Indexing	**Directory of Research Journals Indexing**
ROAD Directory of Open Access Scholarly Resources	**Directory of Open Access Scholarly Resources**
OCLC WorldCat	**World Cat**
Google Scholar	**Google Scholar**
CABI	**CABI**
INDEX COPERNICUS INTERNATIONAL	**Index Copernicus International**
Crossref	**Crossref**

Scien. Tech. Bull-Chem. Food Sci. Eng., Vol. 22(XXIII), 2025, 3-17
doi: 10.62591/Scien.Tech.Bull-Chem.FoodSci.Eng.2025.22.01

Article

CHARACTERIZATION BY FTIR-ATR SPECTROSCOPY OF PM10 AND PM2.5 ATMOSPHERIC PARTICLES IN ARAD (ROMANIA) IN NORMAL PERIODS AND IN EPISODES OF SAHARAN DUST

Andreea-Corina MARCU[1], Andreea Ioana LUPITU[2], Cristian MOISĂ[2], Dorina Rodica CHAMBRE[1]*

[1]Faculty of Food Engineering, Tourism and Environmental Protection, "Aurel Vlaicu" University of Arad, 2 Elena Drăgoi, Arad 310330, Romania
[2] Interdisciplinary Research Institute of the "Aurel Vlaicu" University of Arad, 2 Elena Drăgoi, Arad 310330, Romania
Corresponding author email: dorinachambree@yahoo.com

Abstract: *Atmospheric particulate matter (PM) represents one of the most important air quality indicators due to its significant impact on human health and the environment. FTIR-ATR spectroscopy was employed to investigate the chemical composition of PM10 and PM2.5 aerosols collected at three air quality monitoring stations in Arad County, representative of urban traffic, industrial activities, urban background, and suburban environments, during both normal atmospheric conditions and Saharan dust intrusion events. Variations in filter characteristics and FTIR-ATR spectral features reflected the combined effects of seasonal conditions, local emission sources, and Saharan dust transport. The identified absorption bands corresponding to O–H, C–H, C=O, NO_3^-, CO_3^{2-}, SO_4^{2-}, and Si–O functional groups indicated the presence of both natural and anthropogenic aerosol components. The natural fraction was dominated by silicates, aluminosilicates, quartz, hydrated clay minerals, and carbonates, whereas the anthropogenic fraction included carbonaceous compounds, hydrocarbons, and secondary aerosols such as nitrates and sulfates. Enhanced mineral signatures during Saharan dust episodes confirmed the contribution of long-range transported mineral aerosols rich in illite, smectite, palygorskite, calcite, and dolomite to PM composition. The FTIR-ATR findings demonstrate the combined influence of local emissions, seasonal variability, and Saharan dust transport on particulate matter composition in western Romania.*

Keywords: PM10 and PM2.5; FTIR-ATR spectroscopy; chemical composition; aerosol characterization; Saharan dust intrusion.

INTRODUCTION

Air pollution is one of the major environmental challenges of the 21st century, with significant impacts on human health, ecosystems, and climate. Among air pollutants, particulate matter (PM) is considered a key indicator of air quality due to its ability to penetrate the respiratory system and transport various chemical contaminants (Ofremu et al., 2025; Taha et al., 2025). Atmospheric particles are classified according to their aerodynamic diameter, with PM10 and PM2.5 representing the fractions of greatest relevance for air quality and health assessments.

The health effects of particulate matter depend on both particle size and chemical composition. PM10 particles are mainly deposited in the upper respiratory tract, whereas PM2.5 particles can reach the pulmonary alveoli and enter the bloodstream (Ofremu et al., 2025; Taha et al., 2025, Hamanaka and Mutlu, 2025). Numerous epidemiological studies have linked long-term PM exposure to respiratory and cardiovascular diseases and increased premature mortality (Ofremu et al., 2025; Taha et al., 2025). Consequently, the World Health Organization (WHO) and the European Union have established air quality standards and guideline values for PM10 and PM2.5 concentrations (WHO, 2025; WHO, 2024). Effective monitoring systems and continuous air quality assessment programs are therefore essential for identifying pollution episodes and supporting public health protection measures (EEA, 2024).

Atmospheric particulate matter consists of a complex mixture of organic and inorganic

compounds, including sulfates, nitrates, ammonium salts, elemental carbon, organic matter, trace metals, metalloids, and mineral particles (Seinfeld and Pandis, 2016; Romano et al., 2022). Its composition is influenced by emission sources, meteorological conditions, and atmospheric transport and transformation processes, making PM characterization an important tool for source identification and environmental impact assessment (Harrison and Hester, 2009; Shankar et al., 2022; Mohandoss et al., 2025).

In Central Europe, PM10 and PM2.5 originate from both anthropogenic sources, such as traffic, industry, energy production, residential heating, and agriculture, and natural sources, including soil dust resuspension, wildfires, and long-range transport of mineral aerosols (EEA, 2025; EEA, 2024). Recent studies have highlighted the significant contribution of transboundary pollution to particulate matter levels across Europe (Velásquez-García et al., 2024; Oduber et al., 2026; Basart et al., 2023).

Particular attention has been given to Saharan dust transport events, during which large quantities of mineral aerosols originating from North Africa reach the Mediterranean Basin and subsequently Central and Eastern Europe. These episodes can substantially increase PM10 concentrations and modify aerosol composition and atmospheric optical properties (Querol et al., 2009; Gkikas et al., 2021; Varrica et al., 2019). Recent studies indicate an increasing frequency and intensity of Saharan dust intrusions, affecting regions located hundreds or even thousands of kilometers from the source areas (Rodríguez et al., 2024; Varga, 2023).

Arad County, located along Romania's western border, is among the first regions affected by air masses originating from southwestern Europe. Its position on major European transport corridors and its proximity to important industrial and urban areas in Romania and Hungary expose the region to both local and transboundary sources of air pollution. Consequently, during Saharan dust intrusion events, Arad is often among the first areas in Romania to experience increased particulate matter concentrations due to the prevailing southwesterly air mass circulation (https://apmar.anpm.ro).

The municipality of Arad represents the main urban and economic center of the county, characterized by intense road traffic, industrial and logistics activities, and a high population density. Major emission sources include traffic along the E68 and E671 European corridors, urban traffic, activities within the Arad-West industrial area, and centralized and residential heating systems, particularly during the cold season. In addition, the topographic characteristics of the Western Plain may favor the temporary accumulation of pollutants under stable atmospheric conditions.

Air quality monitoring is performed through automatic stations integrated into the National Air Quality Monitoring Network (RNMCA), managed by the Arad Environmental Protection Agency (DJM Arad) (https://anmap.gov.ro/reteaua-nationala-de-monitorizare-automata-a-calitatii-aerului-rnmca/). In Arad County, monitoring is carried out at two stations located in the municipality of Arad (AR1 and AR2) and one station in the Nădlac area (AR3), providing continuous data on major atmospheric pollutants. These measurements support air quality assessment, the identification of pollution episodes, and studies on atmospheric aerosol dynamics and population exposure to air pollutants. The AR1 monitoring station is situated in an urban area characterized by intense road traffic and industrial activities, including emissions associated with the CET-H electrothermal power plant, and is representative of pollution generated by these sources. The AR2 station is located within a residential area and is considered representative of the urban background conditions of Arad. In contrast, the AR3 station is situated near the Nădlac border crossing with Hungary and is representative of the combined influence of international road traffic and the resuspension of mineral particles from surrounding agricultural land and transportation corridors.

PM10 and PM2.5 samples were collected in accordance with the SR EN 12341 standard using automatic samplers equipped with size-selective inlets for the retention of particles with aerodynamic diameters below 10

μm and 2.5 μm, respectively (https://www.mmediu.ro/app/webroot/uploads/files/Ghid%20G1.pdf). Particles were collected on quartz fiber filters during 24-hour sampling periods under controlled operating conditions. PM concentrations were determined gravimetrically following filter conditioning and weighing procedures specified by the standard. After analysis, the filters were individually sealed and stored under controlled temperature and humidity conditions to preserve their physicochemical properties.

The characterization of atmospheric particulate matter is essential for identifying emission sources and understanding aerosol transport and transformation processes. Among the available analytical techniques, FTIR-ATR spectroscopy has proven particularly useful for investigating the chemical composition of atmospheric particles, while complementary methods such as ICP-MS and SEM-EDS provide additional information on elemental composition and particle morphology (Varrica et al., 2019; Gupta et al., 2024; Radulescu et al., 2017).

FTIR-ATR enables the identification of functional groups and major chemical constituents in particulate matter using small sample quantities and minimal preparation (Radulescu et al., 2017; Mahmud et al., 2024; Maria et al., 2002; Coury and Dillner, 2008; Russell, 2003). Its rapid and non-destructive nature allows the simultaneous characterization of both organic and inorganic aerosol components, making it a valuable tool for atmospheric particle analysis.

The aim of this study was to characterize the chemical composition of PM10 and PM2.5 atmospheric particles collected at different air quality monitoring sites in Arad County, Romania, using ATR-FTIR spectroscopy, with a focus on assessing the influence of local emission sources, seasonal variability, and Saharan dust intrusion events on the chemical characteristics of atmospheric aerosols.

MATERIALS AND METHODS

Material:

This study was based on the analysis of PM10 and PM2.5 particulate matter samples collected on quartz fiber filters and selected from the archive of the Chemical Analysis Laboratory of the DJM Arad. The filters were obtained through routine monitoring activities carried out within the National Air Quality Monitoring Network (RNMCA) at the three automatic air quality monitoring stations AR1, AR2, and AR3.The sampling periods corresponding to the investigated filter samples are presented in Table 1, whereas Table 2 summarizes the coding mode. Figure 1 shows the PM10 and PM2.5 filter samples selected for FTIR-ATR analysis

Table 1. Sampling periods of the investigated filters

Sampling period	Type of samples
February 2025	PM10
March 2025	PM10 and PM2.5
July 2025	PM10
24–25 March 2025	PM10 –episode of Saharan dust
March 2018	PM10
April 17–18, 2018	PM10 –episode of Saharan dust

Table 2. Sample identification codes

Sample code	Date	Filter	Saharan dust **(PS)**
AR1 Location			
AR1-25-1	20.02.2025	PM10	NO
AR1-25-2	20.03.2025	PM10	NO
AR1-25-3	27.07.2025	PM10	NO
AR1-25-PS	24.03.2025	PM10	YES
AR1-18-1	16.03.2018	PM10	NO
AR1-18-PS	17.04.2018	PM10	YES
AR2 Location			
AR2-25-1	20.03.2025	PM10	NO
AR2-25-2	20.03.2025	PM2,5	NO
AR2-25-3	27.07.2025	PM10	NO
AR2-25-PS	24.03.2025	PM10	YES
AR2-18-PS	17.04.2018	PM10	YES
AR3 Location			
AR3-25-1	19.03.2025	PM10	NO
AR3-25-2	20.03.2025	PM10	NO
AR3-25-3	27.07.2025	PM10	NO
AR3-25-PS	24.03.2025	PM10	YES
AR3-18-PS	17.04.2018	PM10	YES

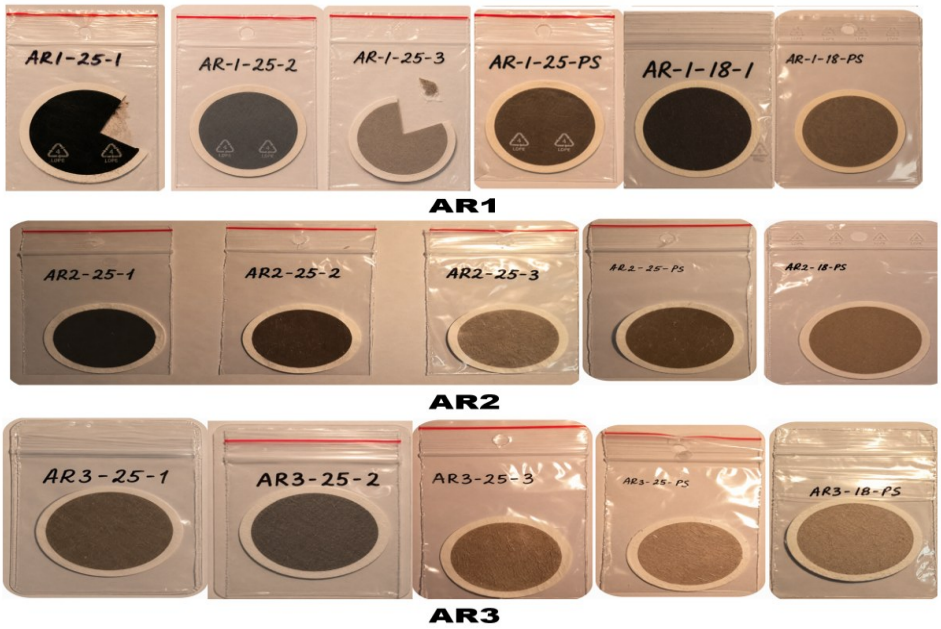

Figure 1. Filter sample images.

Method:

Prior to spectroscopic analysis, the filters were visually examined using a magnifying glass in order to evaluate their general appearance, coloration, surface texture, particle distribution, and particulate matter loading.

For FTIR-ATR analysis, representative fragments were collected from the particulate matter-loaded regions of each filter. The surface layer containing the deposited atmospheric particles was carefully isolated from the filter substrate using stainless-steel tweezers and subsequently used for spectral acquisition.

FTIR-ATR analyses were performed using a Vertex 70 spectrometer (Bruker, Germany) equipped with a ZnSe ATR crystal. Spectra were recorded in the 4000–600 cm^{-1} and 1900–600 cm^{-1} ranges at a resolution of 4 cm^{-1}, with 64 scans accumulated for each measurement. Representative fragments from the particulate matter-loaded areas of the filters were placed directly onto the ATR crystal. Prior to each analysis, a background spectrum was recorded using an unexposed portion of the same filter material to compensate for spectral contributions from the filter substrate. The ATR crystal was cleaned with isopropyl alcohol between successive measurements to prevent cross-contamination. Spectral acquisition and processing, including baseline correction, were performed using OPUS 6.3 software (Bruker). For each sample, three replicate measurements were carried out, and the results are presented as the average spectrum.

RESULTS AND DISCUSSIONS

According to Law No. 104/2011 on ambient air quality, the limit value for PM10 is 50 µg m^{-3} as a daily average, with no more than 35 exceedances permitted per year, and 40 µg m^{-3} as an annual average. For PM2.5, the annual limit value is 25 µg m^{-3}.
(http://www.calitateaer.ro/export/sites/default/.galleries/Legislation/national/Lege-nr.-104_2011-calitatea-aerului-inconjurator.pdf)

Table 3 summarizes the PM10 and PM2.5 concentrations determined by the gravimetric method for the analyzed filter samples collected over a 24-hour sampling period and identifies the instances in which the regulatory limit values were exceeded.

Table 3. Gravimetric PM values for filter samples (DJM Arad, Chemical Analysis Laboratory)

Sample code	PM value (µg/m³)	PM10 limit value exceeded (50 µg/m³)
AR1-25-1	55	YES
AR1-25-2	47	NO
AR1-25-3	26	NO
AR1-25-PS	61	YES
AR1-18-1	34	NO
AR1-18-PS	65	YES
AR2-25-1	51	YES

AR2-25-2	17	NO *
AR2-25-3	22	NO
AR2-25-PS	60	YES
AR2-18-PS	63	YES
AR3-25-1	32	NO
AR3-25-2	35	NO
AR3-25-3	21	NO
AR3-25-PS	68	YES
AR3-18-PS	72	YES

* For PM2.5 there is no daily limit value in the Romanian legislation; The comparison is made only as a guideline against the annual limit value of 25 μg/m³.

The PM concentrations revealed variations among the three monitoring sites (AR1, AR2, and AR3), as well as between normal atmospheric conditions and Saharan dust intrusion events. The highest PM10 concentrations were recorded during Saharan dust episodes, frequently exceeding the daily limit value of 50 μg m^{-3} established by national legislation. Maximum values were observed for samples AR3-18-PS (72 μg m^{-3}), AR3-25-PS (68 μg m^{-3}), and AR1-18-PS (65 μg m^{-3}), highlighting the significant contribution of long-range transported mineral aerosols.

Among the investigated sites, AR1, influenced by both road traffic and industrial activities, generally exhibited the highest particulate matter concentrations, with PM10 values ranging from 26 to 55 μg m^{-3} under non-Saharan conditions. In contrast, AR2, representative of the urban background environment, recorded lower concentrations, reflecting a reduced influence of local anthropogenic sources. The substantial difference between samples AR2-25-1 (PM10 = 51 μg m^{-3}) and AR2-25-2 (PM2.5 = 17 μg m^{-3}), collected on the same day, indicates a significant contribution of coarse particles (2.5–10 μm) to the total aerosol burden. AR3, showed intermediate concentration levels influenced by both traffic emissions and the resuspension of mineral particles from surrounding open areas.

Lower particulate matter concentrations were generally recorded during the summer period, with PM10 values decreasing to approximately 21 μg m^{-3}. Overall, 8 of the 16 analyzed samples exceeded the daily PM10 limit value, most of them being associated with Saharan dust intrusion events. However, exceedances were also observed under non-Saharan conditions at sites strongly affected by road traffic.

These findings demonstrate the combined influence of local anthropogenic emissions and long-range transport of mineral aerosols on particulate matter levels in the Arad region.

Preliminary characterization of the filtres

During the warm season, atmospheric mineral particle concentrations generally increase due to soil drying, road dust resuspension, agricultural activities, and construction work (Harrison and Hester, 2009; Amato, 2018). In addition, Saharan dust intrusion events occur more frequently during spring and summer. Consequently, PM10 filters typically exhibit light gray to brownish shades associated with mineral deposits (Querol et al., 2009).

During Saharan dust events, the filters often display yellowish-brown, reddish-brown, or grayish-brown coloration due to the increased contribution of mineral particles rich in silicates, carbonates, and iron oxides transported from North Africa (Seinfeld and Pandis, 2016; Querol et al., 2009).

In the cold season, high soil moisture and snow cover reduce the resuspension of mineral particles, while emissions from residential heating and road traffic increase, leading to a greater contribution of combustion-derived compounds (Basart et al., 2023; Gkikas et al., 2021). Consequently, PM10 filters collected during winter generally exhibit darker shades, ranging from dark gray to black, reflecting the increased presence of elemental carbon.

The visual examination of the PM10 and PM2.5 filters (Fig.1) revealed noticeable differences in coloration and particle loading depending on the season, sampling location, and the occurrence of Saharan dust intrusion events. Filters collected during the cold season generally exhibited dark gray to black coloration and a high degree of particle loading, reflecting the increased contribution of carbonaceous aerosols associated with road traffic, residential heating, and other combustion processes. In contrast, filters collected during the warm season showed lighter gray, beige, or brownish shades, indicating a greater contribution of mineral particles originating from road dust

resuspension, agricultural activities, and other natural sources. Samples associated with Saharan dust intrusion events were characterized by grayish-brown, beige-brown, or reddish-brown coloration. Differences were also observed among the monitoring sites, with filters collected in areas strongly influenced by traffic and anthropogenic activities displaying darker coloration and higher particle loading than those collected in locations with a greater contribution of mineral dust. Overall, the visual characteristics of the filters reflected the combined effects of seasonal conditions, local emission sources, and Saharan dust transport on the composition of atmospheric particulate matter.

Interpretation of FTIR-ATR spectra

In recent years, Fourier Transform Infrared Spectroscopy (FTIR) has become an important tool for the characterization of atmospheric aerosols, enabling the identification of both organic and inorganic constituents of particulate matter (Romano et al., 2022; Shankar et al., 2022; Varrica et al., 2019). The combination of FTIR with Attenuated Total Reflectance (ATR) significantly expands its applicability to solid samples, allowing rapid, non-destructive analysis with minimal sample preparation (Mohandoss et al., 2025; Gupta et al., 2024; Mahmud et al., 2024). The study published by Varrica D. et al. (Varrica et al., 2019) demonstrates that ATR-FTIR analysis can be successfully used for the chemical characterization of PM10 and PM2.5 and for highlighting the influence of Saharan dust episodes on the composition and concentration of atmospheric particles.

Figures 2–4 show the FTIR-ATR spectra of the PM10 samples collected on 20 March 2025 at the AR1, AR2, and AR3 monitoring stations, whereas Table 4 presents the vibrational assignments of the principal absorption bands observed in the recorded spectra.

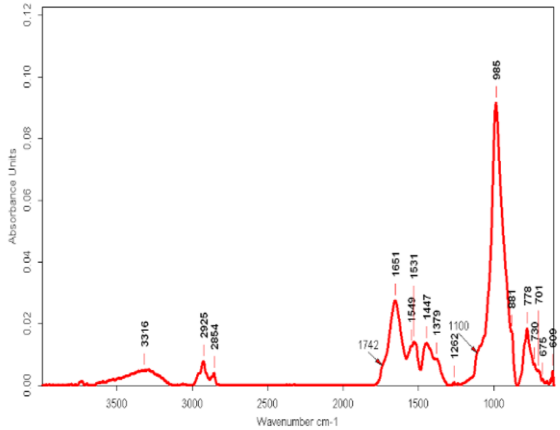

Figure 2. FTIR-ATR spectrum of sample **AR1-25-2**

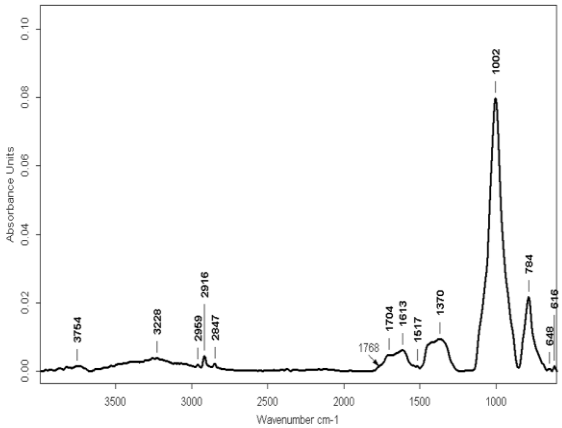

Figure 3. FTIR-ATR spectrum of sample **AR2-25-1**

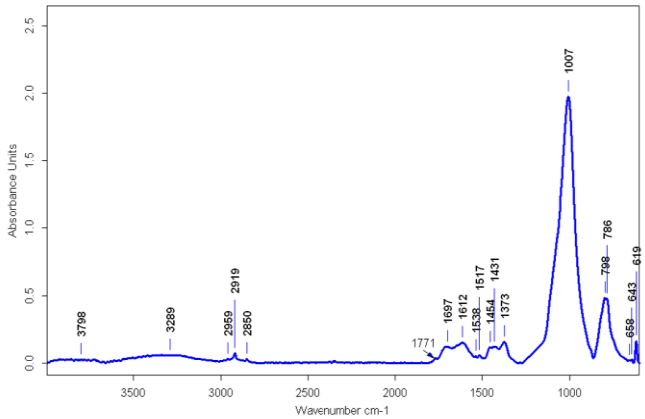

Figure 4. FTIR-ATR spectrum of the **AR3-25-2 sample**

Table 4. Vibrational assignment of FTIR-ATR bands for PM10 samples collected on 20.03.2025

Wavenumber (cm^{-1})	AR1-25-2	AR2-25-1	AR3-25-2	Vibrational assignment	Probable compounds	Ref.
~3800–3200	3316	3754, 3228	3798, 3289	ν(O–H) stretching	Adsorbed water, hydroxyl groups of clays, silicates and hydrated minerals	(Coury and Dillner, 2008; Gupta et al., 2024; Mahmud et al., 2024; Maria et al., 2002; Mohandoss et al., 2025; Romano et al., 2022; Russell, 2003; Shankar et al., 2022; Varrica et al., 2019)
~2960–2915	2925	2959, 2916	2959, 2919	ν as(C–H)	Aliphatic hydrocarbons, carbonaceous compounds from traffic and combustion	
~2855–2845	2854	2847	2850	νs(C–H)	Aliphatic chains of hydrocarbons	
~1775–1690	1742	1768, 1704	1771, 1697	ν(C=O) stretching	Esters, aldehydes, ketones, carboxylic acids and secondary organic aerosols	
~1655–1600	1651	1613	1612	δ(H–O–H), ν(C=C)	Adsorbed water, oxidized organic matter, aromatic compounds	
~1550–1500	1549, 1531	1517	1538, 1517	$\nu(NO_3^-)$, ν(C=C) aromatic	Nitrates and aromatic compounds	
~1455–1370	1447, 1373	1370	1454, 1431, 1373	$\nu_3(CO_3^{2-})$, $\delta(CH_3)$	Carbonates (calcite, dolomite), organic matter	
~1265–1100	1262, 1100	–	–	ν (C–O), ν (SO_4^{2-})	organic compounds Secondary sulphates	
~1030–980	985	1002	1007	ν(Si–O–Si), ν(Si–O)	Quartz, silicates, aluminosilicates, clays	
~800–770	778	784	798, 786	ν(Si–O)	Quartz and crystalline silicates	
~700–560	701, 675, 609	648, 616	643, 619, 568	δ(Si–O), Al–O–Si	Aluminosilicates, clays, feldspars	

The FTIR-ATR spectra of samples AR1-25-2, AR2-25-1, and AR3-25-2 (Figs. 2–4) exhibit similar spectral features, indicating the presence of both organic and inorganic constituents typical of atmospheric aerosols. The identified absorption bands suggest that PM10 particles collected at the three monitoring stations consist of a complex mixture of mineral phases, including silicates, quartz, aluminosilicates, and carbonates, together with organic compounds originating from combustion processes and secondary atmospheric transformations. These findings are consistent with previous studies on the chemical composition of atmospheric particulate matter (Romano et al., 2022; Shankar et al., 2022; Varrica et al., 2019; Gupta et al., 2024). The observed differences among the samples reflect the influence of local emission sources and site-specific conditions, with a more pronounced mineral contribution in sample AR3-25-2 and a stronger anthropogenic influence in samples AR1-25-2 and AR2-25-1.

The most intense absorption band, observed in the 986–1007 cm^{-1} region, represents the dominant spectral feature of all analyzed samples. Although the sampling filters are composed of quartz fibers, their spectral contribution was compensated by recording the background spectrum using an unexposed

portion of the same filter material. As illustrated in Fig. 5, the quartz fiber filter exhibits characteristic absorption bands at approximately 1027 and 802 cm^{-1}; however, these bands are effectively removed during background correction. Consequently, the remaining absorption band in the 986–1007 cm^{-1} region can be attributed to particulate matter deposited on the filters, indicating a significant contribution of silicate-rich mineral particles.

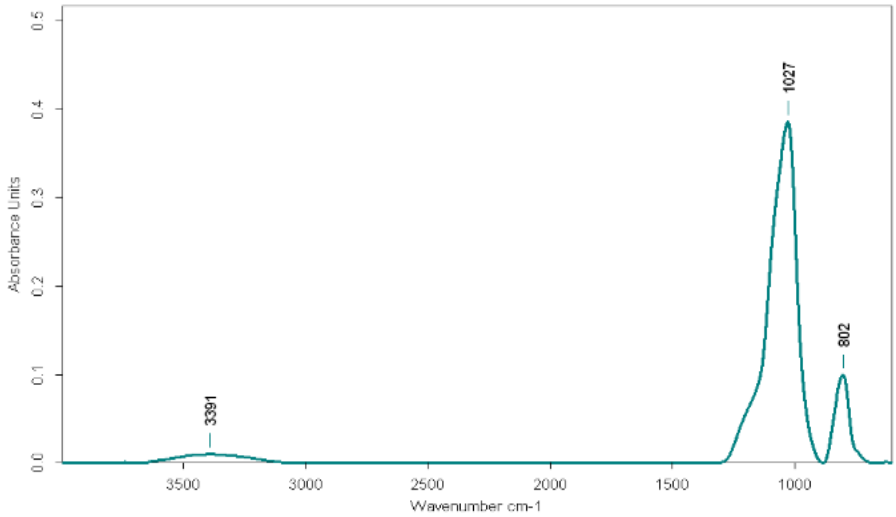

Figure 5. FTIR-ATR Spectrum of quartz fiber filter

Table 5. Comparison of PM10 samples collected on 20.03.2025

Parameter	AR1-25-2	AR2-25-1	AR3-25-2
Station type	Traffic and Industrial	Urban Background	Suburban Traffic
PM10 (μg m^{-3})	47	51	35
Dominant absorption band (cm^{-1})	985	1002	1007
Organic signature (C–H, C=O)	Pronounced	Pronounced	Moderate
Nitrates Secondary aerosols	Pronounced	Moderate	Pronounced
Carbonates	Moderate	Weak	Pronounced
Silicates and alumino-silicates	High	High	Very high
Predominant pollution sources	Traffic and industry	Mixed urban background	Resuspended mineral particles and traffic

In all three spectra, a broad band at 3800–3200 cm^{-1} is attributed to O–H stretching vibrations associated with hydroxyl groups and adsorbed water (Mohandoss et al., 2025; Varrica et al., 2019; Rodríguez et al., 2024). Bands in the 2960–2850 cm^{-1} region correspond to C–H stretching vibrations of aliphatic hydrocarbons, indicating contributions from combustion processes and road traffic (Shankar et al., 2022; Varrica et al., 2019). Absorption bands between 1770 and 1600 cm^{-1} are associated with carbonyl (C=O) groups and oxygenated organic compounds, suggesting the presence of secondary organic aerosols (Romano et al., 2022; Mohandoss et al., 2025; Maria et al., 2002), while bands at 1550–1500 cm^{-1} indicate nitrates and other secondary inorganic species (Coury and Dillner, 2008; Russell, 2003). The most intense bands, observed in the 1030–980 cm^{-1} region, are attributed to Si–O–Si and Si–O vibrations characteristic of silicates, quartz, and aluminosilicates (Varrica et al., 2019; Coury and Dillner, 2008). Together with the bands detected at 800–600 cm^{-1}, they confirm a significant contribution of mineral particles derived from crustal materials and soil dust resuspension. The bands in the 1455–1370 cm^{-1} range, assigned to CO_3^{2-} asymmetric stretching vibrations, indicate the presence of carbonate minerals such as calcite and dolomite (Varrica et al., 2019; Russell, 2003). Among the analyzed samples, AR3-25-2 exhibited the strongest mineral signature, evidenced by the higher intensity of silicate- and carbonate-related bands, whereas AR1-25-2 and AR2-25-1 showed a relatively

greater contribution of organic compounds and secondary aerosols associated with anthropogenic activities (Mohandoss et al., 2025; Gupta et al., 2024; Mahmud et al., 2024; Romano et al., 2022). These findings are consistent with the gravimetrically determined PM10 concentrations and the characteristics of the monitoring sites summarized in Table5.

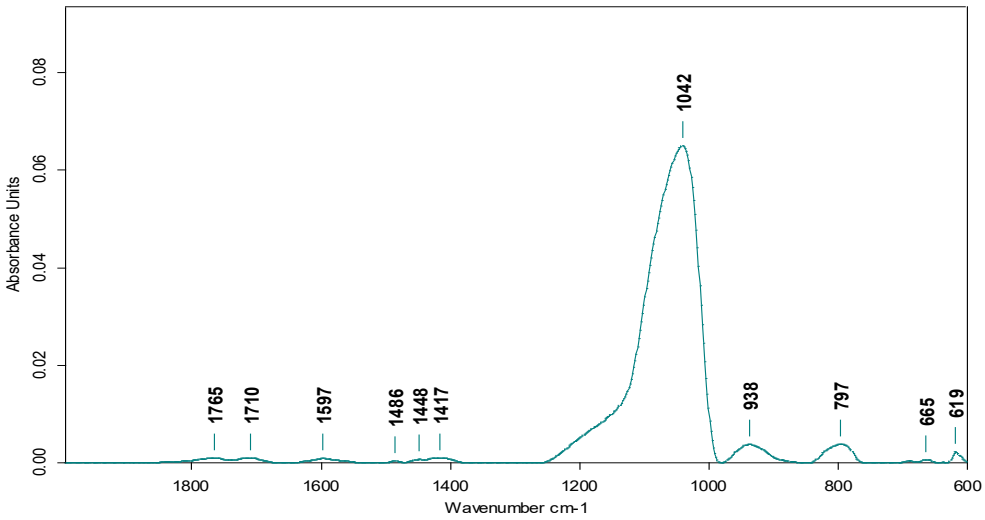

Figure 6. FTIR-ATR spectrum of sample **AR2-25-2 (PM2.5)**

Table 6. Vibrational assignment of FTIR-ATR bands, sample **AR2-25-2 (PM2.5)**

Wavenumber (cm^{-1})	**Vibrational assignment**	**Probable compounds**	**Ref.**
~1640–1650	δ(H–O–H), ν(C=C)	Adsorbed water, oxidized organic compounds, aromatic structures	(Coury and Dillner, 2008; Gupta et al., 2024; Mahmud et al., 2024; Maria et al., 2002; Mohandoss et al., 2025; Radulescu et al., 2017; Russell, 2003; Shankar et al., 2022; Varrica et al., 2019)
~1570–1550	ν(NO_3^-), ν(C=C) aromatic	Secondary nitrates and aromatic compounds	
~1530	ν (NO_3^-)	Inorganic nitrates and secondary aerosols	
~1460–1450	$\nu_s(CO_3^{2-})$, δ(CH_2)	Carbonates (calcite, dolomite) and organic matter	
~1420	$\nu_{as}(CO_3^{2-})$	Carbonates and carbonate compounds of mineral origin	
~1000–1010	ν(Si–O–Si), ν(Si–O)	Quartz, silicates, aluminosilicates	
~940	ν(Si–OH)	Hydrated silicates and clays	
~835	δ(Si–O)	Quartz and crystalline silicates	
~795–780	ν(Si–O)	Quartz (α-quartz)	
~620–610	δ(Si–O), Al–O–Si	Aluminosilicates and clays	

The FTIR-ATR spectrum of sample AR2-25-2 (PM2.5) is dominated by a very intense absorption band at approximately 1000–1010 cm^{-1}, attributed to Si–O–Si and Si–O stretching vibrations characteristic of silicates, aluminosilicates, and other crustal mineral particles (Varrica et al., 2019; Coury and Dillner, 2008). The high intensity of this band indicates a substantial contribution of mineral material, likely associated with soil dust resuspension and mineral aerosol transport. Several low-intensity bands observed in the 1650–1400 cm^{-1} region are assigned to oxygenated organic compounds, carbonyl groups, and secondary inorganic species such as nitrates and carbonates (Shankar et al., 2022; Mohandoss et al., 2025; Varrica et al., 2019; Gupta et al., 2024; Radulescu et al., 2017; Mahmud et al., 2024; Maria et al., 2002; Russell, 2003). Additional bands in the 800–600 cm^{-1} range further confirm the presence of quartz and aluminosilicates (Mohandoss et al., 2025; Varrica et al., 2019; Gupta et al., 2024; Mahmud et al., 2024; Coury and Dillner, 2008).

The spectra of AR2-25-1 (PM10) and AR2-25-2 (PM2.5) display a similar mineral-dominated profile, suggesting common sources of atmospheric particles at the AR2 station. However, the PM10 sample exhibits more pronounced bands associated with organic compounds and secondary aerosols, particularly at 1742, 1651, 1549, and 1531 cm^{-1}, indicating a more complex chemical composition. In contrast, the PM2.5 fraction is dominated by silicate-rich mineral particles. A similar pattern was reported by Radulescu et al. (Radulescu et al., 2017) for PM2.5 samples collected in Târgoviște.

The comparative analysis of the FTIR-ATR spectra of PM10 samples collected during the cold and warm seasons at the AR1, AR2, and AR3 monitoring stations revealed clear seasonal differences in aerosol composition (Figs. 7–9, Table 7). Samples collected during the cold season showed more pronounced bands associated with carbonyl compounds, nitrates, and secondary aerosols, reflecting the influence of combustion-related emissions and atmospheric conditions favorable to pollutant accumulation. In contrast, warm-season samples were characterized by stronger silicate- and carbonate-related bands, indicating an increased contribution of mineral particles derived from soil dust resuspension and regional dust transport.

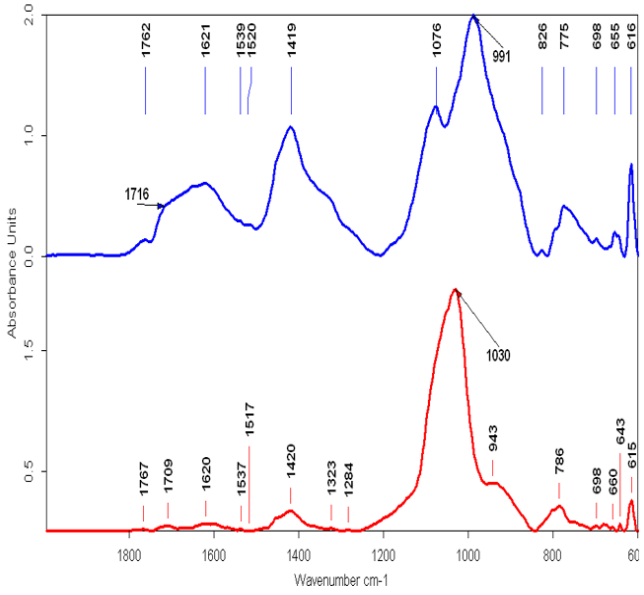

Figure 7. FTIR-ATR spectra of samples collected at AR1 station in different seasons: (____)AR1-25-1- cold season; (____)AR1-25-3 – warm season

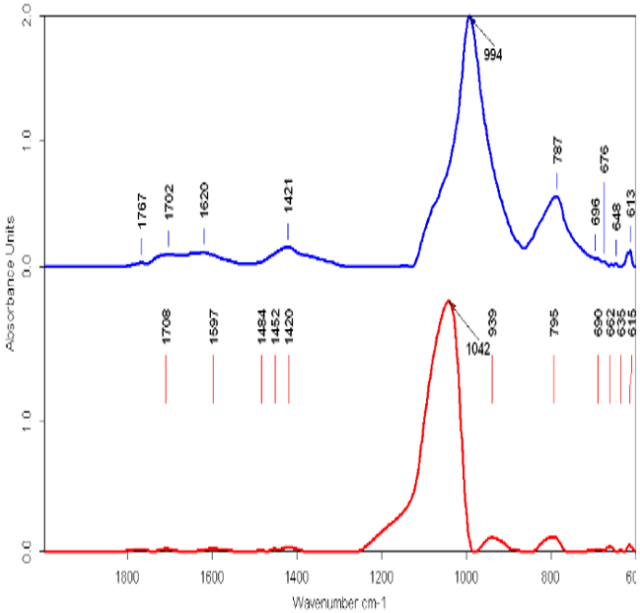

Figure 8. FTIR-ATR spectra of samples collected at AR2 station in different seasons: (____) AR2-25-1 - cold season; (____) AR2-25-3 - warm season

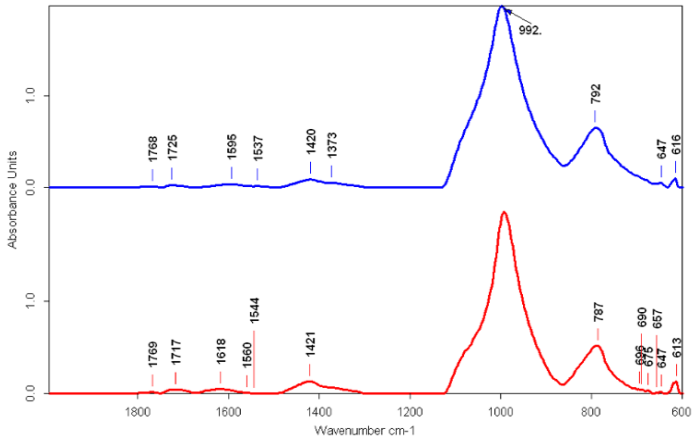

Figure 9. FTIR-ATR spectra of samples collected at AR3 station in different seasons: (____) AR3-25-1- cold season; (____) AR3-25-3 - warm season

Table 7. Comparison between stations

Feature	AR1	AR2	AR3
Difference between Cold Season and Warm Season	High	Very high	Moderate
Organic signature in the cold season	Pronounced	Pronounced	Moderate
Nitrates/secondary aerosols in the cold season	Highlights	Highlights	Highlights
Carbonates in the warm season	Moderate	Moderate	Pronounce
Silicate-mineral component in the warm season	High	Very high	Very high
Annual crustal influence	Moderate	High	Very high

Among the three monitoring stations, AR2 exhibited the greatest seasonal variability, shifting from a relatively complex aerosol composition during the cold season to a profile dominated by mineral particles during the warm season. AR1 showed a stronger influence of anthropogenic sources in the cold season, consistent with the urban and industrial characteristics of the site. In contrast, AR3 maintained the most persistent mineral signature throughout the year, indicating a continuous contribution of crustal particles and resuspended dust associated with both traffic-related and natural sources.

The Saharan dust intrusion events identified in 2018 and 2025 significantly affected air quality in the municipality of Arad, leading to elevated PM10 concentrations and an increased contribution of crustal mineral particles, as shown in Table 3. The FTIR-ATR spectra recorded during the Saharan dust intrusion events (Figs. 10 and 11) exhibited a more pronounced mineral signature than those obtained under normal atmospheric conditions. A comparison of the FTIR-ATR spectra of samples AR1-18-PS and AR1-18-1 presented in Fig. 10 reveals a broadly similar spectral fingerprint dominated by absorption bands characteristic of silicate compounds, while also exhibiting notable differences in the intensity and distribution of specific spectral features. The sample collected during the Saharan dust event (AR1-18-PS) was distinguished from the non-Saharan sample (AR1-18-1) by the presence of a distinct absorption band at approximately 1143 cm^{-1} and a pronounced enhancement of the band at 1624 cm^{-1}. The absorption band observed at 1143 cm^{-1} is associated with Si–O stretching vibrations in aluminosilicate minerals, including illite, smectite, and palygorskite, which are characteristic constituents of Saharan dust originating from Algeria, Tunisia, and Morocco (Caquineau et al.2002, Formenti et al.2011). The band at 1624 cm^{-1} is attributed to hydrated clay minerals and water adsorbed onto their surfaces (Varrica et al., 2019). In addition, the spectra exhibit a distinct absorption band at approximately 1423 cm^{-1}, assigned to carbonate minerals such as calcite and dolomite, which are frequently reported in association with illite, smectite, and palygorskite in Saharan dustransported from North Africa (Varrica et al., 2019.. The occurrence of these mineralogical markers confirms the significant contribution of long-

range transported Saharan aerosols to the PM10 composition. Similar spectral behavior during Saharan dust intrusion events was reported by Varrica et al. (Varrica et al., 2019) for atmospheric particulate matter collected in Palermo.

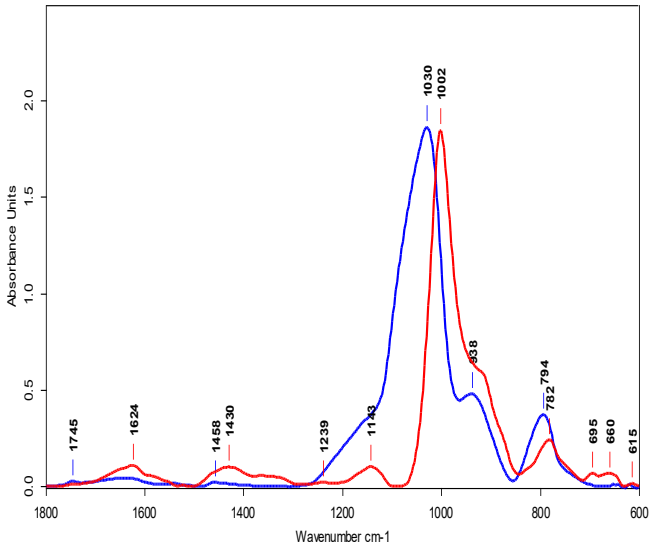

Figure 10. Comparative FTIR-ATR spectra for PM10 samples taken at the AR1 station in 2018 during an intense Saharan dust episode: (___) **AR1-18-PS**; during the normal period (___) **AR1-18-1**

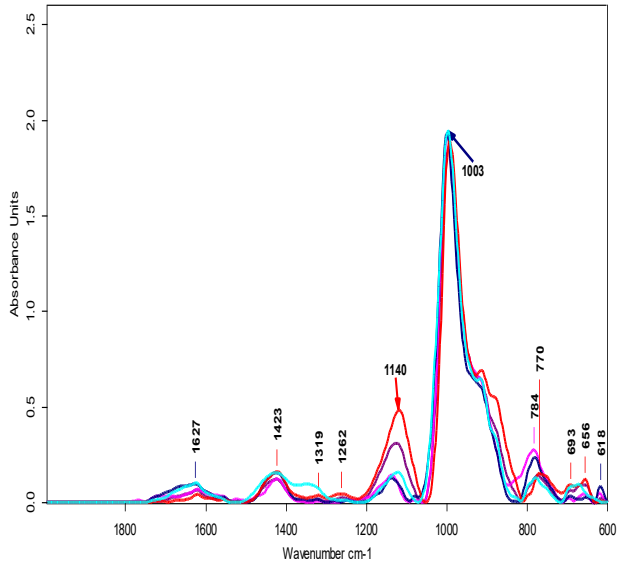

Figure 11. FTIR-ATR spectra for PM10 samples taken during periods of Saharan dust: (___) **AR3-18-PS,** (___) **AR3-25-PS**, (___) **AR1-25-PS**, (___) **AR2-25-PS**, (___) **AR2-18-PS**

Figure 11 shows a consistent FTIR-ATR spectral fingerprint for PM10 samples collected during the Saharan dust events of 2018 and 2025. All spectra are dominated by mineral absorption bands associated with silicates, aluminosilicates, and carbonates, confirming the influence of Saharan mineral aerosols on PM10 composition in Arad County.

Among the investigated sites, AR3 exhibited the highest intensity of the 1140 cm^{-1} band during both Saharan dust events, consistent with the highest PM10 concentrations recorded at this station (72 $\mu g/m^3$ in 2018 and 68 $\mu g/m^3$ in 2025; Table 3.). These results indicate a stronger impact of long-range transported Saharan dust at the AR3 site.

Limitations

This study is based exclusively on FTIR-ATR spectroscopy; therefore, mineral phases such as illite, smectite, palygorskite, calcite, and dolomite were identified from characteristic absorption bands and literature correlations only. These assignments were not independently verified by complementary techniques such as XRD, SEM-EDS, or ICP-MS. Future studies combining FTIR-ATR with these methods would provide a more reliable mineralogical and chemical characterization of atmospheric particulate matter.

CONCLUSIONS

PM10 and PM2.5 samples collected at three representative sites in Arad County were successfully characterized using FTIR-ATR spectroscopy, demonstrating the applicability of this technique for the rapid identification of major chemical components and potential aerosol sources. FTIR-ATR analysis identified characteristic absorption bands attributed to O–H, C–H, C=O, NO_3^-, CO_3^{2-}, SO_4^{2-}, and Si–O functional groups, indicating the presence of both natural and anthropogenic aerosol constituents.

The analyzed particulate matter consisted of a complex mixture of natural and anthropogenic components. The natural fraction was dominated by silicates, aluminosilicates, quartz, hydrated clay minerals, and carbonates, whereas the anthropogenic fraction included carbonaceous compounds, aliphatic and aromatic hydrocarbons, carbonyl compounds, and secondary aerosols such as nitrates and sulfates. Seasonal variations were evident,

with a greater contribution of combustion-related compounds during the cold season and enhanced mineral signatures during the warm season.

Site-specific differences reflected the influence of local emission sources. The AR1 station was predominantly affected by traffic and industrial activities, resulting in a stronger contribution of carbonaceous compounds and secondary aerosols. The AR2 site exhibited characteristics typical of an urban background environment, while the AR3 station showed a greater influence of mineral particles, indicating a stronger contribution of crustal material and Saharian dust.

Saharan dust events significantly influenced both PM10 concentrations and aerosol composition, as evidenced by the enhanced FTIR-ATR absorption bands associated with aluminosilicates, carbonates, and hydrated clay minerals. The occurrence of characteristic absorption bands consistent with illite, smectite, palygorskite (1140 cm^{-1}), calcite, and dolomite (1423 cm^{-1}) suggests the contribution of long-range transported Saharan dust from North Africa. However, these mineral phase assignments are inferred from FTIR-ATR band positions and were not independently confirmed by XRD, SEM-EDS, or ICP-MS analyses. Overall, the results highlight the combined effects of local anthropogenic emissions, seasonal variability, and long-range atmospheric transport on particulate matter composition in Arad County. FTIR-ATR spectroscopy proved to be a valuable tool for identifying the major chemical constituents of atmospheric particles and assessing the impact of Saharan dust intrusions on regional air quality.

REFERENCES

Amato, F. (Ed.), 2018. Non-Exhaust Emissions: An Urban Air Quality Problem for Public Health. Academic Press.

Basart, S., Rémy, S., Mona, L., Cornacchia, C., Benincasa, F., Karanikolas, A., Pey, J., Querol, X., 2023. Saharan dust outbreaks over Europe: Atmospheric transport, impacts on air quality and recent trends. Atmospheric Environment 301, 119690. https://doi.org/10.1016/j.atmosenv.2023.119690

Caquineau, S., Gaudichet, A., Gomes, L., Legrand, M., Papineau, F,. 2002. Mineralogy of Saharan dust transported over northwestern tropical Atlantic Ocean in relation to source regions. Journal of Geophysical Research: Atmospheres, 107(D15), 4251. https://doi.org/10.1029/2000JD000247

Coury, C., Dillner, A.M., 2008. ATR-FTIR characterization of ambient aerosol samples. Atmospheric Environment 42(23), 5923–5932. https://doi.org/10.1016/j.atmosenv.2008.03.026

European Environment Agency (EEA), 2024. Air Quality in Europe – 2024 Report. Publications Office of the European Union, Luxembourg.

European Environment Agency (EEA), 2024. Europe's Air Quality Status 2024. European Environment Agency, Copenhagen.

European Environment Agency (EEA), 2025. Particulate Matter – PM10. Air Quality Status Report 2025. European Environment Agency, Copenhagen. https:///www.eea.europa.eu/en/analysis/publications/air-quality-status-report-2025/particulate-matter

Formenti, P., Schütz, L., Balkanski, Y., Desboeufs, K., Ebert, M., Kandler, K., Petzold, A., Scheuvens, D., Weinbruch, S., & Zhang, D., 2011. Recent progress in understanding physical and chemical properties of African and Asian mineral dust. Atmospheric Chemistry and Physics, 11, 8231–8256. https://doi.org/10.5194/acp-11-8231-2011

Gkikas, A., Proestakis, E., Amiridis, V., Kazadzis, S., Koukouli, M.E., Tsekeri, A., Mihalopoulos, N., 2021. Modelling and assessment of desert dust episodes in the Mediterranean Basin and Europe. Atmospheric Chemistry and Physics 21(10), 7915–7938. https://doi.org/10.5194/acp-21-7915-2021

Gupta, S., Shankar, S., Kuniyal, J.C., et al., 2024. Identification of sources of coarse mode aerosol particles (PM10) using ATR-FTIR and SEM-EDX spectroscopy over the Himalayan Region of India. Environmental Science and

Pollution Research 31, 15788–15808. https://doi.org/10.1007/s11356-024-31973-3
Hamanaka, R.B., Mutlu, G.M., 2025. Particulate matter air pollution: Effects on the respiratory system. Journal of Clinical Investigation 135(19). https://doi.org/10.1172/JCI190560
Harrison, R.M., Hester, R.E. (Eds.), 2009. Air Quality in Urban Environments. Royal Society of Chemistry.
Mahmud, M., Mohiuddin, K.A.B., et al., 2024. Micro-characterization of indoor deposited particles using FTIR, SEM-EDS, and XRD techniques: A case study of a university campus, Bangladesh. Aerosol and Air Quality Research 24, 230236. https://doi.org/10.4209/aaqr.230236
Maria, S.F., Russell, L.M., Turpin, B.J., Porcja, R.J., 2002. FTIR measurements of functional groups and organic mass in aerosol samples. Atmospheric Environment 36(33), 5185–5196. https://doi.org/10.1016/S1352-2310(02)00627-4
Mohandoss, R., Jain, C.D., Madhavan, B.L., Madineni, V.R., 2025. Spectroscopic and chemical compositional analysis of the atmospheric aerosols in urban and rural tropical environment of southern India. Atmospheric Environment, 121431. https://doi.org/10.1016/j.atmosenv.2025.121431
Ofremu, G.O., et al., 2025. Exploring the relationship between climate change, air pollutants, and human health: A review. Environmental Challenges 18, 101086. https://doi.org/10.1016/j.envc.2024.101086
Querol, X., Pey, J., Pandolfi, M., Alastuey, A., Cusack, M., Pérez, N., Moreno, T., Mihalopoulos, N., 2009. African dust contributions to mean ambient PM10 mass levels across the Mediterranean Basin. Atmospheric Environment 43(28), 4266–4277. https://doi.org/10.1016/j.atmosenv.2009.06.013
Radulescu, C., Stihi, C., Iordache, S., Dunea, D., Dulama, I.D., 2017. Characterization of urban atmospheric PM2.5 by ATR-FTIR, ICP-MS and SEM-EDS techniques. Revista de Chimie 68(4), 805–810. https://doi.org/10.37358/RC.17.4.5557
Rodríguez, S., López-Darias, J., et al., 2024. Extreme Saharan dust events expand northward over the Atlantic and Europe, prompting record-breaking PM10 and PM2.5 episodes. Atmospheric Chemistry and Physics 24, 12031–12053. https://doi.org/10.5194/acp-24-12031-2024
Russell, L.M., 2003. Aerosol organic-mass-to-organic-carbon ratio measurements by FTIR spectroscopy. Aerosol Science and Technology 37(10), 819–828. https://doi.org/10.1080/02786820300941
Seinfeld, J.H., Pandis, S.N., 2016. Atmospheric Chemistry and Physics: From Air Pollution to Climate Change, 3rd ed. John Wiley & Sons.
Shankar, S., Gadi, R., Sharma, S.K., Mandal, T.K., 2022. Identification of carbonaceous species and FTIR profiling of PM2.5 aerosols for source estimation in Old Delhi region of India. MAPAN 37(1–3), 1–16. https://doi.org/10.1007/s12647-022-00575-0
Taha, S.S., et al., 2025. Comprehensive review of health impacts of the exposure to air pollutants: Carbon dioxide, nitrogen oxides and particulate matter. Results in Engineering, 100182. https://doi.org/10.1016/j.rineng.2025.100182
Varga, G., 2023. Increasing frequency and changing nature of Saharan dust storm events in Europe. Hungarian Geographical Bulletin 72(4), 335–352. https://doi.org/10.15201/hungeobull.72.4.2
Varrica, D., Tamburo, E., Vultaggio, M., Di Carlo, I., 2019. ATR-FTIR spectral analysis and soluble components of PM10 and PM2.5 particulate matter over the urban area of Palermo (Italy) during normal days and Saharan events. International Journal of Environmental Research and Public Health 16(14), 2507. https://doi.org/10.3390/ijerph16142507
Velásquez-García, M.P., Loria-Salazar, S.M., Alvarez-Ospina, H., 2024. Long-range transport of air pollutants increases the impact of PM2.5 on population exposure and health. Atmospheric Chemistry and Physics 24, 11497–11518. https://doi.org/10.5194/acp-24-11497-2024
World Health Organization (WHO), 2024. Ambient (outdoor) air pollution. Fact sheet.

https:///www.who.int/news-room/fact-sheets/detail/ambient-%28outdoor%29-air-quality-and-health
World Health Organization (WHO), 2025. Air pollution. https://www.who.int/health-topics/air-pollution

ACKNOWLEDGEMENTS
The authors gratefully acknowledge the Arad County Environmental Directorate (DJM Arad) for providing the PM filter samples investigated in this study.

ISSN 1582-1021
e-ISSN 2668-4764
Edited by "Aurel Vlaicu" University Publishing House, Arad, Romania

doi:10.62591/Scien.Tech.Bull-Chem.FoodSci.Eng.2024.21.01

Scien. Tech. Bull-Chem. Food Sci. Eng., Vol. 22(XXIII), 2025, 18-26
doi: 10.62591/Scien.Tech.Bull-Chem.FoodSci.Eng.2025.22.02

Article

SYNTHESIS AND CHARACTERISATION OF A NOVEL PHENANTHROLINE-BASED LIGAND FUNCTIONALIZED WITH AMPHIPILIC GROUPS AND ITS LUMINESCENT Zn(II) COMPLEX

Raluca DANCIAR[1], Evelyn POPA[1], Adelina-Antonia ANDELESCU[1*], Truong Ngoc HUNG[2], Elisabeta I. SZERB[1]

[1] "Coriolan Drăgulescu" Institute of Chemistry, Romanian Academy, 24 Mihai Viteazu Blvd., 300223 Timisoara, Romania
[2]Institute of Chemistry, Vietnam Academy of Science and Technology, 18 Hoang Quoc Viet Str., Nghia Do Ward, Hanoi, Vietnam
Corresponding author email: andelescu.ade@gmail.com

Abstract: *The present paper reports the synthesis of a new phenanthroline-based ligand (phenIm_1) and its Zn(II) coordination compound (phenIm_Zn). Their chemical structure was determined by a combination of FT-IR and NMR spectroscopy, while their purity was confirmed by elemental analysis. Their photophysical properties were investigated in freshly prepared dichloromethane solutions.*

Keywords: heterocycles; N-donor ligand; hydrophilic ligand; coordination compounds

INTRODUCTION

Since antiquity, metals have been used to treat various infectious and chronic conditions, especially when plant-based remedies were not efficient (Abdallah *et al.* 2022, Ma *et al.* 2020). Although conventionally most of the synthetic drugs were based initially on organic molecules, the discovery of *cis*-platin anticancer properties by Rosenberg (Rosenberg et al. 1965, Rosenberg et al. 1969) shifted the researchers focus on the design of new drugs based on *d*-block metal complexes (*d*-MCs). Nowadays, *d*-MCs are currently finding applications in biomedical fields as advanced drugs (Arun *et al.* 2025, Sodhi and Paul 2019, Zhang and Sadler 2017), while specific properties deriving from the metal centre like luminescence are relevant for applications in different fields like photodynamic therapy, sensing and imaging (Monro *et al.* 2019, Mari *et al.* 2015). While *d*-MCs are known for excellent therapeutic and luminescence efficiencies, several limitations like the poor solubility, lack of targeted and local delivery still need to be overcome (Zhuo *et al.* 2024, Sanz Mendiguchia *et al.* 2013).

Varying the ligand structure and its functionalisation is a key strategy for enhancing the solubility and, consequently, the bioavailability of *d*-MCs (Wani *et al.* 2016). It has been demonstrated that neutral lipophilic *d*-MCs can passively diffuse through the lipid bilayer of biological membranes (Zhao *et al.* 2016).

Nowadays, non-platinum metallodrugs containing 3*d* metals like Cu and Zn are being investigated because of their biocompatibility and because they exhibit favourable toxicity profiles alongside potent DNA-binding, cleavage, and cytotoxic responses under physiological conditions (Khursheed *et al.* 2022). Among the biocompatible metals, zinc serves a wide range of essential biochemical and physiological functions, playing critical catalytic, structural, and regulatory roles in biological systems (Roohani *et al.* 2013), therefore making it a promising metal centre ion in medicinal bio-inorganic chemistry (Yoshikawa and Yasui 2012).

Due to their low toxicity and minimal side effects, Zn(II) complexes are widely investigated as DNA-binding agents, tumour photosensitizers, and antimicrobial therapeutics (Porchia et al. 2020). Moreover, N-donor ligands are the key structural components in

biologically active Zn(II) complexes (Porchia *et al.* 2020).

Therefore, in this present paper, we report the synthesis and characterization of a new ligand functionalized with amphiphilic chains, phenIm_1 (2-(3,4-bis(2-ethoxyethoxy)phenyl)-3b,7a-dihydro-1H-imidazo[4,5-f][1,10]phenanthroline) obtained by the reaction of 1,10-phenanthroline-5,6-dione with a functionalized aromatic aldehyde and ammonium acetate (See experimental section) and its zinc coordination compound (*phenIm_Zn*, **Figure 1**).

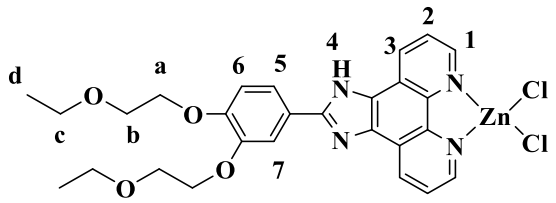

phenIm_Zn

Figure 1. The proposed chemical structure of *phenIm_Zn* and the proton labelling.

The structure of the intermediates and the phenanthroline derivative (*phenIm_1*) were assessed by No-D ^{1}H-NMR spectroscopy, whereas the purity of the *phenIm_1* ligand was confirmed by elemental analysis. The *phenIm_Zn*, complex was characterized by FT-IR, ^{1}H-NMR and ^{13}C-NMR spectroscopies. Moreover, the photophysical properties were investigated for the phenanthroline ligand and its corresponding zinc complex.

MATERIALS AND METHODS

All commercially available starting materials were used as received without further purification: 2-ethoxyethan-1-ol, 4-methylbenzenesulfonyl chloride (p-TsCl), 3,4-dihydroxybenzaldehyde, 1,10-phenanthroline hydrate (phen), $ZnCl_2$, $KBrO_3$, K_2CO_3, CH_3COONH_4, were purchased from Sigma Aldrich. NaOH, Na_2SO_4, H_2SO_4, Na_2CO_3, CH_3COOH were from Chimreactiv. The solvents used for the current study were: *N,N*-Dimethylformamide (DMF), ethyl acetate (AcOEt), tetrahydrofuran (THF), diethyl ether (Et_2O), dichloromethane (DCM), acetonitrile (AcN) and were purchased from Honeywell.

Infrared spectra (KBr pellets) were recorded in the range 4000-400 cm^{-1} on a Cary 630 FT-IR spectrophotometer.

The formation of the ligand and the intermediates was assessed on a Fourier 80 MHz benchtop by Bruker using No-Deuterium Proton-NMR in DCM (CH_2Cl_2) as solvent, by solvent suppression technique.

For the zinc complex, the ^{1}H-NMR and ^{13}C-NMR spectra were recorded on Bruker Avance III HD – 500 MHz spectrometer in DMSO-d_6.

In order to confirm the purity of the samples, elemental analyses (C, H, N) were employed on an Elementar UNICUBE CHNS analyser with helium as the carrier gas.

Molar electrical conductivity was measured with a Mettler Toledo FiveEasy plus (FP30) conductivity meter equipped with a Lab conductivity sensor LE740.

Spectrofluorimetric grade DCM from VWR was used for photophysical investigations in the solution without further purification.

Absorption spectra were recorded using an Agilent Cary 60 spectrophotometer. Emission spectra were recorded on a Perkin Elmer LS 55 fluorimeter. For all measurements quartz cuvettes of a 1 cm path length were used.

The luminescence quantum yields of the samples (*phenIm_1* and *phenIm_Zn*) in solution were determined by the optical dilution method (Demas and Crosby 1971) using 2 - aminopyridine in DCM solution as a reference standard ($\Phi = 0.33$, Rusakowicz and Testa 1968) for the ligand, and $[Ru(bpy)_3]^{2+}$ in water ($\Phi = 0.04$, Suzuki et al. 2009) for the zinc complex.

Absorbance values used for quantum-yield measurements are 0.157 for Zn complex and for the ligand 0.140. The slits used for both excitation and emission were 4 nm and 4 nm, respectively speed of acquisition is 100nm/min. Integration ranges for ligand were 350 – 680 nm and for Zn complex 320 – 580 nm, nr of cycles

is 1. The refractive indexes for DCM is 1.4240, and for water is 1.3325.

EXPERIMENTAL SECTION

Synthesis of 2-ethoxyethyl 4-methylbenzenesulfonate, ***1***

Compound 1 was obtained following a reported procedure for similar derivatives (Zhang *et al.* 2022):

2-ethoxyethan-1-ol (2g, 0.0222 mol) was added over 10 mL NaOH (1.62 g, 0.0406 mol) solution in THF/H_2O (V/V=1/1), cooled on an ice bath under inert atmosphere. The mixture was stirred for 15 min, then 10 mL of THF solution containing 4-methylbenzenesulfonyl chloride (4.23 g, 0.0222 mol) was added dropwise. The reaction mixture was allowed to reach room temperature, and stirred for 2 hours. Then THF was evaporated under reduced pressure and the aqueos phase was extracted with 50 mL Et_2O (3x), the combined organic phase was dried over anhydrous Na_2SO_4, filtered and taken to dryness, to yield **1** as a colourless liquid. The compound was characterized by No-D NMR spectroscopy.

(1): colourless liquid (3.7 g, 0.01514 mol, η=68%).

No-D ^{1}H-NMR (80 MHz, CH_2Cl_2) δ-ppm 7.83 (d, *J* = 7.9 Hz, 2H), 7.41 (d, *J* = 8.0 Hz, 2H), 4.40 – 3.94 (m, 4H), 3.85 – 3.21 (m, 4H), 2.49 (s, 3H), 1.16 (t, *J* = 6.9 Hz, 3H).

Synthesis of 3,4-bis(2-ethoxyethoxy)benzaldehyde, ***2***

Compound 2 was obtained following a Williamson ether synthesis procedure (Percec *et al.* 2009):

0.514 g of 3,4-dihydroxybenzaldehyde (0.00372 mol) and 2.26 g of K_2CO_3 (0.01634 mol) in 25 mL of DMF were added to a 100 mL single neck round-bottom flask; the reaction mixture was then stirred at 60°C for approximately 30 minutes, then compound 1 (2 g, 0.008186 mol) dissolved in DMF was added. The temperature was raised to 80°C, and the reaction mixture is kept under stirring for 24 hours. Following, the reaction mixture was cooled to room temperature, filtered through Celite and washed thoroughly with DCM; the mother liquor was then taken to dryness using a rotary evaporator. The residue was dissolved in DCM and washed with brine. The organic phase was then dried over anhydrous sodium sulfate and evaporated to dryness on a rotary evaporator. The pure compound was obtained by column chromatography (SiO_2; Hexane:Ethyl acetate = 7:4).

(2): colorless oil (0.652 g, 0.002310 mol, 62.1%)

The compound was characterized through No-D NMR.

No-D ^{1}H-NMR (80 MHz, CH_2Cl_2) δ-ppm: 9.84 (s, 1H), 7.47 (overlapped peaks, 2H), 7.22 – 6.84 (m, 1H), 4.24 – 3.92 (m, 4H), 3.90 – 3.73 (m, 4H), 3.69 – 3.36 (m, 4H), 1.23 (t, *J* = 7.0 Hz, 6H).

Synthesis of 1,10-phenanthroline-5,6-dione, ***3***

1,10-phenanthroline-5,6-dione was obtained following a reported procedure (Zheng *et al.* 2010):

10 g of 1,10-phenanthroline hydrate (0.0505 mol) was added to a solution of 32 mL H_2SO_4 60%, cooled on an ice bath, then $KBrO_3$ (11 g, 0.0658 mol) was added in portions avoiding the rise of temperature above 20°C. After the addition of $KBrO_3$ the reaction mixture was stirred at room temperature overnight, then, the mixture was poured over ice and was carefully neutralized to pH= 5.5 using a saturated solution of sodium carbonate (Na_2CO_3). The formed precipitate was filtered out and the mother liquor was extracted with 100 mL DCM (2x). The combined organic layer was washed with H_2O, dried over anhydrous Na_2SO_4, filtered and taken to dryness. 1,10-phenanthroline-5,6-dione was isolated after recrystallizations from hot EtOH as a yellow powder (2 g, 0.00952 mol, η=18.9 %). The compound was characterized through ^{1}H-NMR NMR.

^{1}H-NMR (80 MHz, DMSO-d_6) δ-ppm: 8.99 (dd, *J* = 4.7, 1.8 Hz, 2H), 8.39 (dd, *J* = 7.8, 1.8 Hz, 2H), 7.67 (dd, *J* = 7.8, 4.7 Hz, 2H).

Synthesis of 2-(3,4-bis(2-ethoxyethoxy)phenyl)-3b,7a-dihydro-1H-imidazo[4,5-f][1,10]phenanthroline, phenIm_1

The ligand was obtained adapting a procedure reported for similar phenanthroline-imidazole compounds (Cardinaels *et al.* 2005)

0.310 g of 1,10-phenanthroline-5,6-dione (compound **3**, 0.001475 mol) and 0.909 g of ammonium acetate (0.0118 mol) were added to

a single neck 100 mL round-bottom flask containing 40 mL of glacial acetic acid, and the reaction mixture was brought to reflux. Initially, the dione (**3**) did not appear to dissolve completely, but upon reaching 100°C, it formed a clear, yellow solution. Once the reaction mixture reached 100°C and the dione was fully dissolved, the aldehyde (**2**, 0.500 g, 0.00177 mol) dissolved in 15 mL of warm acetic acid was added dropwise to the reaction mixture. The pale orange reaction mixture was stirred overnight at 125°C. Following, the reaction mixture was cooled to room temperature and poured into a large Berzelius flask containing ice; the pH was adjusted to 7 with ammonia solution and then extracted with DCM (4x). The organic layer was dried over anhydrous Na_2SO_4, filtered and concentrated under reduced pressure. The final product was recrystallized by DCM/Et_2O, and isolated as a pale orange powder. The compound was characterized by FT-IR and No-D NMR spectroscopy and its purity was confirmed by elemental analysis.

(*phenIm_1*): pale orange powder (0.389 g, 0.000820 mol, η=56%).

FT-IR (KBr, cm^{-1}): 2969, 2934, 2869 ν(C-H);1 607, 1559 (ν (C=C)), (ν (C=N)); 1123 ν(C-O-C);

No-D ^{1}H-NMR (80 MHz, CH_2Cl_2) δ-ppm: 9.56 – 8.36 (broad, 4H), 7.88 (d, J = 9.9 Hz, 2H), 7.34 (broad, 2H), 6.81 (d, J = 7.9 Hz, 1H), 4.14 – 3.93 (m, 8H), 3.44 (ddt, J = 17.7, 13.9, 6.3 Hz, 8H), 1.09 (dt, J = 8.8, 6.9 Hz, 6H, Hd).

Anal. Calcd. for $C_{27}H_{30}N_4O_4$ (474.561 g·mol^{-1}): C, 68.34; H, 6.37; N, 11.81%. Found: C, 68.81; H, 6.08; N, 12.27%

Synthesis of phenIm_Zn

A clear solution of $ZnCl_2$ (0.129 g, 0.0009523 mol) in 10 mL of MeOH was added to an orange solution of *phenIm_1* (0.300 g, 0.0006349 mol) in 25 mL of MeOH. The resulting orange reaction mixture was stirred at room temperature for 4 hours. Following, the solvent was evaporated and the pure produce was obtained after precipitation from DCM/Et_2O, followed by filtration and washings with small volumes of Et_2O and AcOEt.

(*phenIm_Zn*): pale yellow solid (0.290 g, 0.000476 mmol, 75%)

FT-IR (KBr, cm^{-1}): 2969, 2934, 2869 ν(C-H); 1607, 1581 (ν (C=C)) and (ν (C=N)); 1123 ν(C-O-C); 427 ν(Zn-N)

^{1}H NMR (500 MHz, DMSO-d_6) δ: 14.00 (s, 1H, H^4), 9.16 (d, J = 33.3 Hz, 2H, H^1), 8.77 (broad, 2H, H^3), 8.04 (broad, 2H, H^2), 7.86 (d, J = 30.8 Hz, 2H, H^5,H^7), 7.18 (d, J = 7.9 Hz, 1H, H^6), 4.22 (dt, J = 35.1, 4.0 Hz, 4H, H^a), 3.76 (dt, J = 17.9, 4.7 Hz, 4H, H^b), 3.55 (dq, J = 10.6, 7.0 Hz, 4H, H^c), 1.15 (td, J = 6.9, 5.3 Hz, 6H, H^d).

^{13}C NMR (126 MHz, DMSO-d_6) δ 152.30, 150.72 148.93, 133.49, 125.90, 125.75, 120.53, 114.30, 112.74, 69.18, 68.88, 68.78, 66.28, 40.56, 40.39, 40.22, 40.06, 39.89, 15.61, 15.59.

Anal. Calcd. for $C_{27}H_{30}Cl_2N_4O_4Zn$ (610.841 g·mol^{-1}): C, 53.09; H, 4.95; N, 9.17%. Found: C, 53.68; H, 4.80; N, 9.28%

RESULTS AND DISCUSSIONS

To induce solubility in polar solvents for the targeted complex we have designed a 2-phenylimidazo [4,5-*f*],[1,10]phenanthroline (phenIm_1) ligand functionalized with ethoxyethoxy chains as depicted in the reaction **Scheme 1**.

In order to obtain the phenanthroline derivative *phenIm_1*, firstly we isolated 3,4-bis(2-ethoxyethoxy)benzaldehyde (compound 2 in Scheme 1) in two steps. First, we converted the hydroxyl group of ethoxyethanol to a tosylate. Then, a Williamson etherification reaction between the isolated tosylate and 3,4-dihydroxybenzaldehyde was carried out (Percec *et al.* 2009). 1,10-phenanthroline-5,6-dione (compound **3**) was obtained under mild reaction conditions at r.t. from 1,10-phenanthroline hydrate using potassium bromate ($KBrO_3$) and 60% sulfuric acid (H_2SO_4) as oxidant, according to a published procedure (Zheng *et al.* 2010).

Then, the *phenIm_1* ligand was obtained through a Debus-Radziszewski reaction in a single step from three components: compound 2, compound 3 and CH_3COONH_4 in acetic acid (Cardinaels *et al.* 2005).

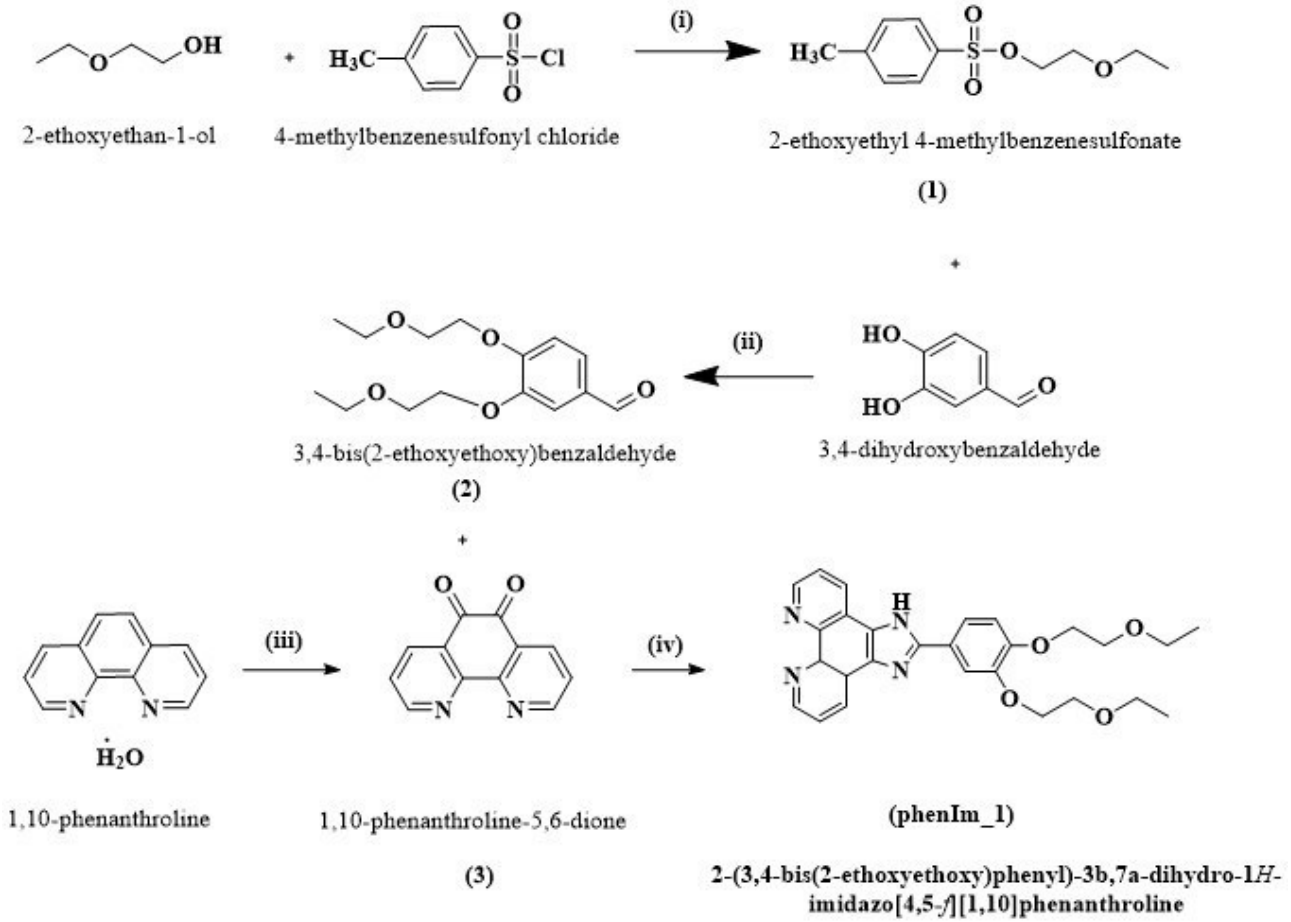

Scheme 1. Reaction pathway for the synthesis of *phenIm_1*. Reagents and conditions: (i) NaOH, THF/H_2O, r.t, 2h, inert atmosphere; (ii) K_2CO_3, DMF, 80°C, 24 h, inert atmosphere; (iii) H_2SO_4 60%, $KBrO_3$, r.t, overnight; (iv) CH_3COONH_4, CH_3COOH, 125°C, overnight.

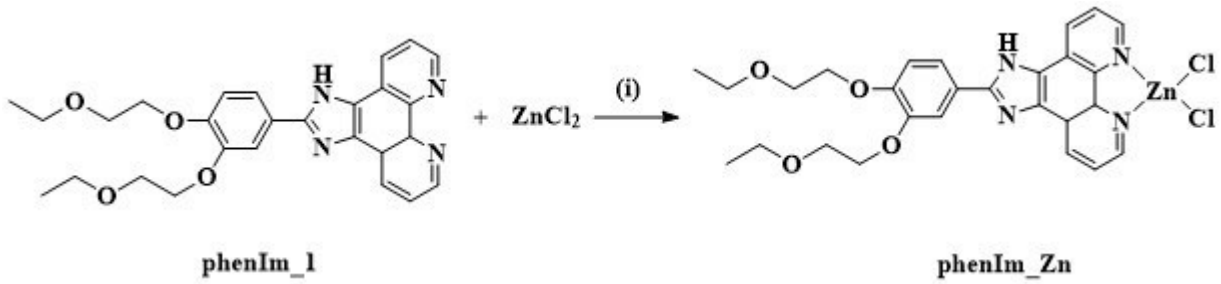

Scheme 2. Reaction pathway for the synthesis of *phenIm_Zn.* Reagents and conditions: (i) MeOH, r.t, 4 h.

The reaction of the *phenIm_1* with an excess of $ZnCl_2$ favoured the formation of the neutral complex *phenIm_Zn* (**Scheme 2**) with the metal centre tetracoordinated by the bidentate phenanthroline derivative and two monodentate chlorine ligands.

The targeted complex resulted to be scarcely soluble in water, but presented a good solubility in polar solvents (DMSO, methanol, acetonitrile) and non-polar solvents (dichloromethane, tetrahydrofuran).

Figure 2 presents the FT-IR spectra of the complex *phenIm_Zn* plotted against *phenIm_1* ligand. The FT-IR spectra of the ligand and its corresponding complex presents the characteristic absorption bands related to the functional groups present in the molecule. Thus, the absorption bands at 2969, 2934 and 2869 cm^{-1} are characteristic for the C-H bond stretching vibration while $\nu_{C\text{-}O\text{-}C}$ bonds, originating from the ethoxyethoxy chains are observed at 1125 cm^{-1} (Chen *et al* 2021).

The successful coordination of the ligand to the metal centre is proven by the shift with about 20 cm^{-1} of the $\nu_{C=N}$ characteristic band (Burger *et al.* 2001). The formation of the Zn(II) complex is further supported by the presence of the absorption band at 427 cm^{-1} which is characteristic for metal-nitrogen stretching (Pook 2023).

The ^{1}H-NMR spectra of complex *phenIm_Zn*, recorded in DMSO-d_6 revealed the presence of the protons corresponding to the phenanthroline ligand. The purity of the compounds is confirmed by elemental analysis (see Experimental Section).

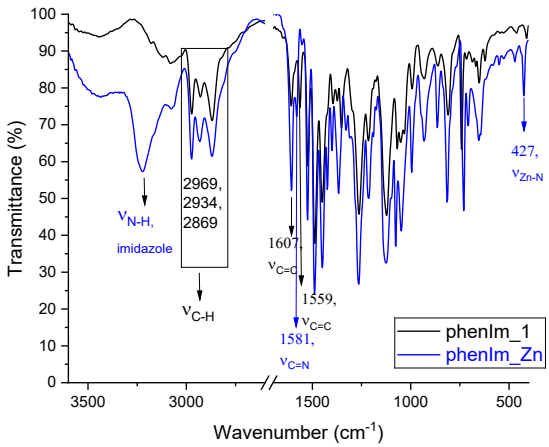

Figure 2. FT-IR spectra of Zn(II) (*phenIm_Zn* – blue) complex plotted against the phenanthroline ligand (*phenIm_1* – black)

The experimental conductivity value for *phenIm_Zn* measured for 10^{-3} mol·L^{-1} solution in acetonitrile at room temperature, falls in the range for non-electrolytes, confirming the neutral character of the complex (Geary 1971).

The photophysical studies (absorption and emission spectra) for the ligand and the Zn(II) complex were carried out. The spectra were recorded in diluted DCM solutions, at a concentration of $5\cdot10^{-6}$ mol·L^{-1} in order to minimize concentration-dependent artifacts.

Figures 3 and **4** present the absorption and emission spectra of the analysed samples, while their data is summarized in **Table 1**.

The absorption bands between 260 – 300 nm, present in the spectrum of both the ligand and the complex are characteristic for π – π* transitions (Zhong *et al.* 2016). Moreover, the absorption bands centred at 311 nm and 328 nm for *phenIm_1* and 307 nm for *phenIm_Zn* respectively, were assigned to an intramolecular charge transfer from the fused imidazole to the phenanthroline core (Devi *et al.* 2020, Zhong *et al.* 2016)

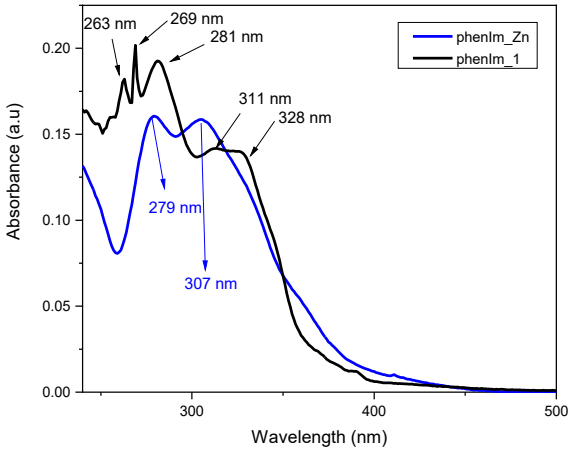

Figure 3. UV-Vis spectra of Zn(II) (*phenIm_Zn* – blue) complex plotted against the phenanthroline ligand (*phenIm_1* – black) recorded in DCM at $5\cdot10^{-6}$ mol·L^{-1}

Regarding the emission spectra (**Figure 4**, **Table 1**), *phenIm_1* presents an emission band centred at 439 nm, which originates from the π→π* singlet excited state, which upon complexation to *phenIm_Zn* suffers a bathochromic shift to 539 nm. Also, a large Stokes shift ($\Delta\lambda = \Delta\lambda_{max,em} - \Delta\lambda_{max,abs}$) of 232 nm is observed for Zn(II) complex.

The increase of the Zn(II) complex emission quantum yield with respect to the ligand is due to the stabilisation of the excited states of the ligand following coordination to the metal centre, suggested by the red shift of the emission maxima of the complex with respect to the emission maxima of the ligand. (Szerb *et al.* 2022)

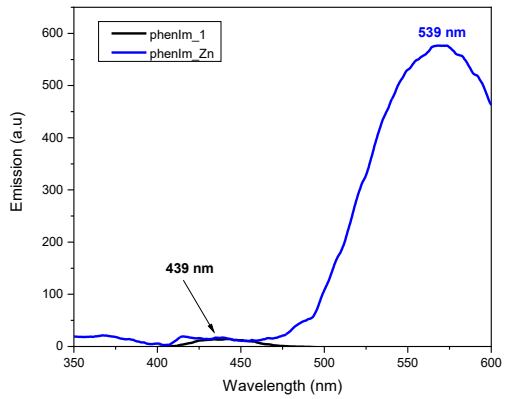

Figure 4. Emission spectra of Zn(II) (*phenIm_Zn* – blue) complex plotted against the phenanthroline ligand (*phenIm_1* – black) recorded in DCM at $5 \cdot 10^{-6}$ mol·L^{-1}

Table 1. Photophysical data of *phenIm_1* and *phenIm_Zn* complex in DCM at $5 \cdot 10^{-6}$ mol·L^{-1}.

Sample	Abs, λ_{max}/nm (ε/M^{-1} cm^{-1})	Em, λ_{max}/nm	QY (%)
phenIm_1	263(36400), 269(40600), 281(38600), 311(28400), 328(27600)	439 (λ_{ex}=325 nm)	1
phenIm_Zn	279(31800) 307(31600)	539 (λ_{ex}=305 nm)	24.13

CONCLUSIONS

A new ligand functionalised with lipophilic chains and its Zn(II) coordination complex were designed, synthesized and characterized.

Although insoluble in water, the complex resulted highly soluble in organic solvents, especially in DMSO which renders it proper for biological studies. Moreover, while the ligand emits modestly, with an emission centred at 439 nm, the coordination to Zn(II) centre stabilises the excited states of the ligand and thus 24 fold increase of the emission quantum yield is obtained. Also, the large Stokes shift value observed for the complex makes it suitable for bioimaging applications, where it is important to avoid the scattered light from the excitation beam overlapping with emission signal.

ACKNOWLEDGEMENTS

We acknowledge the financial support of the Romanian Academy via the research project with title "Luminescent biocompatible coordination complexes based on *d*-block metals and derivatives of natural alkaloids as ligands for biomedical applications", in the framework of Romanian Academy – Vietnam Academy of Science and Technology Joint Research Project 2026-2027.

RD, EP, AAA, EIS acknowledge the Romanian Academy, Program 4 and the infrastructure support granted by the project RO-OPENSCREEN, MySMIS code: 127952, Contract no. 371/20.07.2020, co-financed by European Regional Development Fund through the Competitiveness Operational Program 2014-2020.

REFERENCES

Abdallah, B., Seguin, C., Aubert, E., Ait BenHassou, H., Sbabou, L., Choulier, L., Vonthron, C., Schalk, I.J., Mislin, G.L.A., Fournel, S., Pitchon, V., Fechter, P., 2022. Past mastering of metal transformation enabled physicians to increase their therapeutic potential. Journal of Trace Elements in Medicine and Biology 73, 127027. DOI: 10.1016/j.jtemb.2022.126926

Arun, P.P., Patel, R. R., Singh, S. K.,Parmar, K., Singh, M., 2025. Exploring Metal Complexes for Cancer Treatment: Mechanistic Insights and Therapeutic Potential. Journal of Organometallic Chemistry 1031, 123512. DOI: 10.1016/j.jorganchem.2025.123682

Burger, K., Wagner, F.E., Vértes, A., Bencze, É., Mink, J., Labádi, I., Nemes-Vetéssy, Z., 2001. Structural Study of Terpyridine and O-Phenanthroline Complexes of Iridium(III). Journal of Physics and Chemistry of Solids 62, 2059–2068.
DOI: 10.1016/S0022-3697(01)00075-0

Cardinaels, T., Driesen, K., Parac-Vogt, T.N., Heinrich, B., Bourgogne, C., Guillon, D., Donnio, B., Binnemans, K., 2005. Design of High Coordination Number Metallomesogens

by Decoupling of the Complex-Forming and Mesogenic Groups: Nematic and Lamello-Columnar Mesophases. Chemistry of Materials 17, 6589–6598.
DOI: 10.1021/cm0513177
Chen, L., He, C., Liu, D., Zheng, Y., Li, W., Zu, Y., 2021. Third-order nonlinear optical properties of axially modified indium phthalocyanines with alkyl chains. New Journal of Chemistry 45, 10021–10030. DOI: 10.1039/d1nj00775k
Demas, J.N., Crosby, G.A, 1971. Measurement of photoluminescence quantum yields. Review. The Journal of Physical Chemistry, 75, 991-1024. DOI: 10.1021/j100678a001
Devi, R., Boddula, R., Tagare, J., Kajjam, A. B., Singh, K., Vaidyanathan, S., 2020. White Emissive Europium Complex with CRI 95%: Butterfly vs. Triangle Structure. Journal of Materials Chemistry C 8, 11715–11723. DOI: 10.1039/d0tc02724c
Geary, W.J., 1971. The use of conductivity measurements in organic solvents for the characterisation of coordination compounds. Coordination Chemistry Reviews 7, 81–122. DOI: 10.1016/S0010-8545(00)80009-0
Khursheed, S., Siddique, H.R., Tabassum, S., Arjmand, F., 2022. Water soluble transition metal [Ni(II), Cu(II) and Zn(II)] complexes of N-phthaloylglycinate bis(1,2-diaminocyclohexane). DNA binding, pBR322 cleavage and cytotoxicity. Dalton Transactions 51, 11713–11729. DOI: 10.1039/d2dt01312f
Ma, D.L., Wu, C., Li, G., Yung, T.L., Leung, C.H., 2020. Transition metal complexes as imaging or therapeutic agents for neurodegenerative diseases. Journal of Materials Chemistry B 8(22), 4715–4725. DOI: 10.1039/c9tb02669j
Mari, C., Pierroz, V., Ferrari, S., Gasser, G., 2015. Combination of Ru(II) complexes and light: new frontiers in cancer therapy. Chemical Science 6, 2660–2686.
DOI: 10.1039/c4sc03759f
Monro, S., Colón, K.L., Yin, H., Roque, J., Konda, P., Gujar, S., Thummel, R.P., Lilge, L., Cameron, C.G., McFarland, S.A., 2019. Transition Metal Complexes and Photodynamic Therapy from a Tumor-Centered Approach: Challenges, Opportunities, and Highlights from the Development of TLD1433. Chemical Reviews 119, 797–828.
DOI: 10.1021/acs.chemrev.8b00211
Percec, V., Peterca, M., Tsuda, Y., Rosen, B.M., Uchida, S., Imam, M.R., Ungar, G., Heiney, P.A., 2009. Elucidating the Structure of the Pm3n Cubic Phase of Supramolecular Dendrimers through the Modification of their Aliphatic to Aromatic Volume Ratio. Chemistry – A European Journal 15, 8994–9004.
DOI: 10.1002/chem.200901324
Pook, N.-P., 2023. Supramolecular Structure of Tris(1,10-phenanthroline)zinc(II)-Cation and N,N′,N″-tris(carboxymethyl)-1,3,5-benzenetricarboxamide-Anion: Synthesis, Crystal Structure, Vibrational Spectra, and Theoretical Investigations. Crystals 13, 569. DOI: 10.3390/cryst13040569
Porchia, M., Pellei, M., Del Bello, F., Santini, C., 2020. Zinc Complexes with Nitrogen Donor Ligands as Anticancer Agents. Molecules 25, 5814. DOI: 10.3390/molecules25245814
Roohani, N., Hurrell, R., Kelishadi, R., Schulin, R., 2013. Zinc and its importance for human health: An integrative review. Journal of Research in Medical Sciences 18, 144–157.
Rosenberg, B., VanCamp, L., Krigas, T., 1965. Inhibition of cell division in Escherichia coli by electrolysis products from a platinum electrode. Nature 205, 698–699. DOI: 10.1038/205698a0
Rosenberg, B., VanCamp, L., Trosko, J.E., Mansour, V.H., 1969. Platinum Compounds: A New Class of Potent Antitumour Agents. Nature 222, 385–386. DOI: 10.1038/222385a0
Rusakowicz, R., Testa, A.C., 1968. 2-Aminopyridine as a standard for low-wavelength spectrofluorimetry. The Journal of Physical Chemistry 72(7), 2680–2681. DOI: 10.1021/j100853a084
Sanz Mendiguchia, B., Pucci, D., Mastropietro, T. F., Ghedini, M., Crispini, A. 2013. Non-classical anticancer agents: on the way to water soluble zinc(II) heteroleptic complexes. Dalton Transactions 42, 6768–6774. DOI: 10.1039/c3dt50367d
Szerb, E.I., Crispini, A., Aiello, I., La Deda, M., 2022. Springer Handbook of Inorganic Photochemistry; Part XII: Inorganic Materials for Optoelectronics, 62: Liquid Crystals, Section editor: Eli Zysman-Colman; Bahnemann, D.W.,

Patrocinio, A.O.T., Eds.; Springer Nature: Cham, Switzerland, 1811–1848.
Sodhi, R.K., Paul, S., 2019. Metal Complexes in Medicine: An Overview and Update from Drug Design Perspective. Cancer Therapy & Oncology International Journal 14, 555883. DOI:10.19080/CTOIJ.2019.14.555883
Suzuki, K., Kobayashi, A., Kaneko, S., Takehira, K., Yoshihara, T., Ishida, H., Shiina, Y., Oishi, S., & Tobita, S., 2009. Reevaluation of absolute luminescence quantum yields of standard solutions using a spectrometer with an integrating sphere and a back-thinned CCD detector. Physical Chemistry Chemical Physics 11(42), 9850–9860. DOI: 10.1039/b912178a
Wani, W.A., Prashar, S., Shreaz, S., Gómez-Ruiz, S., 2016. Nanostructured materials functionalized with metal complexes: in search of alternatives for administering anticancer metallodrugs. Coordination Chemistry Reviews 312, 67–98.
DOI: 10.1016/j.ccr.2016.01.001
Yoshikawa, Y., Yasui, H., 2012. Zinc Complexes Developed as Metallopharmaceutics for Treating Diabetes Mellitus based on the Bio-Medicinal Inorganic Chemistry. Current Topics in Medicinal Chemistry 12, 210–218.
DOI: 10.2174/156802612799078874
Zhang, P., Sadler, P.J., 2017. Redox-Active Metal Complexes for Anticancer Therapy. European Journal of Inorganic Chemistry 2017, 1541-1548.
DOI: 10.1002/ejic.201600908
Zhang, J., Che, J., Luo, X., Wu, M., Kan, W., Jin, Y., Wang, H., Pang, A., Li, C., Huang, W., Zeng, S., Zhuang, W., Wu, Y., Xu, Y., Zhou, Y., Li, J., Dong, X., 2022. Structural Feature Analyzation Strategies toward Discovery of Orally Bioavailable PROTACs of Bruton's Tyrosine Kinase for the Treatment of Lymphoma. Journal of Medicinal Chemistry 65, 9096–9125.
DOI: 10.1021/acs.jmedchem.2c00324
Zhao, C.-M., Campbell, P.G.C., Wilkinson, K.J., 2016. When are metal complexes bioavailable? Environmental Chemistry 13, 425–433. https://doi.org/10.1071/EN15205
Zheng, R.H., Guo, H.C., Jiang, H.J., Xu, K.H., Liu, B.B., Sun, W.L., Shen, Z.Q., 2010. A new and convenient synthesis of phendiones oxidated by KBrO3/H2SO4 at room temperature. Chinese Chemical Letters 21, 1270–1272.
DOI: 10.1016/j.cclet.2010.05.030
Zhong, R., Xu, S., Wang, J., Zhao, F., Xia, H., Wang, Y., 2016. Experimental and theoretical investigations on spectroscopic properties of the imidazole-fused phenanthroline and its derivatives. Spectrochimica Acta Part A: Molecular and Biomolecular Spectroscopy 161, 27–32. DOI: 10.1016/j.saa.2016.02.019
Zhuo, Y., Zhao, Y.-G., Zhang, Y., 2024. Enhancing Drug Solubility, Bioavailability, and Targeted Therapeutic Applications through Magnetic Nanoparticles. Molecules 29, 4854. DOI: 10.3390/molecules29204854

ISSN 1582-1021
e-ISSN 2668-4764
Edited by "Aurel Vlaicu" University Publishing House, Arad, Romania


Open Access

doi: 10.62591/Scien.Tech.Bull-Chem.FoodSci.Eng.2025.22.02

Scien. Tech. Bull-Chem. Food Sci. Eng., Vol. 22(XXIII), 2025, 27-40
doi: 10.62591/Scien.Tech.Bull-Chem.FoodSci.Eng.2025.22.03

Article

AN EXPLORATORY ANALYSIS OF METHODOLOGICAL PREFERENCES IN SCIENCE EDUCATION AMONG FUTURE TEACHERS

Simona GAVRILAȘ

Faculty of Food Engineering, Tourism and Environmental Protection, "Aurel Vlaicu" University of Arad, Romania, 2 Elena Dragoi St., Arad 310330, Romania
Corresponding author email: simona.gavrilas@uav.ro

Abstract: *Preparing future teachers to teach science plays an essential role in developing scientific literacy and promoting educational approaches based on investigation and active learning. This study aims to analyze students' methodological preferences in the Primary and Preschool Education Pedagogy specialization and their perceptions of the usefulness of different categories of teaching resources used in science education activities. The research was conducted with a sample of 44 students, using a questionnaire structured on a 5-point Likert scale. The frequency of intention to use didactic experiments, systematic observation, didactic games, the project method, heuristic conversation, and discovery learning was investigated, as well as the perceived usefulness of digital resources, multimedia, worksheets, recyclable materials used in experiments, and manipulative materials. Statistical analysis was performed using XLSTAT, including descriptive statistics, Cronbach's alpha, the Spearman correlation coefficient, and the nonparametric Friedman test. The results revealed excellent internal consistency for the teaching methods scale (Cronbach's α = 0.912) and good consistency for the usefulness of teaching resources scale (Cronbach's α = 0.773). At the same time, moderate and strong positive correlations were identified between active-participatory methods and educational resources, suggesting a pedagogical profile oriented toward interactive and investigative approaches. The conclusions support the need to strengthen initial teacher training by integrating strategies and resources specific to STEM education and inquiry-based learning.*

Keywords: STEM; inquiry-based learning; didactic experiment; active-participatory strategies; pedagogical competencies

INTRODUCTION

In recent decades, science education has become a priority in educational policy, given the need to develop scientific literacy, problem-solving, and critical thinking skills from the early years of schooling. Roy et al.'s study identified some gaps in the area. Considerations related to the legislation in the field or the implications for parents could contribute to improving domain performance (Roy et al., 2025). In this context, the specialized literature points out the importance of promoting teaching strategies that emphasize investigation, experimentation, and active participation, allowing students to construct knowledge through direct interaction with the phenomena and processes under study (Kim et al., 2019). The tendency is to promote active learning (AL) and inquiry-based learning (IBL) (Rezai et al., 2025, Morris, 2025, Thomas et al., 2025). The methodology used could be influenced by the teacher's practical experience (Photo, 2025, Kotsis, 2024), gained during the study period or as an employee. Another aspect that may impact educational outcomes is the educator's ability to connect with students and to set realistic goals (Zhang et al., 2024).

For preschool and primary education, these principles are embodied in methods such as the didactic experiment, systematic observation, the project method, heuristic conversation, and discovery learning, all of which have the potential to facilitate the understanding of scientific concepts and the development of investigative skills. Besides the professor's expertise, the children's prior knowledge in a field can also influence the level of acquisition (Grenell et al., 2024).

However, the effectiveness of these methods depends closely on the use of appropriate teaching resources. Manipulative and concrete materials, digital and multimedia resources, worksheets, and recyclable materials used in experimental activities can transform the

learning process into an authentic experience and support the development of students' practical and cognitive skills. Consequently, the initial training of future teachers must include not only the development of methodological skills but also the ability to select and effectively integrate teaching resources into teaching and learning activities (Ochogboju and Díez-Palomar, 2025, Furner and Worrell, 2017).

The motivation for this study stems from the need to understand how students in the Primary and Preschool Education specialization perceive the relationship between teaching strategies and the educational resources used to teach science. Although much research examines the effectiveness of different teaching methods, fewer studies simultaneously analyze future teachers' methodological preferences and how these preferences correlate with perceptions of the usefulness of teaching resources. Such an approach can provide relevant information to optimize the university curriculum and develop initial training programs focused on STEM education and inquiry-based learning.

In this context, three research hypotheses were formulated. The first hypothesis (H1) to confirm that methodological preferences and appreciation of teaching resources configure a coherent pedagogical profile of future teachers, a result compatible with constructivist perspectives on science teaching. The substantiation of this hypothesis is based on the fact that methods such as the didactic experiment, the project method, or discovery learning typically integrate material and digital resources that facilitate the observation, exploration, and validation of results obtained in the learning process.

The second hypothesis (H2) presumes there are significant differences in prospective teachers' stated preferences for different teaching methods in science education.

The third hypothesis (H3) postulates that there are notable variations in the perceived usefulness of different categories of teaching resources used in science education.

The study addresses a theme at the intersection of scientific education and initial teacher training. Although the research has a pronounced psychopedagogical character, it is directly relevant to the science fields, as it analyzes the factors that can influence the implementation of teaching practices that facilitate understanding of phenomena specific to the natural sciences and support the development of the skills necessary for future citizens in a knowledge-based society. The results provide empirical data on the readiness of future teachers to use methods and resources compatible with STEM education and modern inquiry-based learning approaches, thereby strengthening the link between science research and its transfer into educational practice.

Based on these considerations, the research aims to investigate students' methodological preferences and perceptions of the usefulness of the teaching resources used in science instruction, as well as to determine whether pre-service teachers exhibit different levels of preference for inquiry-oriented instructional methods in the field. To this end, responses were analyzed using descriptive and inferential statistics in XLSTAT, including Cronbach's alpha to assess the instrument's internal consistency (Tavakol and Dennick, 2011, Taber, 2018), the Spearman correlation coefficient to examine relationships among variables (Rebekić et al., 2015), and nonparametric Friedman tests to assess possible differences between the dependent measurements. This approach provides a rigorous methodological basis for characterizing the methodological profiles of future teachers and for formulating recommendations to optimize initial training in science education.

Unlike many studies that examine methodological preferences or the use of teaching resources separately, the present study analyzes the relationship between these two dimensions. It highlights how they shape the pedagogical profile of future science teachers. The integration of internal consistency analyses, Spearman correlations, and comparisons using the Friedman test offers an exploratory perspective on the coherence between methodological orientations and the selection of teaching resources.

MATERIALS AND METHODS

Participants and Data Collection Procedure

The research consisted of collecting pedagogical preferences in science teaching among students in the field of psychopedagogy of primary and preschool education. The survey was conducted in May 2026 and was administered to second-year students, towards the end of the science and science didactics course. Respondents' anonymity was ensured, with no personal data collected. Participation was voluntary and involved completing an online Google Forms questionnaire.

The questionnaire was specifically developed for this study based on the learning objectives of the Sciences and Science Teaching course, prior literature on inquiry-based science education (Strat et al., 2024, Ganajová et al., 2025), and the methodological competencies expected of pre-service primary teachers. It was conceived as a feedback instrument to explore students' perceptions of science teaching methodologies and instructional resources. The conceptual framework comprised two complementary dimensions. The first one, methodological preferences, assessed respondents' stated intention to use selected science teaching methods in their future professional practice. The second, perceived usefulness of instructional resources, evaluated respondents' perceptions of the educational value of various instructional materials commonly used in science teaching. The methods was choses to reflect respondents' self-reported inclination toward learner-centered instructional approaches, which are considered essential in contemporary science education (Erhabor and Reis, 2026, Vidal-Esteve and Martín-Gómez, 2023, Prajoko et al., 2017, Janštová et al., 2023). The second component was intended to reflect respondents' evaluation of the pedagogical usefulness of different instructional resources that support inquiry-based science teaching.

In this analysis, six items evaluated methodological preferences and five evaluated the perceived usefulness of instructional resources. Particular attention was paid to ensuring that each item captured a distinct aspect of the construct under investigation while maintaining conceptual coherence within each dimension.

The participation rate among those enrolled in the mentioned course this academic year was around 37%. The respondents were informed that their responses would be used exclusively for academic and scientific research.

The questions used to determine students' priorities for the methods applied were designed using a Likert scale (1-never, 2-rarely, 3-sometimes, 4-often, 5-very often). The range for determining the perceived usefulness of the different teaching resources was as follows: 1-very low, 2-low, 3-moderate, 4-high, 5-very high.

Statistical Analysis

The data were evaluated using XLSTAT 2025.2.0 software. To establish the degree of correlation between the frequency of using active methods and the concrete resources, Spearman's correlation coefficient was used. The Friedman test was utilised to assess differences among six methods and within the five instruments treated as dependent variables. The approach was considered given the study's preliminary characteristics. To assess the internal reliability of the results, Cronbach's Alpha was applied. The statistical coefficients were selected considering the sample size at the time of data processing.

RESULTS AND DISCUSSIONS

The study aimed to analyze respondents' methodological preferences and their perceptions of the usefulness of different resource categories. The analysis was based on participants' responses to a Likert-type (Vagias et al., 2006) questionnaire that assessed both the frequency with which they would use certain teaching methods and the usefulness of resources commonly encountered in science education activities.

Because developing specific science skills requires teaching strategies focused on investigation, exploration, and active student involvement, preferences for methods such as the didactic experiment, systematic observation, didactic game, project, heuristic conversation, and discovery learning were analyzed. In addition, students' perceptions of the usefulness of various teaching resources were investigated,

ranging from concrete, reusable materials used in didactic experiments to digital and multimedia resources.

The degree of correlation and its meaning between the frequency of use of active methods (experiment, discovery, project) and concrete resources (recyclable materials and worksheets) were determined using Spearman's coefficient (Schober et al., 2018). From the correlation matrix (Table 1), moderate and strong positive relationships are observed between active-investigative methods and teaching resources perceived as useful. The strength of the relationship between the elements considered determines the most relevant values supporting the acceptance of the first hypothesis. Additionally, the consideration is sustained by the fact that most associations between methods and resources are statistically significant ($p<0.001$) (Table 2).

Almost all correlations among the six methods are statistically significant (most $p<0.001$) (Table 2). Such a result suggests that students who report they would frequently use an active method also report frequently using other similar ones. The result could suggest that methodological preferences are not independent but form a relatively coherent pedagogical profile.

This conclusion aligns with Cronbach's alpha values (≈0.91).

Results, such as observation↔worksheets ($p=0.206$), observation↔multimedia ($p=0.094$), concrete materials↔digital resources ($p=0.081$), and concrete materials↔worksheets ($p=0.242$), indicate that not all resources are perceived as equally relevant across all teaching strategies.

The correlation analysis revealed a strong positive association between the preference for systematic observation and the perceived usefulness of manipulative/concrete materials (0.62). The result is consistent with the specificity of this method, which involves the direct investigation of objects and phenomena through material supports that facilitate exploration and the formulation of conclusions based on observation. A strong positive association was also identified between heuristic conversation and the use of recyclable materials in experiments (0.60), suggesting that students perceive heuristic dialogue and experimental activities using accessible materials as complementary elements of interactive teaching. Both results support the existence of an orientation toward didactic practices that center on students' active involvement and the valorization of concrete resources in early science education. Sowmya and Rani underlined the positive effects of studying science from an early age (Sowmya and Rani, 2025). The design and implementation of exploratory activities are also suggested by the results of Dejonckheere et al.'s study (Dejonckheere et al., 2016).

Several situations with moderate to strong correlations (0.56-0.58) and moderate ones (0.40-0.53) were observed. The moderate-to-strong positive association identified between the project method and the perceived usefulness of digital, multimedia, and recyclable materials used in experiments (0.58) suggests that students who value project-based learning strategies tend to view these resources as essential supports for investigation and practical application activities. Such a result could be seen as consistent with the project method's specificity, which involves documentation, collaboration, the creation of educational products, and the integration of concrete learning experiences. Naseer et al.'s study provides additional data that underscore the benefits of project learning (Naseer et al., 2025). Such an approach appears to impact learners' future development, independent of the educational levels they were involved in. Thus, the preference for projects appears to be associated with an orientation toward active, interdisciplinary didactic approaches, characteristic of contemporary science and STEM education. A path to encourage the transition to project-based learning implementation was suggested in Martin-Garcia et al.'s study (Martín-García et al., 2024). Their research focused on implementing this approach in learning clubs. An observed limitation of such a procedure could be related to the teachers' experience in the field.

The moderate correlation between didactic experiment and concrete resources (0.53) shows that students associate experimental activities with the use of material supports. They perceive practical materials as essential for learning sciences. The result could

be seen as a natural relationship in experimental didactics (Oliveira and Bonito, 2023, Kranz et al., 2023). The manipulative materials also show a moderate correlation with discovery learning (0.54). Such a result suggests that students value exploratory learning contexts, and supports the orientation towards constructivist pedagogies and inquiry-based learning. The worksheets seem to present less important correlations, with most coefficients falling in the weak association range.

It could be considered that students who prefer active, participatory methods also find concrete teaching resources useful. As the frequency of preference for methods based on investigation and active involvement increases, so does the perception of the usefulness of practical and applicative resources.

Correlation analysis revealed a coherent pedagogical profile in which a preference for active teaching methods is associated with a positive appreciation of a diverse range of teaching resources. However, the lack of significant associations between systematic observation and worksheets or multimedia resources suggests that participants distinguish between resources appropriate for observation-based activities and those used primarily to organize or present information.

The scale's internal consistency was evaluated using Cronbach's alpha (Table 3).

Table 3. Consistency global coefficient

	Methods	**Materials**
Cronbach's alpha	0.912	0.773
Standardized Cronbach's Alpha	0.914	0.778
Split-Half 1	didactic experiment	concrete/manipulative materials
	didactic game	digital resources
	heuristic conversation	worksheets
Split-Half 2	systematic observation	multimedia resources
	project method	recyclable materials used in experiments
	discovery learning	

Reliability analysis shows excellent internal consistency for the scale measuring the frequency of use of didactic methods (Cronbach's α=0.912) and good internal consistency for the scale measuring the perceived usefulness of didactic resources (Cronbach's α=0.773). These results support the instrument's internal consistency (Dorsah, 2026).

The methodological preferences aspect highlights higher internal homogeneity than the perceived usefulness of teaching resources (Table 4). This result is expected because the investigated teaching methods represent complementary pedagogical strategies used in science teaching. In contrast, teaching resources include more heterogeneous categories (digital, multimedia, and concrete and recyclable materials), which may lead to greater variability in responses.

Table 4. Corrected Item-Total Correlation Values

Variable	**Item-total correlation**	**Interpretation correlation**
Methodological preferences		
Didactic experiment	0.807	Very strong
Systematic observation	0.744	Strong
Didactic game	0.672	Strong
Project method	0.709	Strong
Heuristic conversation	0.786	Very strong
Discovery learning	0.828	Very strong
Perceived usefulness of materials		
Concrete materials	0.454	Moderate
Digital resources	0.609	Strong
Worksheets	0.435	Moderate
Multimedia resources	0.699	Strong
Recycled materials	0.562	Moderate–strong

Internal consistency was evaluated using Cronbach's alpha and item-level statistics. For the methodological preferences scale, corrected item-total correlations ranged from 0.672 to 0.828, indicating strong associations between each item and the overall construct. The highest correlations were observed for discovery learning (0.828) and didactic experiments (0.807), while didactic games showed the lowest, yet still high, correlation (0.672). Furthermore, Cronbach's alpha did not improve

after deleting any item, supporting the retention of all six items.

The perceived usefulness of the different instruments scale also indicate satisfactory internal consistency. Corrected item-total correlations ranged from 0.435 to 0.699, exceeding the commonly accepted threshold of 0.30. Multimedia resources (0.699) and digital resources (0.609) showed the strongest relationships with the total score, whereas worksheets had the lowest correlation (0.435), which was still acceptable. No improvement in Cronbach's alpha was observed after deleting individual items.

Friedman's test suggests the existence of global differences between teaching methods, but does not identify pairs of methods that differ significantly (Table 5 and 6).

Table 5. Friedman's test results for the methods considered

Q (Observed value)	**23.220**
Q (Critical value)	11.070
DF	5
p-value (one-tailed)	**0.000**
alpha	0.05

An approximation has been used to compute the p-value.

Table 6. Methods summary statistics

Variable	Mean	Median O_1-Q3
didactic experiment	4.21±0.73	4(4-5)
systematic observation	4.36±0.72	4.5(4-5)
didactic game	4.57±0.70	5(4-5)
project method	4.23±0.80	4(4-5)
heuristic conversation	4.43±0.70	5(4-5)
discovery learning	4.52±0.66	5(4-5)

Descriptive analysis indicates that all investigated teaching methods were evaluated favorably, with means ranging from 4.205 to 4.568 on a five-point Likert scale. The highest scores were recorded for the didactic game (4.568 ± 0.695). The didactic experiment (4.205 ± 0.734) and the project method (4.227 ± 0.803) recorded slightly lower values, but remained above the level of frequent use. All data considered have an IQR of 1, indicating that the responses are concentrated between ”Frequent” and ”Very frequent”. Medians consistently indicated high preferences for all instructional methods. The didactic game, heuristic conversation, and discovery learning reached a median score of 5 (Q1–Q3: 4–5), indicating that at least half of respondents reported using these methods frequently or very frequently. The didactic experiment and project method had slightly lower median values of 4 (Q1–Q3: 4–5), although their mean scores were also generally favorable.

To assess whether these differences are statistically significant, the Friedman test for repeated measures was applied. The results revealed significant differences among the six methods investigated ($Q=23.220$, $df=5$, $p<0.001$), indicating that participants do not intend to use all teaching methods with the same frequency. This result suggests a hierarchy of methodological preferences, with a stronger orientation toward active, student-centered strategies. However, the Friedman test does not identify which pairs of methods differ significantly. Post hoc analyses would be necessary to identify the specific differences.

Therefore, the null interpretation of the second hypothesis, according to which all methods are evaluated similarly, is rejected, and the alternative form, which specifies that at least one teaching method is evaluated differently from the others, is accepted.

Regarding the instruments used, the Friedman test results indicate that the differences between the means are not statistically significant at the $\alpha = 0.05$ threshold (Tables 7 and 8).

Table 7. Friedman's test results for the instruments considered

Q (Observed value)	**9.328**
Q (Critical value)	9.488
DF	4
p-value (one-tailed)	0.053
alpha	0.05

An approximation has been used to compute the p-value.

Table 8. Instruments summary statistics

Variable	Mean	Median O_1-Q3
concrete/manipulative materials	4.43±0.87	5(4-5)
digital resources	4.16±0.71	4(4-5)
worksheets	4.14±0.80	4(4-5)
multimedia resources	4.11±0.78	4(3.75-5)
recyclable materials used in experiments	4.34±0.74	4.5(4-5)

Participants rated all categories of educational resources investigated favorably, with averages ranging from 4.114 to 4.432. Concrete/manipulative materials (4.432 ± 0.873) and recyclable materials used in experiments (4.341 ± 0.745) had the highest values, while multimedia resources (4.114 ± 0.784) and worksheets (4.136 ± 0.795) had slightly lower values.

The only variable that is somewhat more dispersed is multimedia resources (IQR=1.25). Perceived usefulness of instructional resources was similarly high. Concrete/manipulative materials had the highest median score (Median=5; Q1-Q3:4-5), whereas digital resources, worksheets, and multimedia resources all had a median of 4 and relatively narrow interquartile ranges, suggesting a generally consistent appreciation across participants. For the variable ”multimedia resources”, Q1=3.75 indicates the use of an interpolation method for calculating quartiles.

The Friedman test did not reveal statistically significant differences among the evaluations of the five resource categories ($Q=9.328$; $df=4$; $p=0.053$). Although the result is close to the conventional significance threshold, it does not provide sufficient evidence to conclude that participants systematically prioritize certain resources over others. These results suggest a relatively balanced appreciation of the various teaching resources used in science education. In this case, the null formulation of the third assumption is accepted.

The median results (Q_1-Q_3) support the Friedman data, with differences detected for the methods used and being less significant for the instruments.

Spearman correlations indicated moderate to strong associations between active-participatory methods and didactic resources. Overall, the results suggest a coherent pedagogical profile oriented toward interactive, investigative, and specific approaches to STEM education. Independent of the didactic methods and materials used, the teaching activity's success could be considered highly dependent on the educator's professional and personal capacities to adapt and implement appropriate strategies to the educable's capacities and interests (Kucharčíková and Tokarčíková, 2016).

CONCLUSIONS

The results suggest that future teachers are oriented toward interactive teaching strategies. Inquiry-based methods are conceptualized alongside practical resources. There are favorable conditions for integrating STEM and inquiry-based approaches into initial teacher education. Combined interpretation of Spearman correlation coefficients and Friedman results revealed a statistically coherent pattern of methodological preferences among pre-service teachers. Strong positive associations were found between inquiry-based teaching methods and the perceived usefulness of practical and digital instructional resources, and the Friedman test confirmed significant variations in stated preferences for different teaching methods in science education ($p<0.0003$). These findings suggest an educational orientation toward interactive, student-centered, and resource-supported science teaching practices. Successful results regarding future teachers' capacities to implement different didactic approaches are linked to both their theoretical studies and practical experience (Sizer et al., 2021).

The results support the finding that prospective teachers have a favorable orientation toward teaching methods that promote active student engagement and knowledge construction through direct learning experiences. The high scores for didactic games, discovery learning, and heuristic conversation are consistent with current science-teaching guidelines, which recommend active strategies to develop critical thinking, investigation, and problem-solving skills.

In contrast, the lack of significant differences across the teaching resource categories suggests that respondents view these resources as complementary instead of competing. This perspective aligns with contemporary approaches to science education, which promote integrating concrete materials, digital resources, and recyclable materials based on teaching objectives and the context of learning activities (Park et al., 2023).

The preferences for discovery learning and heuristic conversation can be interpreted in

light of constructivist perspectives on learning, which hold that knowledge is actively constructed through exploration, hypothesis-making, and reflection on learning experiences. From this perspective, the teacher's role shifts from transmitting information to facilitating investigation and argumentation.

The favorable orientation toward active methods aligns with numerous studies on science teacher education, which have shown that inquiry-based university experiences increase acceptance of student-centered teaching strategies (Jerrim et al., 2022, Aidoo, 2024). At the same time, our results indicate that the didactic experiment does not rank first in the hierarchy of preferences, which may reflect perceived constraints on organizing experimental activities or students' confidence in managing them.

The results are based on self-reported preferences, instead of observations of teaching practice. Therefore, it cannot be concluded that participants will actually use the methods and resources evaluated in their professional work. Additionally, the small sample size (44 students from the same specialization) limits the generalizability of the conclusions.

The data obtained suggest the need to strengthen university activities through investigation, projects, and the integrated use of digital resources and concrete materials. The development of methodological skills should be achieved through authentic activities of designing and implementing science lessons, which allow students to directly experience the relationship between teaching strategies and the resources used.

The preference for active strategies is consistent with recent research on initial teacher education, which shows that inquiry-based university experiences foster the acceptance of student-centered methods. At the same time, our study complements these results by highlighting the relationships between methodological preferences and the appreciation of specific teaching resources.

The association between the project method and digital resources can be explained by the characteristics of educational projects, which involve documentation, collaboration, and information organization. Digital resources facilitate these processes and become natural supports for the implementation of project-based learning.

The correlation between systematic observation and concrete materials aligns with the principles of inquiry-based learning, as the observation of natural phenomena involves the use of real objects and manipulable materials.

LIMITATIONS AND FUTURE PERSPECTIVES

The results of the study highlight a tendency among future teachers toward active-participatory teaching methods and the use of various teaching resources in science education activities. The high internal consistency of the research instrument (Cronbach's α=0.912 for the methodological preferences scale), along with the positive associations identified between teaching methods and educational resources, supports the need to strengthen these dimensions in initial training programs. A person's innate abilities along with acquired competencies form their personality. Independent of the future field of activity, shaping will begin in the initial stages of the educational process. Designing and implementing participatory activities in which learners, regardless of their level of education, are integral to the process can help shape their future professional development by increasing the stimulation of acquisitions, dynamic and conscious persons (Cortes, 2025, Ma, 2023, Jakob et al., 2026, Gáspár et al., 2021).

Training programs could include more applied activities in which students design, implement, and evaluate teaching sequences based on experimentation, systematic observation, and discovery learning. Practicing these methods in authentic contexts contributes to the development of professional skills and facilitates their transfer to teaching practice.

The research results suggest that investigative-exploratory methods are perceived as complementary. Therefore, the initial training curriculum could be built on pedagogical models centered on questioning, hypothesis development, data collection, and result interpretation, in line with international recommendations for science education.

The correlations identified between the project method and digital and multimedia

resources indicate the need to develop future teachers' digital skills. University activities might include lesson design using educational platforms, interactive simulations, data-collection applications, and digital presentation and collaboration tools, more than just general technical training.

Direct contact with real teaching situations can facilitate the development of skills in selecting and appropriately using teaching methods and resources. Declared preferences are not equivalent to actual teaching practices. The questionnaire measures intentions and perceptions, not observed classroom behaviors. Therefore, even if participants declare a preference for active methods and for certain resources, it cannot be concluded that these will actually be used in professional activity.

The training of future teachers could encourage the design of interdisciplinary activities that connect the natural sciences with technology, engineering, and mathematics. The project method and the didactic experiment provide favorable contexts for developing such approaches and integrating digital resources. Experimental materials can support the use of authentic, relevant problems for students.

Initial training might not be limited to presenting teaching methods. Still, it should also include systematic activities for developing learning scenarios, selecting resources for argumentative purposes, and constructing assessment tools appropriate to the competencies under investigation. Such an approach can help increase coherence among curricular objectives, teaching strategies, and the assessment of learning outcomes.

The associations observed between systematic observation and manipulative materials, and between heuristic conversation and recyclable materials used in experiments, highlight the importance of concrete learning experiences. It could be recommended that university practical activities include workshops on the design and implementation of experiments using accessible, reusable materials, in line with the principles of education for sustainable development (Levina et al., 2025, Arnab et al., 2025, Botella et al., 2022).

Statistical analyses of methodological preferences and student perceptions can provide valuable information for revising school curricula. Introducing periodic feedback collection and analysis can help adapt training content and strategies to the real needs of future teachers.

The recommendations support developing an initial training model that combines theoretical training with practical experience and promotes the integrated use of active, participatory methods and diversified teaching resources. Such an approach can help prepare teachers to design and implement science education activities that are adapted to students' current needs in preschool and primary education, and to facilitate the development of investigative skills and scientific literacy (Halimi et al., 2024). In the Gahrizsangi et al. study, the importance of adapting teaching approaches to current technological developments was highlighted. Transdisciplinarity could increase scientific knowledge and interest in science from early ages (Salehi Gahrizsangi et al., 2026). Future post hoc analyses are recommended to identify which methods differ after a significant Friedman result is obtained.

The findings should be interpreted in light of several limitations. First, the study relied on a relatively small sample (N=44) from a single teacher education program, limiting the generalizability of the results. The response rate (37%) represents an additional limitation of the study. Although similar response rates are frequently reported in voluntary surveys conducted in higher education, the possibility of non-response bias cannot be ruled out. Consequently, the findings should be interpreted as reflecting the characteristics of the participating students, not the entire population of pre-service primary teachers.

A subsequent limitation concerns the data, which were collected via self-reported Likert-scale responses and therefore reflect participants' perceived preferences, not the observed teaching practices. All variables exhibit a ceiling effect, as most responses cluster around values 4 and 5. This limits variability and may reduce the ability of statistical tests to detect more subtle differences between methods or resources.

Also, the cross-sectional design does not allow causal inferences or the examination of

changes in methodological preferences over time. Although the statistical analyses revealed significant associations between teaching methods and instructional resources, these relationships might be better interpreted as correlational instead of causal. Future research should include larger, more diverse samples, longitudinal designs, and complementary observational methods to provide a more comprehensive understanding of pre-service teachers' science teaching practices.

Table 1. Correlation matrix (Spearman)

Variables	Methods						Materials				
	didactic experiment	systematic observation	didactic game	project method	heuristic conversation	discovery learning	concrete/manipulative materials	digital resources	worksheets	multimedia resources	recyclable materials used in experiments
didactic experiment	1	0.74	0.55	0.69	0.68	0.66	*0.53*	***0.56***	0.32	*0.43*	*0.53*
systematic observation	0.74	1	0.55	0.49	0.65	0.53	***0.62***	0.31	0.19	0.26	*0.50*
didactic game	0.55	0.55	1	0.48	0.47	0.72	*0.48*	0.38	0.33	*0.50*	*0.40*
project method	0.69	0.49	0.48	1	0.68	0.68	0.37	***0.58***	*0.55*	***0.58***	***0.58***
heuristic conversation	0.68	0.65	0.47	0.68	1	0.61	*0.52*	*0.48*	0.31	*0.45*	***0.60***
discovery learning	0.66	0.53	0.72	0.68	0.61	1	*0.54*	***0.56***	0.39	***0.57***	*0.40*
concrete/manipulative materials	0.53	0.62	0.48	0.37	0.52	0.54	1	0.27	0.18	0.45	0.52
digital resources	0.56	0.31	0.38	0.58	0.48	0.56	0.27	1	0.52	0.72	0.35
worksheets	0.32	0.19	0.33	0.55	0.31	0.39	0.18	0.52	1	0.48	0.41
multimedia resources	0.43	0.26	0.50	0.58	0.45	0.57	0.45	0.72	0.48	1	0.42
recyclable materials in experiments	0.53	0.50	0.40	0.58	0.60	0.40	0.52	0.35	0.41	0.42	1

Values in bold are different from 0 with a significance level alpha=0.05

Table 2. p-values (Spearman)

Variables	Methods						Materials				
	didactic experiment	systematic observation	didactic game	project method	heuristic conversation	discovery learning	concrete/manipulative materials	digital resources	worksheets	multimedia resources	recyclable materials used in experiments
didactic experiment	0	<0.0001	0.000	<0.0001	<0.0001	<0.0001	0.000	<0.0001	0.037	0.003	0.000
systematic observation	<0.0001	0	0.000	0.001	<0.0001	0.000	<0.0001	0.044	0.206	0.094	0.001
didactic game	0.000	0.000	0	0.001	0.001	<0.0001	0.001	0.010	0.030	0.001	0.008
project method	<0.0001	0.001	0.001	0	<0.0001	<0.0001	0.013	<0.0001	0.000	<0.0001	<0.0001
heuristic conversation	<0.0001	<0.0001	0.001	<0.0001	0	<0.0001	0.000	0.001	0.044	0.003	<0.0001
discovery learning	<0.0001	0.000	<0.0001	<0.0001	<0.0001	0	0.000	<0.0001	0.010	<0.0001	0.007
concrete/manipulative materials	0.000	<0.0001	0.001	0.013	0.000	0.000	0	0.081	0.242	0.002	0.000
digital resources	<0.0001	0.044	0.010	<0.0001	0.001	<0.0001	0.081	0	0.000	<0.0001	0.020
worksheets	0.037	0.206	0.030	0.000	0.044	0.010	0.242	0.000	0	0.001	0.006
multimedia resources	0.003	0.094	0.001	<0.0001	0.003	<0.0001	0.002	<0.0001	0.001	0	0.005
recyclable materials in experiments	0.000	0.001	0.008	<0.0001	<0.0001	0.007	0.000	0.020	0.006	0.005	0

REFERENCES

AIDOO, B. 2024. A reflective study on adopting inquiry-based science teaching methods. *Disciplinary and Interdisciplinary Science Education Research,* 6**,** 29. https://doi.org/10.1186/s43031-024-00119-3

ARNAB, S., MASTERS, A., PURNOMO, R. A., MAHON, D. & MINOI, J.-L. 2025. Playful and frugal learning design: A value-based approach to inclusive and sustainable STEM education. *Social Sciences & Humanities Open,* 12**,** 101923. https://doi.org/10.1016/j.ssaho.2025.101923

BOTELLA, P., BAENA-MORALES, S., GARCÍA-TAIBO, O. & FERRIZ-VALERO, A. 2022. Effects of Self-Construction of Materials on the Ecological Awareness of Physical Education Primary School Students. *Journal of Environmental Research and Public Health,* 19**,** 14176. https://doi.org/10.3390/ijerph192114176

CORTES, S. T. 2025. Advancing science education through a participatory action research guide for science teachers. *Social Sciences & Humanities Open,* 12**,** 102077. https://doi.org/10.1016/j.ssaho.2025.102077

DEJONCKHEERE, P. J., DE WIT, N., VAN DE KEERE, K. & VERVAET, S. 2016. Exploring the classroom: Teaching science in early childhood. *European Journal of Educational Research,* 5**,** 149-164. https://files.eric.ed.gov/fulltext/EJ1109852.pdf

DORSAH, P. 2026. The Use of Cronbach's Alpha Reliability in Educational Research: A Systematic Review. *European Journal of Contemporary Education E-Learning,* 4**,** 39-50. https://doi.org/10.59324/ejceel.2026.4(2).04

ERHABOR, N. I. & REIS, G. 2026. Low-Cost Educational Materials and University Student Teachers' Recycling Knowledge and Attitudes: A Quasi-Experimental Study. *Education Sciences,* 16**,** 325. https://doi.org/10.3390/educsci16020325

FURNER, J. M. & WORRELL, N. L. 2017. The importance of using manipulatives in teaching math today. *Transformations,* 3**,** 2. https://nsuworks.nova.edu/transformations/vol3/iss1/2

GANAJOVÁ, M., OROSOVÁ, R., SOTÁKOVÁ, I. & LETOŠNíKOVÁ, P. 2025. The effect of inquiry-based teaching on students' attitudes toward science as an academic subject as well as science and technology in general. *Frontiers in Education,* Volume 10 - 2025. https://doi.org/10.3389/feduc.2025.1708139

GÁSPÁR, J., HIDEG, É. & KÖVES, A. 2021. Future in the present: Participatory futures research methods in economic higher education–the development of future competencies. *Journal of Futures Studies,* 26**,** 1-18. https://doi.org/10.6531/JFS.202112_26(2).0001

GRENELL, A., ERNST, J. R. & CARLSON, S. M. 2024. Preschool Children's Science Learning: Instructional Approaches and Individual Differences. *Early education development,* 35**,** 1891-1919. https://doi.org/10.1080/10409289.2024.2360884

HALIMI, F., TRYZNA, M. & BRUNSTEIN, A. 2024. Motivational orientation and perception of active learning instruction by pre-service language teachers. *Frontiers in Psychology,* 15**,** 1307733. https://doi.org/10.3389/fpsyg.2024.1307733

JAKOB, M., BÜCHEL, K., STEFFEN, D. & BRUNETTI, A. 2026. Participatory teaching improves learning outcomes: Evidence from a field experiment in Tanzania. *Journal of Development Economics***,** 103742. https://www.econstor.eu/bitstream/10419/278646/1/1859899595.pdf

JANŠTOVÁ, V., NOVOTNÝ, P., CHLEBOUNOVÁ, I., GUITART, F., FORNE, E. & TORTOSA, M. 2023. Identifying key features of digital resources used during online science practicals. *PloS one,* 18**,** e0283054. https://doi.org/10.1371/journal.pone.0283054

JERRIM, J., OLIVER, M. & SIMS, S. 2022. The relationship between inquiry-based teaching and students' achievement. New evidence from a longitudinal PISA study in England. *Learning and Instruction,* 80**,** 101310. https://doi.org/10.1016/j.learninstruc.2020.101310

KIM, S., RAZA, M. & SEIDMAN, E. 2019. Improving 21st-century teaching skills: The key to effective 21st-century learners. *Research in Comparative International Education,* 14**,** 99-117. https://doi.org/10.1177/1745499919829214

KOTSIS, K. T. 2024. Integrating inquiry-based learning in the new Greek primary science curriculum. *European Journal of Education Pedagogy,* 5**,** 63-71. https://doi.org/10.24018/ejedu.2024.5.6.899

KRANZ, J., BAUR, A. & MÖLLER, A. 2023. Learners' challenges in understanding and performing experiments: a systematic review of the literature. *Studies in Science Education,* 59**,** 321-367. https://doi.org/10.1080/03057267.2022.2138151

KUCHARČÍKOVÁ, A. & TOKARČÍKOVÁ, E. J. 2016. Use of participatory methods in teaching at the university. *TOJSAT-The Online Journal of Science and Technology,* 6**,** 82-90. https://dergipark.org.tr/tr/download/article-file/210211

LEVINA, O., LINDAUER, F. & REVINA, A. 2025. A Participatory Workshop Design for Engaging Young People in IT Sustainability. *Education Sciences,* 15**,** 1570. https://doi.org/10.3390/educsci15121570

MA, Y.-C. 2023. Using Participatory Teaching in Hands-On Courses: Exploring the Influence of Teaching Cases on Learning Motivation. *Education Sciences,* 13**,** 547. https://doi.org/10.3390/educsci13060547

MARTÍN-GARCÍA, J., DIES ÁLVAREZ, M. E. & AFONSO, A. S. 2024. Understanding Science Teachers' Integration of Active Methodologies in Club Settings: An Exploratory Study. *Education Sciences,* 14**,** 106. https://doi.org/10.3390/educsci14010106

MORRIS, D. L. 2025. Rethinking Science Education Practices: Shifting from Investigation-Centric to Comprehensive Inquiry-Based Instruction. *Education Sciences,* 15**,** 73. https://doi.org/10.3390/educsci15010073

NASEER, F., TARIQ, R., ALSHAHRANI, H. M., ALRUWAIS, N. & AL-WESABI, F. N. 2025. Project based learning framework integrating industry collaboration to enhance student future readiness in higher education. *Scientific Reports,* 15**,** 24985. https://doi.org/10.1038/s41598-025-10385-4

OCHOGBOJU, A. O. & DÍEZ-PALOMAR, J. 2025. Modeling Concrete and Virtual Manipulatives for Mathematics Teacher Training: A Case Study in ICT-Enhanced Pedagogies. *Information,* 16**,** 698. https://doi.org/10.3390/info16080698

OLIVEIRA, H. & BONITO, J. 2023. Practical work in science education: a systematic literature review. *Frontiers in Education,* Volume 8 - 2023. https://doi.org/10.3389/feduc.2023.1151641

PARK, J., TEO, T. W., TEO, A., CHANG, J., HUANG, J. S. & KOO, S. 2023. Integrating artificial intelligence into science lessons: teachers' experiences and views. *International Journal of STEM Education,* 10**,** 61. https://doi.org/10.1186/s40594-023-00454-3

PHOTO, P. 2025. Teaching Experiences Connected To The Implementation Of Inquiry-Based Practical Work In Primary Science Classrooms. *Research in Science Education,* 55**,** 1493-1516. https://doi.org/10.1007/s11165-025-10235-3

PRAJOKO, S., AMIN, M., ROHMAN, F., GIPAYANA, M. J. I. J. O. E. & EDUCATION, R. I. 2017. The Usage of Recycle Materials for Science Practicum: Is There Any Effect on Science Process Skills? *International Journal of Evaluation and Research in Education,* 6**,** 1-8. https://scispace.com/pdf/the-usage-of-recycle-materials-for-science-practicum-is-34vbn6lvjf.pdf

REBEKIĆ, A., LONČARIĆ, Z., PETROVIĆ, S. & MARIĆ, S. 2015. Pearson's or Spearman's correlation coefficient-which one to use? *Agriculture*. https://doi.org/10.18047/poljo.21.2.8

REZAI, A., AHMADI, R., ASHKANI, P. & HOSSEINI, G. H. 2025. Implementing active learning approach to promote motivation, reduce anxiety, and shape positive attitudes: A case study of EFL learners. *Acta Psychologica,* 253**,** 104704. https://doi.org/10.1016/j.actpsy.2025.104704

ROY, G., SIKDER, S. & DANAIA, L. 2025. Adopting scientific literacy in early years from empirical studies on formal education: a systematic review of the literature.

International Journal of STEM Education, 12**,** 26. https://doi.org/10.1186/s40594-025-00547-1-025-00547-1
SALEHI GAHRIZSANGI, H., KEWALRAMANI, S. & RICHARDS, G. 2026. Multimodal Technology-Integrated Approaches for Teaching Early Childhood and Early Primary Science: A Scoping Review. *Education Sciences,* 16**,** 586. https://doi.org/10.3390/educsci16040586
SCHOBER, P., BOER, C. & SCHWARTE, L. A. 2018. Correlation Coefficients: Appropriate Use and Interpretation. *Anesthesia and Analgesia,* 126**,** 1763-1768. https://doi.org/10.1213/ane.0000000000002864
SIZER, A., THARP, H., WRIGLEY, J., AL-BATAINEH, A. & PARK, D.-Y. 2021. The impact of pre-service teachers' orientation on the implementation of inquiry-based science instruction. *EURASIA Journal of Mathematics, Science Technology Education,* 17**,** em2028. https://doi.org/10.29333/ejmste/11247
SOWMYA, A. & RANI, R. N. 2025. Emerging interest in science during early childhood period and evaluating its effectiveness. *Scientific Reports,* 15**,** 38683. https://doi.org/10.1038/s41598-025-22513-1
STRAT, T. T. S., HENRIKSEN, E. K. & JEGSTAD, K. M. 2024. Inquiry-based science education in science teacher education: a systematic review. *Studies in Science Education,* 60**,** 191-249. https://doi.org/10.1080/03057267.2023.2207148
TABER, K. S. 2018. The Use of Cronbach's Alpha When Developing and Reporting Research Instruments in Science Education. *Research in Science Education,* 48**,** 1273-1296. https://doi.org/10.1007/s11165-016-9602-2
TAVAKOL, M. & DENNICK, R. 2011. Making sense of Cronbach's alpha. *International journal of medical education,* 2**,** 53. https://doi.org/10.5116/ijme.4dfb.8dfd
THOMAS, M. B., MUSCAT, A., ZUCCOLO, A., LUGUETTI, C. N. & WATT, A. 2025. Navigating Pedagogical Innovation in Higher Education: Education Academics'Experiences with Active and Inquiry-Based Learning in Intensive Teaching. *Innovative Higher Education,* 50**,** 1917-1943. https://doi.org/10.1007/s10755-025-09807-y
VAGIAS, W. M. J., RESEARCH DEVELOPMENT, D. O. P., RECREATION & TOURISM MANAGEMENT, C. U. 2006. Likert-type scale response anchors. clemson international institute for tourism. 4.
VIDAL-ESTEVE, M. I. & MARTÍN-GÓMEZ, S. 2023. Digitalization of Classrooms: A Comparative Study on Teachers' Perceptions about the Use of Digital Teaching Materials in Early Childhood and Primary Education. *Education Sciences,* 13**,** 1156. https://doi.org/10.3390/educsci13111156
ZHANG, H., YANG, J. & LIU, Z. 2024. Effect of teachers' teaching strategies on students' learning engagement: moderated mediation model. *Frontiers in Psychology,* Volume 15 - 2024. https://doi.org/10.3389/fpsyg.2024.1475048

ISSN 1582-1021
e-ISSN 2668-4764
Edited by "Aurel Vlaicu" University Publishing House, Arad, Romania

doi: 10.62591/Scien.Tech.Bull-Chem.FoodSci.Eng.2025.22.03

Scien. Tech. Bull-Chem. Food Sci. Eng., Vol. 22(XXIII), 2025, 41-46
doi: 10.62591/Scien.Tech.Bull-Chem.FoodSci.Eng.2025.22.04

Article

CHANGES IN ANTIOXIDANT ACTIVITY, PHENOLIC CONTENT AND COLOUR CHARACTERISTICS OF RED WINES FOLLOWING DEALCOHOLISATION

Claudia MURESAN[1◆], Flavia BORTES[2,3◆], Alexandru GANCEA[1], Sergiu PALCU[1], Dana Maria COPOLOVICI[1], Lucian COPOLOVICI[1,2], Andreea LUPITU[2], Cristian MOISA[2*]

[1]Faculty of Food Engineering, Tourism and Environmental Protection, "Aurel Vlaicu" University of Arad, Romania, 2 Elena Dragoi, Arad 310330, Romania
[2]Institute for Interdisciplinary Research, "Aurel Vlaicu" University of Arad, Elena Dragoi St. 2, Arad, 310330, Romania
[3]Interdisciplinary Doctoral School of "Aurel Vlaicu" University of Arad, Elena Dragoi St. 2, Arad, 310330, Romania

◆These authors have contributed equally.
Corresponding author email: moisa.cristian@yahoo.com

Abstract: *The increasing interest and demand for low-alcohol and alcohol-free beverages has encouraged wine producers to invest in the development of processes able to reduce ethanol content while preserving the main characteristics of wine. This study evaluated the effect of dealcoholisation by rotary evaporation under reduced pressure on the antioxidant, phenolic and chromatic properties of two experimental red wine blends, designated as Rubra Nova and Armony. Antioxidant activity was determined by the DPPH assay, total phenolic content by the Folin–Ciocâlteu method, while colour characteristics and visible absorption profiles were evaluated by UV–Vis spectrophotometry. Dealcoholisation caused only a slight decrease in DPPH radical inhibition in both wines, while total phenolic content showed a small increase. More evident changes were observed in the chromatic parameters, particularly in colour intensity and hue. However, the overall shape of the UV–Vis spectra remained similar before and after treatment. These results indicate that rotary evaporation under reduced pressure largely preserved the antioxidant and phenolic characteristics of the analysed wines, although some minor changes in their colour properties were observed.*

Keywords: dealcoholised wine; rotary evaporation; antioxidant activity; total phenolic content; chromatic characteristics.

INTRODUCTION

Wine is conventionally defined as the product obtained exclusively through the partial or complete alcoholic fermentation of fresh grapes, either crushed or not, or grape must. Both the International Organisation of Vine and Wine and the European Union regulatory framework establish a minimum actual alcoholic strength of 8.5% vol. for products classified as wine (EU Regulation No 1308/2013, 2013; Kumar et al., 2024; Wine, 2026).

Wine, and particularly red wine is known for being a complex mixture of phenolic compounds, flavonoids, anthocyanins (El Rayess et al., 2024; Muñoz-Bernal et al., 2023), all which contribute to its antioxidant properties, colour and flavour, while several studies associate light-moderate drinking of red wine with the possibility of reducing the risk of cardiovascular diseases (Baxevanis and Kanellos, 2024; Cândido et al., 2026; Castaldo et al., 2019; Monagas et al., 2005).

In recent years, interest in low-alcohol and alcohol-free beverages (beer, wine) has increased considerably, mainly due to changing consumer preferences toward products perceived as more compatible with a healthy lifestyle and moderate alcohol consumption (Catarino and Mendes, 2011; Desk, 2026; Oshima et al., 2022). In Great Britain an increase in the consumption of alcohol-free drinks was observed from 35.0% to 43.9% during 2020 and 2024, and from 25.5% to 38.8% in the attempt to cut down on overall alcohol consumption (Buss et al., 2025).

Demand for these products is also supported by consumers who try to limit or avoid alcohol for health, safety, religious, or other lifestyle reasons, as well as by the need for responsible behaviour in situations such as driving (Kumar et al., 2024; Piornos et al., 2020;

Ruggeri et al., 2026). In this context, dealcoholised wines represent a growing product category aimed at preserving, as closely as possible, the sensory and compositional characteristics of conventional wine while reducing its ethanol content. Some alternatives available to wine producers for obtaining low-alcohol wines include pre-fermentation strategies, such as using grapes with a lower sugar content or reducing the concentration of fermentable sugars in the must by dilution, as well as fermentation-stage approaches, such as interrupting fermentation or using selected or modified yeast strains. Although these methods can effectively reduce ethanol formation, they may negatively affect the sensory characteristics of the final product. Consequently, post-fermentation techniques, including reverse osmosis, osmotic distillation, vacuum distillation, spinning cone column, pervaporation, and diafiltration, are often preferred when the aim is to obtain dealcoholised wines while preserving overall product quality (Akhtar et al., 2025).

In parallel with these consumer-driven trends, recent climate changes and overall increase of annually temperatures, especially during grape ripening season, can result in a higher sugar accumulation in grapes and therefore lead to wines with a higher alcohol content (Parker et al., 2020), further increasing the interest in alcohol-reduction technologies.

In this context, evaluating the effect of dealcoholisation on wines produced from traditional Romanian grape varieties may provide useful information on the preservation of their phenolic and chromatic characteristics.

Therefore, the aim of this study was to investigate the effect of dealcoholisation by rotary evaporation under reduced pressure on the antioxidant activity, total phenolic content, and chromatic characteristics of red wines, with particular emphasis on the preservation of these properties after ethanol removal.

MATERIALS AND METHODS

Wine samples and abbreviations

Two experimental red wine blends, designated as Armony and Rubra Nova, were prepared for this study from local commercially available wines. They were produced as a blend of Cadarcă and Fetească Neagră grapes in the following proportions: 50-50 for Armony and 20-80 for Rubra Nova.

Cadarcă is a traditional red grape variety strongly associated with the Miniș wine-growing region, producing wines typically characterized by a ruby-red colour and distinctive aroma and flavour (Geza et al., 2023), while Fetească Neagră is an autochthonous Romanian variety known for producing deeply coloured wines with a rich phenolic profile and good anthocyanin content (Yao et al., 2026).

Each blend was analysed both in its original form and after dealcoholisation by rotary evaporation under reduced pressure.

Table 1. Abbreviations

Wine name	Original wine	Dealcoholised wines
Rubra Nova	RN	RND
Armony	A	AD

Dealcoholisation by rotary evaporation

Dealcoholisation of both wine blends was performed using a rotary evaporator equipment IKA RV 10 controller and HB 10 heating bath (IKA-Werke GmbH & Co. KG, Staufen, Germany). The samples were processed using the automatic distillation mode with ethanol selected as solvent, a rotation speed of 100 rpm, a heating bath temperature of 60 °C, and an automatically regulated vacuum. The distillation was continued until the automatic endpoint was reached. After dealcoholisation, the samples were restored to their initial volume using distilled water.

Antioxidant activity

The antioxidant activity of the samples was determined using the DPPH radical scavenging assay, according to the method described by (Moisă et al., 2018), with minor modifications. Briefly, 100 µL of wine sample was mixed with 3 mL of freshly prepared 0.2 mM DPPH solution in ethanol and incubated in the dark for 30 minutes at room temperature. Absorbance was measured at 517 nm using a Specord 200 UV-Vis spectrophotometer (Analytik Jena, Germany). The antioxidant activity was expressed as DPPH radical inhibition (%) and was calculated as follows:

DPPH inhibition (%) = $[(A_0-A_s)/A_0] \times 100$

Where A_0 is the absorbance of the DPPH solution and A_s is the absorbance of the sample.

Total phenolic content

The total phenolic content (TPC) of the wine samples was determined using the Folin-Ciocâlteu method described by (Moisă et al., 2018), with minor modifications. Briefly, 1 mL diluted wine sample 1:25 with distilled water, was mixed with 0.5 mL Folin-Ciocâlteu reagent, 2 mL of 20% Na_2CO_3 solution, and 5 mL of distilled water. The mixture was incubated for 45 minutes at room temperature in the dark, and the absorbance was measured at 765 nm using a Specord 200 UV-Vis spectrophotometer (Analytik Jena, Germany). Total phenolic content was calculated using a gallic acid calibration curve and expressed as mg gallic acid equivalents per liter (mg GAE/L).

UV-Vis spectral and chromatic characteristics of wine

The UV-Vis spectra of the original and dealcoholised wine samples were recorded in the 400-650 nm range using a Specord 200 UV-Vis spectrophotometer (Analytik Jena, Germany). The resulting spectra were overlaid to evaluate changes in the absorption profile following dealcoholisation.

The chromatic characteristics were determined spectrophotometrically according to the method described by (Glories, 1984) and subsequently applied in wine colour studies (Gambuti et al., 2022). The absorbance was measured at 420, 520 and 620 nm using a UV-Vis spectrophotometer. Colour intensity (CI) was calculated as the sum of the absorbance values at the three wavelengths (A420 + A520 + A620), while hue was expressed as the A420/A520 ratio. The relative contributions of the yellow, red and blue components were calculated as percentages of the total colour intensity. The dA% parameter that represents the contribution of the red component associated with flavylium forms of free and combined anthocyanins, was calculated according to Glories method.

RESULTS AND DISCUSSIONS

The impact of dealcoholisation by rotary evaporation was assessed by comparing each dealcoholised wine with its corresponding original sample in terms of antioxidant activity, total phenolic content and chromatic characteristics (Figure 1).

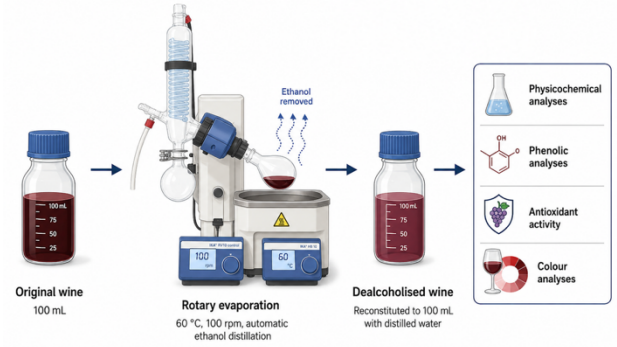

Figure 1. Schematic representation of the experimental workflow used for wine dealcoholisation and analysis (image generated using AI)

Antioxidant activity and phenolic content

Antioxidant activity, expressed as DPPH radical inhibition, remained high in all analysed samples, with values ranging from 83.04 to 87.08% (Table 2). Following dealcoholisation, only a slight decrease was observed for both wines, from 87.08% to 86.40% in Rubra Nova and from 83.77% to 83.04% in Armony. In contrast, total phenolic content showed a slight increase after treatment, from 1723.40 to 1743.59 mg GAE/L for Rubra Nova and from 2373.78 to 2425.80 mg GAE/L for Armony (Table 2). Overall, Armony exhibited a higher phenolic content than Rubra Nova, whereas Rubra Nova showed slightly higher DPPH radical inhibition.

Table 2. DPPH radical inhibition and total phenolic content of original and dealcoholised wines

Sample	DPPH Inhibition (%)	TPC (mg GAE/L)
RN	87.08 ± 0.14	1723.40 ± 7.24
RND	86.40 ± 0.10	1743.59 ± 5.58
A	83.77 ± 0.36	2373.78 ± 27.74
AD	83.04 ± 0.34	2425.80 ± 3.12

Values are expressed as mean ± SEM (n = 3).

According to (Belisario-Sánchez et al., 2009) the antioxidant activity expressed as DPPH radical inhibition remained high and was similar after dealcoholisation with minor decreases observed for the analysed samples. In

the present study, the same variations were observed after rotary evaporation: both wine blends preserved their antioxidant capacity with minor decreases under 1%. In the case of phenolic compounds, several studies (Belisario-Sánchez et al., 2009; Motta et al., 2017) present a slight increase in total phenolic content after dealcoholisation, an effect associated with ethanol removal and a part of the volatile fraction.

These results suggest that rotary evaporation had only a limited effect on the antioxidant capacity of the wines, while the small increase in total phenolic content (20-50 mg GAE/L) may be related to changes in sample concentration or matrix composition during dealcoholisation or even variations of the Folin–Ciocâlteu assay.

UV-Vis spectral and chromatic characteristics of wine

The chromatic parameters showed clear differences between the two wines and between the original and dealcoholised samples (Figure 2). Armony exhibited a higher colour intensity than Rubra Nova both before and after dealcoholisation. Following rotary evaporation, colour intensity increased from 1.6342 to 2.0281 in Rubra Nova and from 3.3222 to 3.9553 in Armony, corresponding to increases of approximately 24% and 19%, respectively (Table 3). Changes were also observed in the relative contribution of the individual colour components. In Rubra Nova, dealcoholisation slightly increased the red component from 44.55% to 45.61% and dA from 61.89% to 66.15%, while hue decreased from 1.0032 to 0.9348 (Table 3). In contrast, Armony showed a decrease in the relative red contribution from 48.22% to 44.51% and in dA from 69.53% to 65.36%, accompanied by an increase in hue from 0.8417 to 0.9696. The blue component increased slightly after dealcoholisation in both wines.

Previous studies on dealcoholised wines observed a colour increase for red wines subjected to vacuum distillation, literature data indicating an increase ranging between 17 to 98%, depending on the type of wine and processing conditions. This behaviour was mainly attributed to concentration effect associated with ethanol removal (Motta et al., 2017; Sam et al., 2021). More recently, (Kumar et al., 2025) reported an increased colour intensity in red dealcoholised wine. The increases observed in the present study, approximately 24% for Rubra Nova and 19% for Armony fall within the range previously reported for dealcoholised wines.

For hue differences, a slight decrease is reported (Kumar et al., 2024), Rubra Nova has a similar trend while Armony presented the opposite behaviour. These differences indicate that the initial pigment composition and wine matrix are important.

Table 3. Chromatic characteristics of original and dealcoholised red wines determined by the Glories method.

Sample	Colour intensity	Hue	Yellow (%)	Red (%)	Blue (%)	dA (%)
RN	1.6342	1.0032	44.70	44.55	10.75	61.89
RND	2.0281	0.9348	42.64	45.61	11.75	66.15
A	3.3222	0.8417	40.58	48.22	11.20	69.53
AD	3.9553	0.9696	43.16	44.51	12.32	65.36

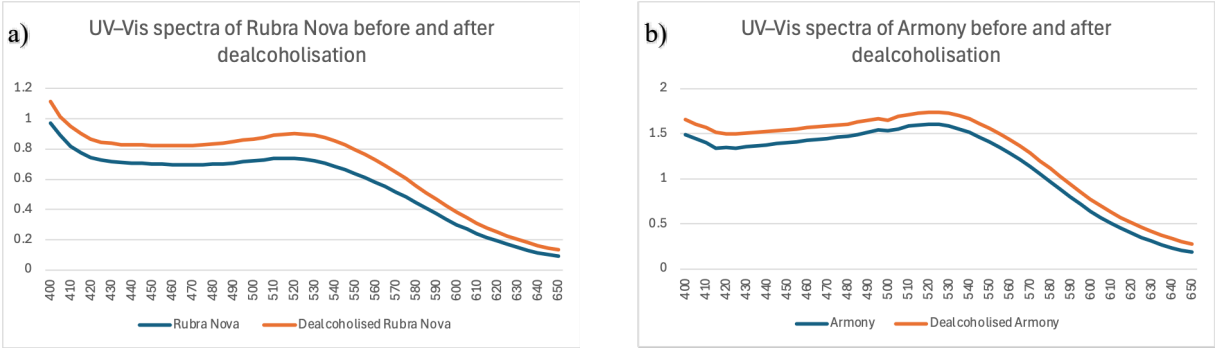

Figure 2. UV–Vis absorption spectra of red wines before and after dealcoholisation: (a) Rubra Nova; (b) Armony

The chromatic changes observed after dealcoholisation were also reflected in the UV–Vis spectral profiles (Figure 2). In both wines, the dealcoholised samples showed higher absorbance over most of the 400–650 nm range, while the overall shape of the spectra remained similar to that of the corresponding original wines. This behaviour is consistent with the increase in colour intensity calculated using the Glories parameters and suggests that dealcoholisation mainly affected the scale of visible absorption rather than producing major changes in the overall spectral profile.

CONCLUSIONS

Dealcoholisation by rotary evaporation under reduced pressure had a limited effect on the antioxidant properties of the analysed red wine blends. DPPH inhibition showed only a slight decrease, while total phenolic content slightly increased after treatment. More evident changes were observed in the chromatic parameters, particularly in colour intensity and hue, with the magnitude and direction of some changes depending on the wine blend. Nevertheless, the overall UV–Vis spectral profiles remained similar before and after dealcoholisation. Overall, within the parameters evaluated in this study, rotary evaporation under reduced pressure largely preserved the antioxidant and phenolic characteristics of the wines, while inducing moderate and wine-dependent changes in their colour properties.

ACKNOWLEDGEMENTS

This work was carried out within the framework of the Erasmus+ BIP Intensive Programme “JOINED BY WINE – JOURNEY OF A CRAFT”, involving the European “University Miguel de Cervantes” (Valladolid, Spain), “Aurel Vlaicu” University of Arad (Romania), University of Maia – UMAIA (Portugal) and Gal Ferenc University, Bekescsaba, Hungary.

Funding for the equipment used in the study has been provided by The European Commission and The Romanian Government (project POSCCE 621/2014).

REFERENCES

Akhtar, W., Ceci, A.T., Longo, E., Marconi, M.A., Lonardi, F., Boselli, E., 2025. Dealcoholised wine: Techniques, sensory impacts, stability, and perspectives of a growing industry. Compr Rev Food Sci Food Saf 24, e70171.

Baxevanis, G.K., Kanellos, P.T., 2024. Red Wine Consumption and the Impact on Cardiovascular Health: The Methodological Barriers of Observational Study Design. Journal of Medicinal Food 27, 1009-1017.

Belisario-Sánchez, Y.Y., Taboada-Rodríguez, A., Marín-Iniesta, F., López-Gómez, A., 2009. Dealcoholised wines by spinning cone column distillation: phenolic compounds and antioxidant activity measured by the 1,1-diphenyl-2-picrylhydrazyl method. J Agric Food Chem 57, 6770-6778.

Buss, V., Kale, D., Oldham, M., Shahab, L., Stevely, A., Kersbergen, I., Brown, J., 2025. Trends in use of alcohol-free or low alcohol drinks in attempts to reduce alcohol consumption in Great Britain, 2020-2024: a population-based study. BMJ Public Health 3, e002775.

Cândido, R., C.Cunha, S., O.Fernandes, J., Faria, A.C., 2026. Dealcoholisation of wine by pervaporation. Food Chemistry: X 36, 103988.

Castaldo, L., Narváez, A., Izzo, L., Graziani, G., Gaspari, A., Minno, G.D., Ritieni, A., 2019. Red Wine Consumption and Cardiovascular Health. Molecules 24.

Catarino, M., Mendes, A., 2011. Dealcoholising wine by membrane separation processes. Innov. Food Sci. Emerg. Technol. 12, 330-337.

Desk, F.M.F.B., 2026. Non-Alcoholic Wine Market. Fact.MR, Market Research Company.

El Rayess, Y., Nehme, N., Azzi-Achkouty, S., Julien, S.G., 2024. Wine Phenolic Compounds: Chemistry, Functionality and Health Benefits. Antioxidants (Basel) 13.

EU Regulation No 1308/2013, p., 2013. The European Parliament and of the Council of 17 December 2013 establishing a common organisation of the markets in agricultural products and repealing Council Regulations (EEC) No 922/72, (EEC) No 234/79, (EC) No 1037/2001 and (EC) No 1234/2007., in: Council, T.E.P.a.o.t. (Ed.), Official Journal of the European Union.

Gambuti, A., Picariello, L., Forino, M., Errichiello, F., Guerriero, A., Moio, L., 2022. How the Management of pH during Winemaking Affects Acetaldehyde, Polymeric Pigments and Color Evolution of Red Wine. Applied Sciences 12, 2555.

Geza, B., Lunka, T., JoÓ, J., Moldován, C., Zsolt, S.-V., Putnoky-Csicsó, B., Kentelky, E., 2023.

Fermentation Temperature And Duration Effect On The Quality And Anthocyanin Content Of Kadarka Wine Produced In The Miniș (Ménes) Wine Region. LXVII, 227-232.
Glories, Y., 1984. La couleur des vins rouges. 2e partie : mesure, origine et interprétation. OENO One 18, 253.
Kumar, Y., Italiano, L., Schmitt, M., Ricci, A., Parpinello, G.P., Versari, A., 2025. Dealcoholisation of wine by vacuum distillation: Volatile and non-volatile profile, and sensory analysis. Food Chem 495, 146499.
Kumar, Y., Ricci, A., Parpinello, G.P., Versari, A., 2024. Dealcoholised Wine: A Scoping Review of Volatile and Non-Volatile Profiles, Consumer Perception, and Health Benefits. Food and Bioprocess Technology 17, 3525-3545.
Moisă, C., Copolovici, L., Bungau, S., Pop, G., Imbrea, I., Lupitu, A.-I., Nemeth, S., Copolovici, D., 2018. Wastes resulting from aromatic plants distillation - bio-sources of antioxidants and phenolic compounds with biological active principles. Revista Farmacia 66, 289-295.
Monagas, M., Bartolomé, B., Gómez-Cordovés, C., 2005. Updated knowledge about the presence of phenolic compounds in wine. Crit Rev Food Sci Nutr 45, 85-118.
Motta, S., Guaita, M., Petrozziello, M., Ciambotti, A., Panero, L., Solomita, M., Bosso, A., 2017. Comparison of the physicochemical and volatile composition of wine fractions obtained by two different dealcoholisation techniques. Food Chem 221, 1-10.
Muñoz-Bernal, Ó.A., Vazquez-Flores, A.A., de la Rosa, L.A., Rodrigo-García, J., Martínez-Ruiz, N.R., Alvarez-Parrilla, E., 2023. Enriched Red Wine: Phenolic Profile, Sensory Evaluation and In Vitro Bioaccessibility of Phenolic Compounds. Foods 12, 1194.
Oshima, S., Shiiya, S., Kato, Y., 2022. Effects of Regular Low-Level Alcohol Consumption in Healthy Individuals: A Randomized, Double-Blind, Placebo-Controlled Crossover Study. Healthcare (Basel) 10.
Parker, A.K., García de Cortázar-Atauri, I., Gény, L., Spring, J.-L., Destrac, A., Schultz, H., Molitor, D., Lacombe, T., Graça, A., Monamy, C., Stoll, M., Storchi, P., Trought, M.C.T., Hofmann, R.W., van Leeuwen, C., 2020. Temperature-based grapevine sugar ripeness modelling for a wide range of Vitis vinifera L. cultivars. Agric. For. Meteorol. 285-286, 107902.
Piornos, J.A., Balagiannis, D.P., Methven, L., Koussissi, E., Brouwer, E., Parker, J.K., 2020. Elucidating the Odor-Active Aroma Compounds in Alcohol-Free Beer and Their Contribution to the Worty Flavor. Journal of Agricultural and Food Chemistry 68, 10088-10096.
Ruggeri, G., Mazzocchi, C., Selicorni, T., 2026. From tradition to moderation: Italian consumers' attitudes and price acceptance for dealcoholised wines. Future Foods 14, 101102.
Sam, F.E., Ma, T., Liang, Y., Qiang, W., Atuna, R.A., Amagloh, F.K., Morata, A., Han, S., 2021. Comparison between Membrane and Thermal Dealcoholisation Methods: Their Impact on the Chemical Parameters, Volatile Composition, and Sensory Characteristics of Wines. Membranes 11, 957.
Wine, I.O.o.V.a., 2026. International Code of Oenological Practices.
Yao, M., Wang, F., Arpentin, G., 2026. Exploratory terroir differentiation of Fetească Neagră wines via volatile aroma compounds in Moldovan regions. Journal of Food Measurement and Characterization 20, 5412-5426.

doi: 10.62591/Scien.Tech.Bull-Chem.FoodSci.Eng.2025.22.04

Scien. Tech. Bull-Chem. Food Sci. Eng., Vol. 22(XXIII), 2025, 47-54
doi: 10.62591/Scien.Tech.Bull-Chem.FoodSci.Eng.2025.22.05

Review

THE USE OF AI IN FINDING NEW ANTIMICROBIALS

Ana Maria Tolos (Vasii)[1,2], Cristian MOISA[3], Lucian COPOLOVICI[1,3], Dana-Maria COPOLOVICI[1,3]*

[1]Institute for Interdisciplinary Research, "Aurel Vlaicu" University of Arad, Elena Dragoi St., Nr. 2, 310330, vArad, Romania
[2] Biomedical Sciences Doctoral School, University of Oradea, Universitatii Str., Nr. 1, 410087, *Oradea, Romania*
[3]Faculty of Food Engineering, Tourism and Environmental Protection, "Aurel Vlaicu" University of Arad, Elena Dragoi St., Nr. 2, 310330, Arad, Romania
**Corresponding author: dana.copolovici@uav.ro*

Abstract: *The pressing need for new antimicrobial drugs has been highlighted by the growing problem of antimicrobial resistance (AMR). The quick creation of efficient medicines is hampered by the time-consuming and expensive nature of traditional drug discovery techniques. Artificial intelligence (AI) has recently surfaced as a potentially useful technology to speed up the discovery of novel antimicrobials. From anticipating chemical interactions to improving drug candidates, artificial intelligence (AI) technologies including machine learning, deep learning, and natural language processing have been used at different phases of antimicrobial development. AI can find previously undiscovered chemicals and forecast their effectiveness against resistant infections by examining enormous datasets of chemical structures, biological activity, and genomic data. This study examines the use of AI in antimicrobial drug discovery, emphasizing how it can expedite the drug development process, increase target identification precision, and encourage the creation of new compounds with improved potency and selectivity. We also go over the drawbacks and difficulties of incorporating AI into antimicrobial research, such as the requirement for interdisciplinary cooperation, data quality, and model interpretability. Finally, AI-driven strategies present a promising opportunity to tackle the worldwide AMR epidemic and quicken the creation of critically required antibiotic treatments. As an alternative to traditional antibiotics, antimicrobial peptides (AMPs) show promise as agents against antimicrobial resistance. AMP discovery was transformed by artificial intelligence (AI) using both generation and discrimination techniques. The vast field of drug discovery is always looking for new and creative ways to find and create peptide-based medicines. The development of novel peptide medications has undergone a radical change since the introduction of artificial intelligence (AI). A variety of computer tools and algorithms provided by AI allow researchers to expedite the development of therapeutic peptides.*

Keywords: artificial intelligence, antimicrobial peptides, antibiotics, machine learning

INTRODUCTION

In recent years, the rise of antimicrobial resistance (AMR) has emerged as a global health crisis, threatening our ability to treat infections effectively. As traditional antimicrobial discovery faces increasing challenges, artificial intelligence (AI) is stepping in as a transformative tool in the search for new antimicrobial agents. Since its recent technological advancement, AI has been quickly used into medication research, significantly increasing the effectiveness of finding new antibiotics (Liu et al., 2024b).

This narrative review explores how AI is being utilized in the discovery of new antimicrobials, the possible benefits it offers, as well as future prospects, with particular attention to antimicrobial peptides.

Antibiotics have emerged as the mainstay of contemporary medicine since the discovery of penicillin. However, because antibiotic-resistance determinants are spreading throughout the world, it is unknown if these

necessary medications will remain effective (Stokes et al., 2020).

Antibacterial peptides (ABPs) are a family of peptides found in nature that play a crucial role in the innate immune systems of organisms. These ABPs offer several advantages over widely used antibiotics. As a result, they have recently received a lot of attention as potential replacements for currently available antibiotics. But it is expensive and time-consuming to identify ABPs from natural sources, AI-based approaches could facilitate screening and optimization of AMP candidates (Sharma et al., 2024).

In reaction to environmental challenges, pathogens undergo various changes in their genomes, resulting in AMR. As a consequence of AMR, these pathogens become unresponsive to antibiotics (Sharma et al., 2024).

AI has significantly sped the development of novel antibiotics in recent years (Cesaro et al., 2023; Stokes et al., 2020; Wong et al., 2023). New AI-based antibiotic candidates can now be discovered in hours due to computational screening, compared to conventional discovery workflows that take years. Millions of individuals still pass away from infections every year despite these scientific and technological advancements (Murray et al., 2022; Naghavi et al., 2024). More than 4 million people died in 2019 alone as a result of pan-drug-resistant bacteria that have emerged because of the overuse and abuse of antibiotics. However, antibiotic-resistant genes are not the only reason why antimicrobial treatments fail to successfully cure people and eradicate infections. Antibiotic failure is caused by a variety of circumstances, including intricate systems underpinning serious clinical situations like sepsis (Cesaro et al., 2023). This complex problem is becoming a major worldwide concern.

Since its recent technological advancement, AI has been quickly used into medication research, significantly increasing the effectiveness of finding new antibiotics (Liu et al., 2024b).

1.Artificial Intelligence in Drug Development

AI is anticipated to streamline and expedite pharmaceutical development in the future. By using robotics and models of genetic targets, medications, organs, diseases and their course, pharmacokinetics, safety, and efficacy, AI can transform the labour-intensive process of drug development into one that requires capital and data (Naik et al., 2022). The drug discovery and development process can be accelerated and made more economical and efficient with the application of AI. AI was previously used to find possible Ebola virus medications, but like with any pharmacological study, finding a lead compound does not ensure the creation of a safe and effective treatment (Stephenson, 2021).

AI has the ability to close gaps in rural communities and resource-poor nations, increasing access to healthcare services. AI could be used to conduct screening and evaluation in settings with limited resources if insufficient medical expertise is available, a common challenge in many resource-poor settings (Stephenson, 2021).

Using algorithms that can produce and assess a huge number of peptide sequences according to desired characteristics, like target affinity, selectivity, and bioavailability, is known as AI-driven peptide design. Compared to conventional techniques, these algorithms are more thorough and effective at exploring vast chemical regions (Nissan et al., 2024).

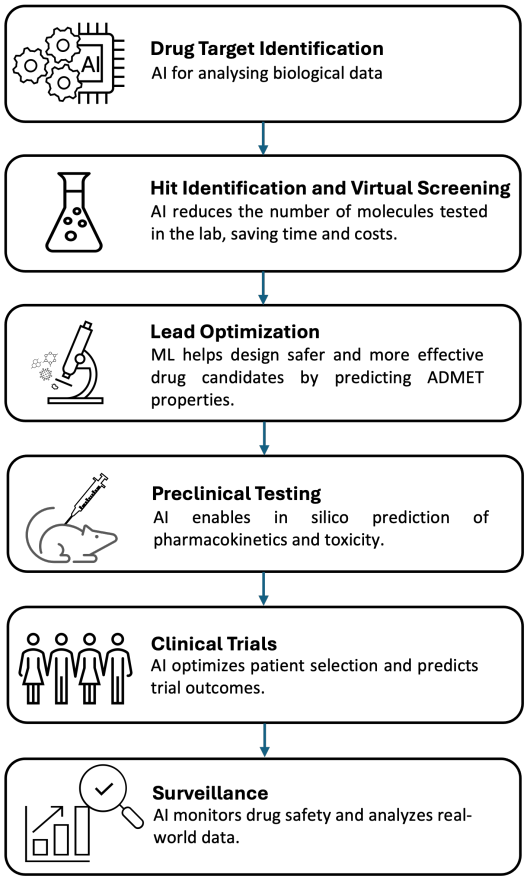

Figure 1. Schematic representation of AI in drug development.

2. Machine learning (ML)

With its many uses in computer vision, language processing, gaming, and computational biology, machine learning (ML), a subfield of artificial intelligence, has advanced significantly. Some machine learning models make use of deep learning (DL), a technique that uses deep networks (DNNs) to predict outcomes and extract hidden features from complicated datasets, such as biomolecular structures and photographs (Liu et al., 2024b; Stokes et al., 2020; Wan et al., 2024a).

In addition to producing medicines, machine-learning (ML) models have been used to forecast antimicrobial resistance, haemolysis, and antimicrobial activity (Wan et al., 2022).

ML can be used to predict macromolecular structures and therapeutic features, including antibiotic activity and absorption, distribution, metabolism, excretion, and toxicity (ADMET) (Wan et al., 2024b).

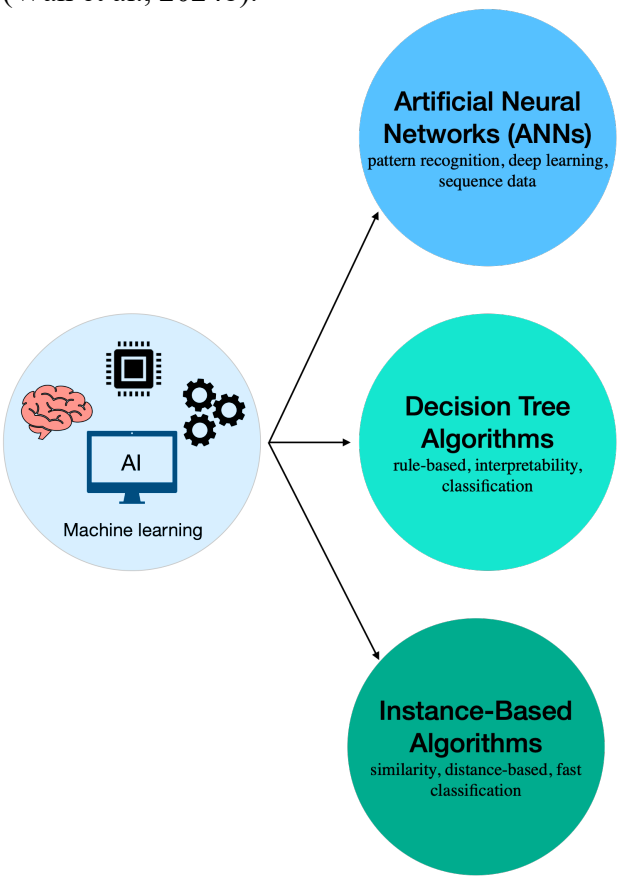

Figure 2. Schematic representation of ML.

The use of AI in the development of novel peptide drugs has bright future prospects and has the potential to completely transform the peptide drug discovery process. To fully realize the potential of AI-driven techniques and guarantee their successful incorporation into the drug development pipeline, a number of obstacles must be overcome. Expanding and improving AI models through the use of more extensive and varied datasets is one of the fundamental prerequisites (Bilal et al., 2025).

For example, machine learning has identified genetic traits associated with antibiotic sensitivity in *Escherichia coli* across various sequence types (STs) (Bilal et al., 2025). These genetic markers help elucidate how STs evolve and spread within populations that are likely to facilitate dissemination (Shaik et al., 2022). Similarly, it was used to predict *Streptococcus pneumoniae* susceptibility to β-lactam antibiotics by correlating penicillin-binding protein (PBP) sequences with minimum inhibitory concentrations (MIC) values (Zhang et al., 2019).

Intricate patterns in a variety of data can be found using AI/ML methods, which can shed light on the processes behind the emergence of drug resistance (Liu et al., 2024a). An AI-based tool called PathogenWatch makes it possible to analyze and visualize microbial genome sequences in real-time in both geographical and phylogenetic settings, which enhances the tracking and monitoring of pathogen outbreaks (Vashisht et al., 2023). Real-time monitoring enabled by AI/ML helps to promptly modify containment and treatment plans (Vashisht et al., 2023).

Using a dataset of 312 antibiotics and 936 non-antibiotic medications, researchers trained eight distinct algorithms—including extreme gradient boosting, random forest, deeper neural networks, and gradient boosting classifier—to predict novel antimicrobial compounds. With five-fold cross-validation, the top four classifiers obtained over 80% accuracy in both test and blind data (Jana et al., 2024).

Table 1. A list of antimicrobial agents and peptides discovered or designed using artificial intelligence (AI) and machine learning (ML)

Antimicrobial Agent	Methods Used	Properties	References
SPR206	Structure-activity relationship (SAR) models	Reduced nephrotoxicity, high efficacy	(Hazrat et al., 2025; Zhang et al., 2020)
QPX9003	AI-guided structure optimization	Improved safety profile, effective at lower doses	(Castanheira et al., 2019)
MRX−8	Predictive modeling	Lower toxicity, enhanced pharmacokinetics	(Duncan et al., 2022)
Murepavadin	Iterative peptidomimetic design	High specificity, effective in biofilms	(Sader et al., 2018)
IB−367	AI peptide design	Safe but limited efficacy in clinical settings	(Mosca et al., 2000)
SCH−79797	ML based dual mechanism profiling	Broad-spectrum efficacy	(Martin et al., 2020; Mosca et al., 2000)
Bactenecin	Machine-learning classifer	Broad-spectrum efficacy	(Wu et al., 1999)
DP7	AI-driven sequence optimization	Low cytotoxicity, strong biofilm activity	(Wu et al., 2014)
Lead AMPs	PanCleave random forest modeling	Low toxicity, high specificity	(Maasch et al., 2023)

3. Deep Learning

Deep learning models have shown promise in predicting molecular properties and biological activities of compounds. Deep-learning approaches applied to antibiotic discovery include graph neural networks (GNN) and message-passing neural networks (MPNN) for molecular activity prediction, convolutional neural networks (CNNs) and transformers for compound or antimicrobial peptide classification, and generative architectures such as autoencoders and variational autoencoders (VAEs), generative adversarial networks (GANs), diffusion models, and reinforcement-learning frameworks for the de novo design and optimization of antibacterial molecules. By training on datasets that include chemical structures and their associated biological responses, these models can suggest novel compounds that may not have been previously considered. HydrAMP is a deep-learning model that learns the main structural features of peptides together with their antimicrobial properties, allowing it to generate new peptide sequences or improved analogues of known peptides. By combining this design process with computational screening and molecular dynamics simulations, HydrAMP can prioritize promising candidates for experimental testing and improve the chances of identifying active antimicrobial peptides. This approach was used to obtain Hydraganan-1, an analogue of pexiganan and showed strong activity against *E. coli* (Szymczak et al., 2023). DeepAMP is a peptide language-based deep generative framework designed to discover potent, broad-spectrum antimicrobial peptides. It was successfully used to generate 18 candidates with strong activity against both Gram-positive and Gram-negative bacteria, reduced potential for resistance development, and three of them demonstrated efficacy in an in vivo wound infection model (Li et al., 2024). AMP-Diffusion is a generative AI platform that combines latent diffusion modeling with protein language embeddings to design novel antimicrobial peptides. By using this model the authors obtained a high experimental success rate of the AMPS tested against both susceptible and multidrug-resistant bacteria, with low toxicity and promising in vivo efficacy for two peptides, comparable to clinically used antibiotics (Torres et al., 2025).

4. Challenges and Future Directions

While the use of AI in antimicrobial discovery is promising, several challenges remain. Data quality, accessibility, and the need for interdisciplinary collaboration are all crucial for advancing this field. Additionally, regulatory and ethical considerations must be addressed as AI-driven solutions become more prevalent in drug development. The use of AI in the development of novel peptide drugs has bright future prospects and has the potential to completely transform the peptide drug discovery process. To fully realize the potential of AI-driven techniques and guarantee their successful incorporation into the drug development pipeline, a number of obstacles must be overcome. Expanding and improving AI models through the use of more extensive and varied datasets is one of the fundamental prerequisites (Nissan et al., 2024).

CONCLUSIONS

AI is revolutionizing and overall, increasingly contributing to the discovery of new antimicrobials, offering efficient, accurate, and innovative approaches to combat antimicrobial resistance. As researchers continue to leverage AI technologies, the hope for effective solutions to tackle resistant infections becomes increasingly attainable. Embracing this interdisciplinary approach may hold the key to safeguarding public health against the ever-evolving threat of resistant pathogens. However, all AI-generated predictions still require an experimental validation process.

ACKNOWLEDGEMENTS

This work was supported by a grant of the Ministry of Research, Innovation and Digitization, CNCS - UEFISCDI, project number PN-III-P4-PCE-2021-0639, within PNCDI III.

DECLARATION OF GENERATIVE AI AND AI-ASSISTED TECHNOLOGIES

During the preparation of this work, the authors used ChatGPT-4 to assist with grammar checking. After utilizing this tool, the authors reviewed and edited the content as necessary and take full responsibility for the final content of the publication.

REFERENCES

Bilal, H., Khan, M.N., Khan, S., Shafiq, M., Fang, W., Khan, R.U., Rahman, M.U., Li, X., Lv, Q.-L., Xu, B., 2025. The role of artificial intelligence and machine learning in predicting and combating antimicrobial resistance. Computational and Structural Biotechnology Journal 27, 423-439.

Castanheira, M., Lindley, J., Huynh, H., Mendes, R.E., Lomovskaya, O., 2019. 690. Activity of a novel polymyxin analog, QPX9003, tested against resistant Gram-negative pathogens, including carbapenem-resistant Acinetobacter, Enterobacterales, and Pseudomonas, Open Forum Infectious Diseases, p. S313.

Cesaro, A., Bagheri, M., Torres, M., Wan, F., de la Fuente-Nunez, C., 2023. Deep learning tools to accelerate antibiotic discovery. Expert Opinion on Drug Discovery 18, 1245-1257.

Duncan, L.R., Wang, W., Sader, H.S.J.A.A., Chemotherapy, 2022. In vitro potency and spectrum of the novel polymyxin MRX-8 tested against clinical isolates of gram-negative bacteria. 66, e00139-00122.

Hazrat, B., Muhammad Nadeem, K., Sabir, K., Muhammad, S., Wenjie, F., Rahat Ullah, K., Mujeeb Ur, R., Xiaohui, L., Qiao-Li, L., Bin, X., 2025. The role of artificial intelligence and machine learning in predicting and combating antimicrobial resistance. Computational and Structural Biotechnology Journal 27, 423-439.

Jana, T., Sarkar, D., Ganguli, D., Mukherjee, S.K., Mandal, R.S., Das, S.J.I.J.o.M.R., 2024. ABDpred: Prediction of active antimicrobial compounds using supervised machine learning techniques. 159, 78-90.

Li, T., Ren, X., Luo, X., Wang, Z., Li, Z., Luo, X., Shen, J., Li, Y., Yuan, D., Nussinov, R., Zeng, X., Shi, J., Cheng, F., 2024. A Foundation Model Identifies Broad-Spectrum Antimicrobial Peptides against Drug-Resistant Bacterial Infection. Nature Communications 15, 7538.

Liu, G.Y., Yu, D., Fan, M.M., Zhang, X., Jin, Z.Y., Tang, C., Liu, X.F., 2024a. Antimicrobial resistance crisis: could artificial intelligence be the solution? Military Medical Research 11.

Liu, G.Y., Yu, D., Fan, M.M., Zhang, X., Jin, Z.Y., Tang, C., Liu, X.F., 2024b. Antimicrobial resistance crisis: could artificial intelligence be the solution? Military Medical Research 11, 7.

Maasch, J.R., Torres, M.D., Melo, M.C., de la Fuente-Nunez, C.J.C.H., Microbe, 2023. Molecular de-extinction of ancient antimicrobial peptides enabled by machine learning. 31, 1260-1274. e1266.

Martin, J.K., Sheehan, J.P., Bratton, B.P., Moore, G.M., Mateus, A., Li, S.H.-J., Kim, H., Rabinowitz, J.D., Typas, A., Savitski, M.M.J.C., 2020. A dual-mechanism antibiotic kills gram-negative bacteria and avoids drug resistance. 181, 1518-1532. e1514.

Mosca, D.A., Hurst, M.A., So, W., Viajar, B.S., Fujii, C.A., Falla, T.J.J.A.a., chemotherapy, 2000. IB-367, a protegrin peptide with in vitro and in vivo activities against the microflora associated with oral mucositis. 44, 1803-1808.

Murray, C.J.L., Ikuta, K.S., Sharara, F., Swetschinski, L., Robles Aguilar, G., Gray, A., Han, C., Bisignano, C., Rao, P., Wool, E., Johnson, S.C., Browne, A.J., Chipeta, M.G., Fell, F., Hackett, S., Haines-Woodhouse, G., Kashef Hamadani, B.H., Kumaran, E.A.P., McManigal, B., Achalapong, S., Agarwal, R., Akech, S., Albertson, S., Amuasi, J., Andrews, J., Aravkin, A., Ashley, E., Babin, F.-X., Bailey, F., Baker, S., Basnyat, B., Bekker, A., Bender, R., Berkley, J.A., Bethou, A., Bielicki, J., Boonkasidecha, S., Bukosia, J., Carvalheiro, C., Castañeda-Orjuela, C., Chansamouth, V., Chaurasia, S., Chiurchiù, S., Chowdhury, F., Clotaire Donatien, R., Cook, A.J., Cooper, B., Cressey, T.R., Criollo-Mora, E., Cunningham, M., Darboe, S., Day, N.P.J., De Luca, M., Dokova, K., Dramowski, A., Dunachie, S.J., Duong Bich, T., Eckmanns, T., Eibach, D., Emami, A., Feasey, N., Fisher-Pearson, N., Forrest, K., Garcia, C., Garrett, D., Gastmeier, P., Giref, A.Z., Greer, R.C., Gupta, V., Haller, S., Haselbeck, A., Hay, S.I., Holm, M., Hopkins, S., Hsia, Y., Iregbu, K.C., Jacobs, J., Jarovsky, D., Javanmardi, F., Jenney, A.W.J., Khorana, M., Khusuwan, S., Kissoon, N., Kobeissi, E., Kostyanev, T., Krapp, F., Krumkamp, R., Kumar, A., Kyu, H.H., Lim, C., Lim, K., Limmathurotsakul, D., Loftus, M.J., Lunn, M., Ma, J., Manoharan, A., Marks, F., May, J., Mayxay, M., Mturi, N., Munera-Huertas, T., Musicha, P., Musila, L.A., Mussi-Pinhata, M.M., Naidu, R.N., Nakamura, T., Nanavati, R., Nangia, S., Newton, P., Ngoun, C., Novotney, A., Nwakanma, D., Obiero, C.W., Ochoa, T.J., Olivas-Martinez, A., Olliaro, P., Ooko, E., Ortiz-Brizuela, E., Ounchanum, P., Pak, G.D., Paredes, J.L., Peleg, A.Y., Perrone, C., Phe, T., Phommasone, K., Plakkal, N., Ponce-de-Leon, A., Raad, M., Ramdin, T., Rattanavong, S., Riddell, A., Roberts, T., Robotham, J.V., Roca, A., Rosenthal, V.D., Rudd, K.E., Russell, N., Sader, H.S., Saengchan, W., Schnall, J., Scott, J.A.G., Seekaew, S., Sharland, M., Shivamallappa, M., Sifuentes-Osornio, J., Simpson, A.J., Steenkeste, N., Stewardson, A.J., Stoeva, T., Tasak, N., Thaiprakong, A., Thwaites, G., Tigoi, C., Turner, C., Turner, P., van Doorn, H.R., Velaphi, S., Vongpradith, A., Vongsouvath, M., Vu, H., Walsh, T., Walson, J.L., Waner, S., Wangrangsimakul, T., Wannapinij, P., Wozniak, T., Young Sharma, T.E.M.W., Yu, K.C., Zheng, P., Sartorius, B., Lopez, A.D., Stergachis, A., Moore, C., Dolecek, C., Naghavi, M., 2022. Global burden of bacterial antimicrobial resistance in 2019: a systematic analysis. The Lancet 399, 629-655.

Naghavi, M., Vollset, S.E., Ikuta, K.S., Swetschinski, L.R., Gray, A.P., Wool, E.E., Robles Aguilar, G., Mestrovic, T., Smith, G., Han, C., Hsu, R.L., Chalek, J., Araki, D.T., Chung, E., Raggi, C., Gershberg Hayoon, A., Davis Weaver, N., Lindstedt, P.A., Smith, A.E., Altay, U., Bhattacharjee, N.V., Giannakis, K., Fell, F., McManigal, B., Ekapirat, N., Mendes, J.A., Runghien, T., Srimokla, O., Abdelkader, A., Abd-Elsalam, S., Aboagye, R.G., Abolhassani, H., Abualruz, H., Abubakar, U., Abukhadijah, H.J., Aburuz, S., Abu-Zaid, A., Achalapong, S., Addo, I.Y., Adekanmbi, V., Adeyeoluwa, T.E., Adnani, Q.E.S., Adzigbli, L.A., Afzal, M.S., Afzal, S., Agodi, A., Ahlstrom, A.J., Ahmad, A., Ahmad, S., Ahmad, T., Ahmadi, A., Ahmed, A., Ahmed, H., Ahmed, I., Ahmed, M., Ahmed, S., Ahmed, S.A., Akkaif, M.A., Al Awaidy, S., Al Thaher, Y., Alalalmeh, S.O., AlBataineh, M.T., Aldhaleei, W.A., Al-Gheethi, A.A.S., Alhaji, N.B., Ali, A., Ali, L., Ali, S.S., Ali, W., Allel, K., Al-Marwani, S., Alrawashdeh, A., Altaf, A., Al-Tammemi, A.B., Al-Tawfiq, J.A., Alzoubi, K.H., Al-Zyoud, W.A., Amos, B., Amuasi, J.H., Ancuceanu, R., Andrews, J.R., Anil, A., Anuoluwa, I.A., Anvari, S., Anyasodor, A.E., Apostol, G.L.C., Arabloo, J., Arafat, M., Aravkin, A.Y., Areda, D., Aremu, A., Artamonov, A.A., Ashley, E.A., Asika, M.O., Athari, S.S., Atout, M.M.d.W., Awoke, T., Azadnajafabad, S., Azam, J.M., Aziz, S., Azzam, A.Y., Babaei, M., Babin, F.-X., Badar, M., Baig, A.A., Bajcetic, M., Baker, S., Bardhan, M., Barqawi, H.J., Basharat, Z., Basiru, A., Bastard, M., Basu, S., Bayleyegn, N.S., Belete, M.A., Bello, O.O., Beloukas, A., Berkley, J.A., Bhagavathula, A.S., Bhaskar, S., Bhuyan, S.S., Bielicki, J.A., Briko, N.I., Brown, C.S., Browne, A.J., Buonsenso, D., Bustanji, Y., Carvalheiro, C.G., Castañeda-Orjuela, C.A., Cenderadewi, M., Chadwick, J., Chakraborty, S., Chandika, R.M., Chandy, S., Chansamouth, V., Chattu, V.K., Chaudhary, A.A., Ching, P.R., Chopra, H., Chowdhury, F.R., Chu, D.-T., Chutiyami, M., Cruz-Martins, N., da Silva, A.G., Dadras, O., Dai, X., Darcho, S.D., Das, S., De la Hoz, F.P., Dekker, D.M., Dhama, K., Diaz, D., Dickson, B.F.R., Djorie, S.G., Dodangeh, M., Dohare, S., Dokova, K.G., Doshi, O.P., Dowou, R.K., Dsouza, H.L., Dunachie, S.J., Dziedzic, A.M., Eckmanns, T., Ed-Dra, A., Eftekharimehrabad, A., Ekundayo, T.C., El Sayed, I., Elhadi, M., El-Huneidi, W., Elias, C., Ellis, S.J., Elsheikh, R., Elsohaby, I., Eltaha, C., Eshrati, B., Eslami, M., Eyre, D.W., Fadaka, A.O., Fagbamigbe, A.F., Fahim, A., Fakhri-Demeshghieh, A., Fasina, F.O., Fasina, M.M.,

Fatehizadeh, A., Feasey, N.A., Feizkhah, A., Fekadu, G., Fischer, F., Fitriana, I., Forrest, K.M., Fortuna Rodrigues, C., Fuller, J.E., Gadanya, M.A., Gajdács, M., Gandhi, A.P., Garcia-Gallo, E.E., Garrett, D.O., Gautam, R.K., Gebregergis, M.W., Gebrehiwot, M., Gebremeskel, T.G., Geffers, C., Georgalis, L., Ghazy, R.M., Golechha, M., Golinelli, D., Gordon, M., Gulati, S., Gupta, R.D., Gupta, S., Gupta, V.K., Habteyohannes, A.D., Haller, S., Harapan, H., Harrison, M.L., Hasaballah, A.I., Hasan, I., Hasan, R.S., Hasani, H., Haselbeck, A.H., Hasnain, M.S., Hassan, I.I., Hassan, S., Hassan Zadeh Tabatabaei, M.S., Hayat, K., He, J., Hegazi, O.E., Heidari, M., Hezam, K., Holla, R., Holm, M., Hopkins, H., Hossain, M.M., Hosseinzadeh, M., Hostiuc, S., Hussein, N.R., Huy, L.D., Ibáñez-Prada, E.D., Ikiroma, A., Ilic, I.M., Islam, S.M.S., Ismail, F., Ismail, N.E., Iwu, C.D., Iwu-Jaja, C.J., Jafarzadeh, A., Jaiteh, F., Jalilzadeh Yengejeh, R., Jamora, R.D.G., Javidnia, J., Jawaid, T., Jenney, A.W.J., Jeon, H.J., Jokar, M., Jomehzadeh, N., Joo, T., Joseph, N., Kamal, Z., Kanmodi, K.K., Kantar, R.S., Kapisi, J.A., Karaye, I.M., Khader, Y.S., Khajuria, H., Khalid, N., Khamesipour, F., Khan, A., Khan, M.J., Khan, M.T., Khanal, V., Khidri, F.F., Khubchandani, J., Khusuwan, S., Kim, M.S., Kisa, A., Korshunov, V.A., Krapp, F., Krumkamp, R., Kuddus, M., Kulimbet, M., Kumar, D., Kumaran, E.A.P., Kuttikkattu, A., Kyu, H.H., Landires, I., Lawal, B.K., Le, T.T.T., Lederer, I.M., Lee, M., Lee, S.W., Lepape, A., Lerango, T.L., Ligade, V.S., Lim, C., Lim, S.S., Limenh, L.W., Liu, C., Liu, X., Liu, X., Loftus, M.J., M Amin, H.I., Maass, K.L., Maharaj, S.B., Mahmoud, M.A., Maikanti-Charalampous, P., Makram, O.M., Malhotra, K., Malik, A.A., Mandilara, G.D., Marks, F., Martinez-Guerra, B.A., Martorell, M., Masoumi-Asl, H., Mathioudakis, A.G., May, J., McHugh, T.A., Meiring, J., Meles, H.N., Melese, A., Melese, E.B., Minervini, G., Mohamed, N.S., Mohammed, S., Mohan, S., Mokdad, A.H., Monasta, L., Moodi Ghalibaf, A., Moore, C.E., Moradi, Y., Mossialos, E., Mougin, V., Mukoro, G.D., Mulita, F., Muller-Pebody, B., Murillo-Zamora, E., Musa, S., Musicha, P., Musila, L.A., Muthupandian, S., Nagarajan, A.J., Naghavi, P., Nainu, F., Nair, T.S., Najmuldeen, H.H.R., Natto, Z.S., Nauman, J., Nayak, B.P., Nchanji, G.T., Ndishimye, P., Negoi, I., Negoi, R.I., Nejadghaderi, S.A., Nguyen, Q.P., Noman, E.A., Nwakanma, D.C., O'Brien, S., Ochoa, T.J., Odetokun, I.A., Ogundijo, O.A., Ojo-Akosile, T.R., Okeke, S.R., Okonji, O.C., Olagunju, A.T., Olivas-Martinez, A., Olorukooba, A.A., Olwoch, P., Onyedibe, K.I., Ortiz-Brizuela, E., Osuolale, O., Ounchanum, P., Oyeyemi, O.T., P A, M.P., Paredes, J.L., Parikh, R.R., Patel, J., Patil, S., Pawar, S., Peleg, A.Y., Peprah, P., Perdigão, J., Perrone, C., Petcu, I.-R., Phommasone, K., Piracha, Z.Z., Poddighe, D., Pollard, A.J., Poluru, R., Ponce-De-Leon, A., Puvvula, J., Qamar, F.N., Qasim, N.H., Rafai, C.D., Raghav, P., Rahbarnia, L., Rahim, F., Rahimi-Movaghar, V., Rahman, M., Rahman, M.A., Ramadan, H., Ramasamy, S.K., Ramesh, P.S., Ramteke, P.W., Rana, R.K., Rani, U., Rashidi, M.-M., Rathish, D., Rattanavong, S., Rawaf, S., Redwan, E.M.M., Reyes, L.F., Roberts, T., Robotham, J.V., Rosenthal, V.D., Ross, A.G., Roy, N., Rudd, K.E., Sabet, C.J., Saddik, B.A., Saeb, M.R., Saeed, U., Saeedi Moghaddam, S., Saengchan, W., Safaei, M., Saghazadeh, A., Saheb Sharif-Askari, N., Sahebkar, A., Sahoo, S.S., Sahu, M., Saki, M., Salam, N., Saleem, Z., Saleh, M.A., Samodra, Y.L., Samy, A.M., Saravanan, A., Satpathy, M., Schumacher, A.E., Sedighi, M., Seekaew, S., Shafie, M., Shah, P.A., Shahid, S., Shahwan, M.J., Shakoor, S., Shalev, N., Shamim, M.A., Shamshirgaran, M.A., Shamsi, A., Sharifan, A., Shastry, R.P., Shetty, M., Shittu, A., Shrestha, S., Siddig, E.E., Sideroglou, T., Sifuentes-Osornio, J., Silva, L.M.L.R., Simões, E.A.F., Simpson, A.J.H., Singh, A., Singh, S., Sinto, R., Soliman, S.S.M., Soraneh, S., Stoesser, N., Stoeva, T.Z., Swain, C.K., Szarpak, L., T Y, S.S., Tabatabai, S., Tabche, C., Taha, Z.M.-A., Tan, K.-K., Tasak, N., Tat, N.Y., Thaiprakong, A., Thangaraju, P., Tigoi, C.C., Tiwari, K., Tovani-Palone, M.R., Tran, T.H., Tumurkhuu, M., Turner, P., Udoakang, A.J., Udoh, A., Ullah, N., Ullah, S., Vaithinathan, A.G., Valenti, M., Vos, T., Vu, H.T.L., Waheed, Y., Walker, A.S., Walson, J.L., Wangrangsimakul, T., Weerakoon, K.G., Wertheim, H.F.L., Williams, P.C.M., Wolde, A.A., Wozniak, T.M., Wu, F., Wu, Z., Yadav, M.K.K., Yaghoubi, S., Yahaya, Z.S., Yarahmadi, A., Yezli, S., Yismaw, Y.E., Yon, D.K., Yuan, C.-W., Yusuf, H., Zakham, F., Zamagni, G., Zhang, H., Zhang, Z.-J., Zielińska, M., Zumla, A., Zyoud, S.e.H.H., Zyoud, S.H., Hay, S.I., Stergachis, A., Sartorius, B., Cooper, B.S., Dolecek, C., Murray, C.J.L., 2024. Global burden of bacterial antimicrobial resistance 1990–2021: a systematic analysis with forecasts to 2050. The Lancet 404, 1199-1226.

Naik, N., Hameed, B.M.Z., Shetty, D.K., Swain, D., Shah, M., Paul, R., Aggarwal, K., Ibrahim, S., Patil, V., Smriti, K., Shetty, S., Rai, B.P., Chlosta, P., Somani, B.K., 2022. Legal and Ethical Consideration in Artificial Intelligence in Healthcare: Who Takes Responsibility? 9.

Nissan, N., Allen, M.C., Sabatino, D., Biggar, K.K., 2024. Future Perspective: Harnessing the Power of Artificial Intelligence in the Generation of New Peptide Drugs. 14, 1303.

Sader, H.S., Dale, G.E., Rhomberg, P.R., Flamm, R.K.J.A.A., Chemotherapy, 2018. Antimicrobial activity of murepavadin tested against clinical isolates of Pseudomonas aeruginosa from the United States, Europe, and China. 62, 10.1128/aac. 00311-00318.

Shaik, S., Singh, A., Suresh, A., Ahmed, N., 2022. Genome Informatics and Machine Learning-Based Identification of Antimicrobial Resistance-Encoding Features and Virulence Attributes in Escherichia coli Genomes Representing Globally Prevalent Lineages, Including High-Risk Clonal Complexes. 13, e03796-03721.

Sharma, R., Shrivastava, S., Singh, S.K., Kumar, A., Singh, A.K., Saxena, S., 2024. Artificial Intelligence-Based Model for Predicting the Minimum Inhibitory Concentration of Antibacterial Peptides Against ESKAPEE Pathogens. Ieee Journal of Biomedical and Health Informatics 28, 1949-1958.

Stephenson, J., 2021. WHO Offers Guidance on Use of Artificial Intelligence in Medicine. JAMA Health Forum 2, e212467-e212467.

Stokes, J.M., Yang, K., Swanson, K., Jin, W., Cubillos-Ruiz, A., Donghia, N.M., MacNair, C.R., French, S., Carfrae, L.A., Bloom-Ackermann, Z., Tran, V.M., Chiappino-Pepe, A., Badran, A.H., Andrews, I.W., Chory, E.J., Church, G.M., Brown, E.D., Jaakkola, T.S., Barzilay, R., Collins, J.J., 2020. A Deep Learning Approach to Antibiotic Discovery. Cell 180, 688-702.e613.

Szymczak, P., Możejko, M., Grzegorzek, T., Jurczak, R., Bauer, M., Neubauer, D., Sikora, K., Michalski, M., Sroka, J., Setny, P., Kamysz, W., Szczurek, E., 2023. Discovering highly potent antimicrobial peptides with deep generative model HydrAMP. Nature Communications 14, 1453.

Torres, M.D.T., Chen, L.T., Wan, F., Chatterjee, P., de la Fuente-Nunez, C., 2025. Generative latent diffusion language modeling yields anti-infective synthetic peptides. Cell Biomaterials 1.

Vashisht, V., Vashisht, A., Mondal, A.K., Farmaha, J., Alptekin, A., Singh, H., Ahluwalia, P., Srinivas, A., Kolhe, R.J.B., 2023. Genomics for emerging pathogen identification and monitoring: Prospects and obstacles. 3, 1145-1177.

Wan, F., Kontogiorgos-Heintz, D., de la Fuente-Nunez, C., 2022. Deep generative models for peptide design. Digital Discovery 1, 195-208.

Wan, F., Torres, M.D.T., Peng, J., de la Fuente-Nunez, C., 2024a. Deep-learning-enabled antibiotic discovery through molecular de-extinction. Nature Biomedical Engineering 8, 854-871.

Wan, F., Wong, F., Collins, J.J., de la Fuente-Nunez, C., 2024b. Machine learning for antimicrobial peptide identification and design. Nature Reviews Bioengineering 2, 392-407.

Wong, F., de la Fuente-Nunez, C., Collins, J.J., 2023. Leveraging artificial intelligence in the fight against infectious diseases. 381, 164-170.

Wu, M., Hancock, R.E.J.A.a., chemotherapy, 1999. Improved derivatives of bactenecin, a cyclic dodecameric antimicrobial cationic peptide. 43, 1274-1276.

Wu, X., Wang, Z., Li, X., Fan, Y., He, G., Wan, Y., Yu, C., Tang, J., Li, M., Zhang, X.J.A.a., chemotherapy, 2014. In vitro and in vivo activities of antimicrobial peptides developed using an amino acid-based activity prediction method. 58, 5342-5349.

Zhang, C., Ju, Y., Tang, N., Li, Y., Zhang, G., Song, Y., Fang, H., Yang, L., Feng, J., 2019. Systematic analysis of supervised machine learning as an effective approach to predicate β-lactam resistance phenotype in Streptococcus pneumoniae. Briefings in Bioinformatics 21, 1347-1355.

Zhang, Y., Zhao, C., Wang, Q., Wang, X., Chen, H., Li, H., Zhang, F., Wang, H.J.J.o.A.C., 2020. Evaluation of the in vitro activity of new polymyxin B analogue SPR206 against clinical MDR, colistin-resistant and tigecycline-resistant Gram-negative bacilli. 75, 2609-2615.

doi: 10.62591/Scien.Tech.Bull-Chem.FoodSci.Eng.2025.22.05

Published by "AUREL VLAICU" University of Arad Publishing House
Arad, Romania, 2025